

Parametric Thermal Models of the Transient Reactor Test Facility (TREAT)

Bradley K. Heath

March 2014



The INL is a U.S. Department of Energy National Laboratory
operated by Battelle Energy Alliance

Parametric Thermal Models of the Transient Reactor Test Facility (TREAT)

Bradley K. Heath¹

¹Idaho State University

March 2014

**Idaho National Laboratory
Idaho Falls, Idaho 83415**

<http://www.inl.gov>

**Prepared for the
U.S. Department of Energy
Under DOE Idaho Operations Office
Contract DE-AC07-05ID14517**

TABLE OF CONTENTS

List of Figures.....	iii
LIST of Tables.....	vii
Abstract.....	viii
Chapter 1: Introduction	1
<i>Background.....</i>	<i>1</i>
<i>Problem</i>	<i>1</i>
<i>Goals.....</i>	<i>2</i>
<i>Achieving the Goals.....</i>	<i>2</i>
<i>Assumptions/Limitations.....</i>	<i>3</i>
<i>Significance</i>	<i>3</i>
Chapter 2: Literature Review.....	5
<i>Reactor Description.....</i>	<i>5</i>
<i>Fuel Description.....</i>	<i>7</i>
<i>Reactor Cooling.....</i>	<i>11</i>
<i>Previous Work</i>	<i>16</i>
Chapter 3: Methodology.....	34
<i>Software Description.....</i>	<i>34</i>
<i>Assumptions.....</i>	<i>37</i>
<i>Parametrics and Model Development</i>	<i>38</i>
<i>Analytical Comparison to BISON.....</i>	<i>45</i>
Chapter 4: Results.....	49
<i>Property Variation.....</i>	<i>49</i>
<i>Steady State</i>	<i>52</i>
<i>Transients</i>	<i>62</i>
CHAPTER 5: CONCLUSION.....	81
References.....	84
Appendix A: Drawings	A1
Appendix B: Mesh file	A13
Appendix C: Input file.....	A23

LIST OF FIGURES

Figure 1: Cutaway view of the TREAT reactor.....	6
Figure 2: Axial view of a standard fuel assembly.....	8
Figure 3: Standard fuel assembly components.	9
Figure 4: Schematic of the TREAT reactor cooling system.	12
Figure 5: Four fuel elements come together to create a coolant channel.....	13
Figure 6: Core alignment is by clamping bars at the top and a grid plate at the bottom. .	15
Figure 7: Grid plate for bottom alignment and core support.	15
Figure 8: Reactor power vs. time for several experimental transients.....	21
Figure 9: Axial temperature curves for several transients.	21
Figure 10: Model of fuel cell used in calculations.....	22
Figure 11: Time lag in heat transfer for various fuel particle sizes during initial stage and runaway. (Pile is on an 80 ms period).....	23
Figure 12: Measured and calculated axial temperature profiles.	24
Figure 13: Calculated axial temperature profiles in center fuel assembly following a 2500 MWs transient without coolant flow.....	25
Figure 14: Measured axial temperature curves following a 800 MW-s transient. Air flow is turned on at 87 minutes at 70% flow.....	26
Figure 15: Calculated axial temperature profiles in coolant channel at 100 kW.....	27
Figure 16: Apparatus used in experimental model.	28
Figure 17: Axial thermocouple placement in apparatus.	29
Figure 18: Radial thermocouple placement in apparatus.....	30

Figure 19: Axial midplane temperature distribution. Left - Steady state power of 1000 W and flow of 108 lb/hr. Right - 30 minutes after heat is turned off.	32
Figure 20: Axial temperature distribution for cooling from steady state power at a flowrate of 260 lbm/hr (zircaloy spacer being used).	33
Figure 21: Outlet air temperatures for steady state and transient power.	33
Figure 22: Axial view of TREAT fuel assembly showing components.	41
Figure 23: Cross-sectional view of the octant and the fueled region.	41
Figure 24: Built-in deflection compared against the elastic model BISON solves. The model on the left does not have pressure applied to cladding.	41
Figure 25: Heat generation curve as a function of time for the transient mode.	42
Figure 26: BISON 2D models to compare against analytical solution (100 kW and 300,000 s).	48
Figure 27: Axial temperature distribution for a steady state power of 100 kW at 300,000 s.	52
Figure 28: Steady State Benchmark –vs- fuel specific heat and thermal conductivity. ...	53
Figure 29: Steady State Benchmark -vs- fuel density and fuel emissivity.	54
Figure 30: Steady State Benchmark -vs- Zr-3 specific heat and thermal conductivity. ...	55
Figure 31: Steady State Benchmark -vs- Zr-3 density and emissivity.	56
Figure 32: Steady State Benchmark -vs- spacer thermal conductivity and canning material type.	57
Figure 33: Temperature distribution of a TREAT fuel assembly at a power of 100 kW and 300,000 s. Shown is an octant of the assembly.	58

Figure 34: Temperature distribution of the fuel. The top of the fuel is coolest as is expected for air that flows downward.....	59
Figure 35: Interface for Zr-3 and Al-6063 cans and interface for fuel and reflector blocks. Observable is the effect the spacer has on delaying heat transfer.....	60
Figure 36: Radial temperature distribution across the fuel showing the cooling takes place primarily where the cladding makes contact.	61
Figure 37: Axial temperature distribution for a transient of 1000 MJ at 0.9 s.	64
Figure 38: Benchmark compared against fuel Cp and k. Fuel k has negligible effects on temperature.....	65
Figure 39: Benchmark compared against fuel ρ and ϵ . Fuel ϵ has negligible effects on temperature.....	66
Figure 40: Temperature distribution at 1000 MJ and 0.9 s. Shown is an octant of the assembly.....	67
Figure 41: Temperature distribution of the fuel. The outside of the fuel is cooler since it is in contact with the Zr-3 can allowing some of the heat to dissipate there.....	68
Figure 42: Zr-3 can temperature distribution. The hotter spots on the can are in contact with the fuel.	69
Figure 43: Radial distribution of the fuel. The side is cooler than the chamfer because the fuel is in contact with the Zr-3 can.	70
Figure 44: Delayed heat transfer from spacer.....	71
Figure 45: Axial temperature distribution 25,000 s after a 1000 MW-s transient.....	72
Figure 46: Benchmark compared against fuel Cp and k. Both these properties affect temperature, however Cp has a greater effect.....	73

Figure 47: Benchmark compared against fuel ρ and ϵ . Fuel ϵ has negligible effects on temperature.....	74
Figure 48: Benchmark compared against Zr-3 can C_p and k . Zr-3 C_p has negligible effects on temperature.	75
Figure 49: Benchmark compared against spacer k and canning material.....	76
Figure 50: Temperature distribution 25,000 s after a 1000 MW-s transient. Shown is an octant of the fuel assembly.....	77
Figure 51: Axial temperature distribution of the fuel section.....	78
Figure 52: Fuel transferring heat across spacer to reflector.....	79
Figure 53: Radial temperature distribution of the fuel. Similar the steady state case the cooler spots where the Zr-3 can makes contact.	80
Figure A1: TREAT Fuel Assembly.....	2
Figure A2: TREAT Fuel Assembly Fuel Block.	3
Figure A3: TREAT Fuel Assembly Reflector Block (Long).....	4
Figure A4: TREAT Fuel Assembly Reflector Block (Short).	5
Figure A5: TREAT Fuel Assembly Reflector Block for vacuum tube (Short).	6
Figure A6: TREAT Fuel Assembly Al-6063 Can.	7
Figure A7: TREAT Fuel Assembly Fuel Section.....	8
Figure A8: TREAT Fuel Assembly Tab to link Al-6063 and Zr-3 cans.	9
Figure A9: TREAT Fuel Assembly Spacer between fuel and reflector.	10
Figure A10: TREAT Fuel Assembly Top handling fixture for TREAT fuel element.....	11
Figure A11: TREAT Fuel Assembly bottom support pin.....	12

LIST OF TABLES

Table 1: Design Parameters for TREAT.....	7
Table 2: Thermal Properties for a Standard Fuel Assembly.....	11
Table 3: Parametrics	39
Table 4: Reynolds Numbers by Axial Position.....	44
Table 5: Nusselt Numbers and Convection Coefficients by Axial Location.....	44
Table 6: Equations for Nusselt Numbers	45
Table 7: Hot Spot Temperatures	49
Table 8: Steady State BISON results compared against literature.	50
Table 9: Transient BISON results compared against the literature.	62

ABSTRACT

This work supports the restart of transient testing in the United States using the Department of Energy's Transient Reactor Test Facility at the Idaho National Laboratory. It also supports the Global Threat Reduction Initiative by reducing proliferation risk of high enriched uranium fuel. The work involves the creation of a nuclear fuel assembly model using the fuel performance code known as BISON. The model simulates the thermal behavior of a nuclear fuel assembly during steady state and transient operational modes. Additional models of the same geometry but differing material properties are created to perform parametric studies. The results show that fuel and cladding thermal conductivity have the greatest effect on fuel temperature under the steady state operational mode. Fuel density and fuel specific heat have the greatest effect for transient operational model. When considering a new fuel type it is recommended to use materials that decrease the specific heat of the fuel and the thermal conductivity of the fuel's cladding in order to deal with higher density fuels that accompany the LEU conversion process. Data on the latest operating conditions of TREAT need to be attained in order to validate BISON's results. BISON's models for TREAT (material models, boundary convection models) are modest and need additional work to ensure accuracy and confidence in results.

CHAPTER 1: INTRODUCTION

Background

The Transient Reactor Test Facility (TREAT) is an air-cooled graphite moderated nuclear reactor. It is owned by the Department of Energy (DOE) and located inside the Materials and Fuels Complex at Idaho National Laboratory (INL) near Idaho Falls, Idaho. The facility operated from 1959 to 1994 undergoing 6,604 reactor startups and 2,885 transient irradiations. The reactor design allows for transient mode producing 1000 MW-s deposition or steady stateⁱ mode of 100 kW. The TREAT was used to study fuel meltdowns, metal-water reactions, interactions between overheated fuel and coolant, and the transient behavior of fuels for high temperature systems. The TREAT has provided valuable information into the behavior of mixed-oxide breeder reactor fuel rods under accident conditions. The reactor was placed in cold standby in 1994 due to funding constraints.

Problem

Recent cases made for advanced accident tolerant fuels (as well as other nuclear fuel systems) have generated a desire to resume transient testing in the United States. The DOE's Office of Nuclear Energy (DOE-NE) is in the process of restarting the TREAT specifically for this application. In taking this course DOE-NE recognizes the facility will need some upgrades in order to meet current standards and regulations. In preparation for the resumption of transient testing at the TREAT INL is gathering

ⁱ Steady state is mentioned in differing contexts throughout: (1) to describe the operation of the reactor at 100 kW (2) to describe the point where the energy generated by the reactor and removed by the coolant is equal (3) to describe the air flow into and out of the reactor as constant.

information on how to approach the use of low enriched fuel (LEU) as an alternative to the current highly enriched fuel. Part of a preliminary study is use of modern computer codes and simulation techniques to model the current reactor configuration to provide a baseline of the TREAT.

Goals

This is motivated to better understand the experiment environment, improve data outputs, define safety margins, and simplify operation. In the case for LEU conversion, computer simulation allows for parametric studies to define best material selection in new fuel development. The goals of this work are to give INL a tool that can be used to: understand the thermal aspects of the TREAT, analyze additional phenomenon, and support nonproliferation efforts in new LEU fuel development. Having the ability to easily manipulate the thermal model through simulation techniques enhances understanding. In the reactor multiple phenomenon including fuel burnup, fission product generation, property and geometrical variation from irradiation, oxidation, etc. are occurring simultaneously. These parametric studies give INL a solid base that is built in a platform where the phenomenon can be added to supplement understanding of the experimental environment. Converting the TREAT to LEU fuel is part of the Global Threat Reduction Initiative to reduce proliferation risk in research and test reactors.

Achieving the Goals

This thesis's objective is to contribute to the accomplishment of the goals by providing INL with a usable model that can model various aspects of thermal behavior. The model also provides a baseline that can be easily expanded to model additional phenomenon

such as those mentioned above. The objective is achieved through literary review, BISON model development, baseline and parametric studies, and analyzed results.

Assumptions/Limitations

The models developed herein only consider the thermal aspects of the nuclear fuel in TREAT. It is well known that in nuclear reactors temperature characteristics of the fuel are only a portion of the information necessary to design, development, and operate a nuclear reactor successfully. The TREAT operated for over 40 years. During that time safety limits (reactor temperature, power, etc.) were modified to better suit the experimenter's needs. Those extensions of the original design and operating limits are not included in this work.

Significance

The significance of this study is it supports the restart of a transient testing capability in the United States that is one of kind and necessary to ensure the future of nuclear security as a reliable and safe energy option and where proliferation risk is greatly reduced. It supports INL's capability in nuclear and material testing and development, fuel modeling and simulation development, and supplements their role as the lead nuclear laboratory in the United States. Additionally it sparks insight and development into what are both relatively new technologies: nuclear energy and computational science.

CHAPTER 2: LITERATURE REVIEW

Reactor Description

The TREAT is an air-cooled graphite moderated heterogeneous nuclear reactor designed to evaluate reactor fuels and structural materials under condition simulating various types of nuclear excursions and transient undercooling situations. The TREAT provides an environment where fuel meltdowns, metal-water reactions, thermal interactions between overheated fuel and coolant, and the transient behavior of ceramic fuel for high temperature systems can be studied.^[1] Construction of the TREAT was started by the Teller Construction Company, Portland, Oregon in February 1958 and completed in November 1958. The facility achieved criticality for the first time on February 23, 1959.

The reactor operated in transient mode delivering 1000 MW-s (peak power of 1000 MW) energy deposition into the core or in steady state mode at power of 100 kW.^[2] Both modes had an upper hot spot temperature limit of 752°F (400°C). The transient mode was used to simulate excursions while the steady state operation was used to support neutron-radiography. Figure 1 shows a cutaway view of the reactor.

The maximum active core size is 6 ft 4 in square by 4 ft high (361 assembliesⁱⁱ). Nominal active core size is 5 ft square (225 assemblies) for transient mode and a slightly smaller (180 assemblies) active core size for steady state operation. When using smaller active core sizes the maximum core size is still maintained by placing dummy (non-fueled) assemblies into unused positions in the core. A permanent reflector surrounds the

ⁱⁱ There are 361 4 in x 4 in locations in the core. Maximum amount of fuel assemblies is less than 361 assemblies. Some locations in the core are reserved for experiment(s), driven rods, or in some cases entire rows are removed for viewing.

core with a 2 in gap between core and reflector and a 2 in gap between reflector and biological shield. The biological shield makes up the rest of the reactor structure. Table 1 shows reactor operating parameters based on the 1958 design.

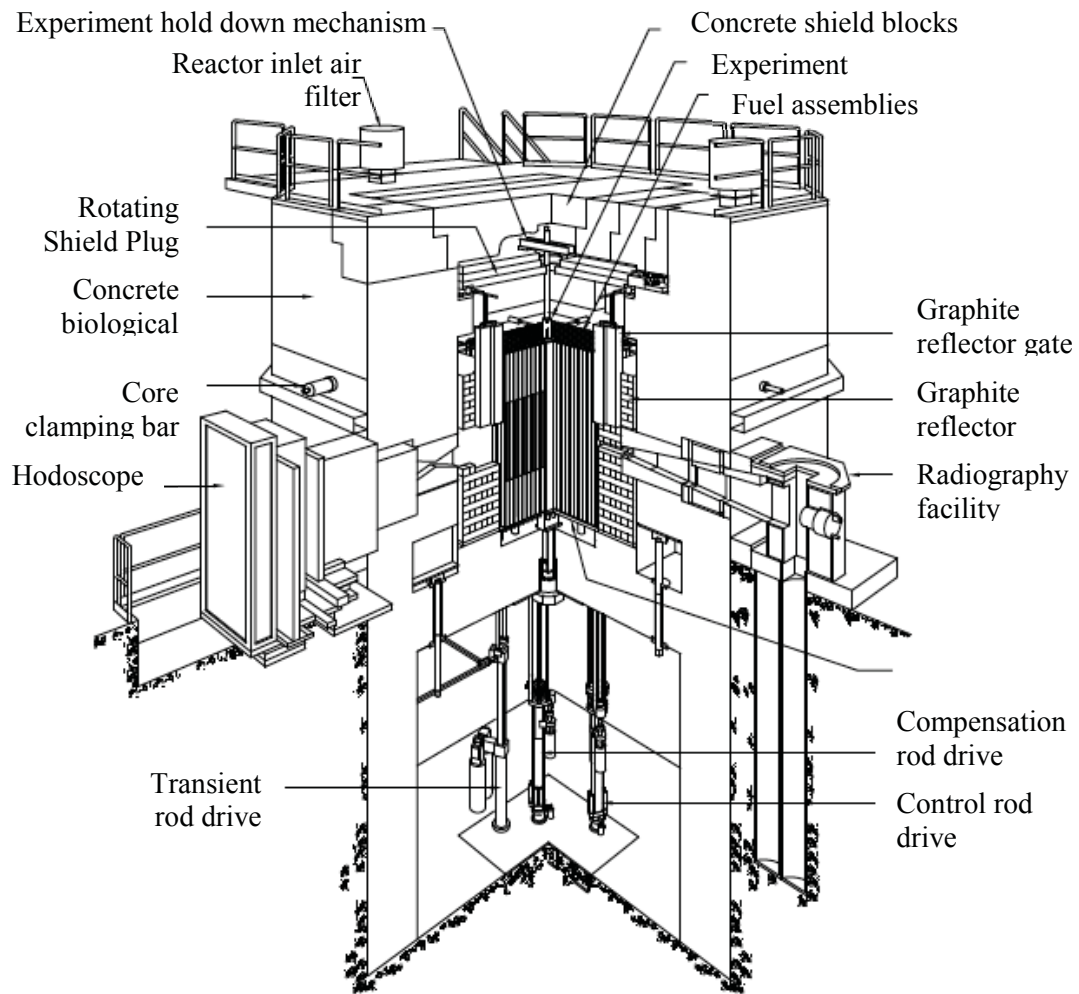


Figure 1: Cutaway view of the TREAT reactor.^[3]

Table 1: Design Parameters for TREAT

Nuclear		
Core Size (Nominal)		5 ft X 5 ft X 4 ft
Core Size (Maximum)		6 ft 4 in X 6 ft 4 in X 4 ft
Reflector		Graphite (2 ft)
Loading		8.44 kg
Carbon-U235 Atomic Ratio		10,000:1
Transient Mode		
Energy Release for Nominal Core		1000 MW-s
Time-Integrated Thermal Flux (avg. over core)		$3.5 \times 10^{15} \text{ n cm}^{-2}$
Corresponding Final Average Graphite Temperature		500°F (260°C)
Final Maximum Hot-Spot Graphite Temperature		752°F (400°C)
Corresponding $\Delta k/k$ in Temperature Coefficient		0.05
Steady State Mode		
Power Level (nominal)		100 kW
Coolant Air Flow		6000 cfm
Coolant Inlet Pressure		12.5 psi
Core Pressure Drop		0.5 psi
Coolant Temperature Rise through Core		118°F (48°C)

Fuel Description

The TREAT fuel fabrication was conducted with a joint effort from Argonne National Laboratory and the Great Lakes Carbon Corporation. The standard fuel assembly length is approximately 8.94 ft.^[4] The fueled section of the assembly is made up of six 8-in long 3.8-in square graphite uranial blocks totaling 4 ft (see Figure 2 and Figure 3). The fueled portion is canned in 0.025-in thick zircaloy-3 (Zr-3) with a nominal gap between can and fuel of 0.055 in. The Zr-3 can is made from two sections that are cold rolled, formed to shape in a bending fixture, and welded together.^[5] The finished length of the Zr-3 can is 49-3/8 in. All graphite uranial blocks are thermally outgassed at high temperature before placement in Zr-3 cans to avoid subsequent pressure buildup during reactor operation.

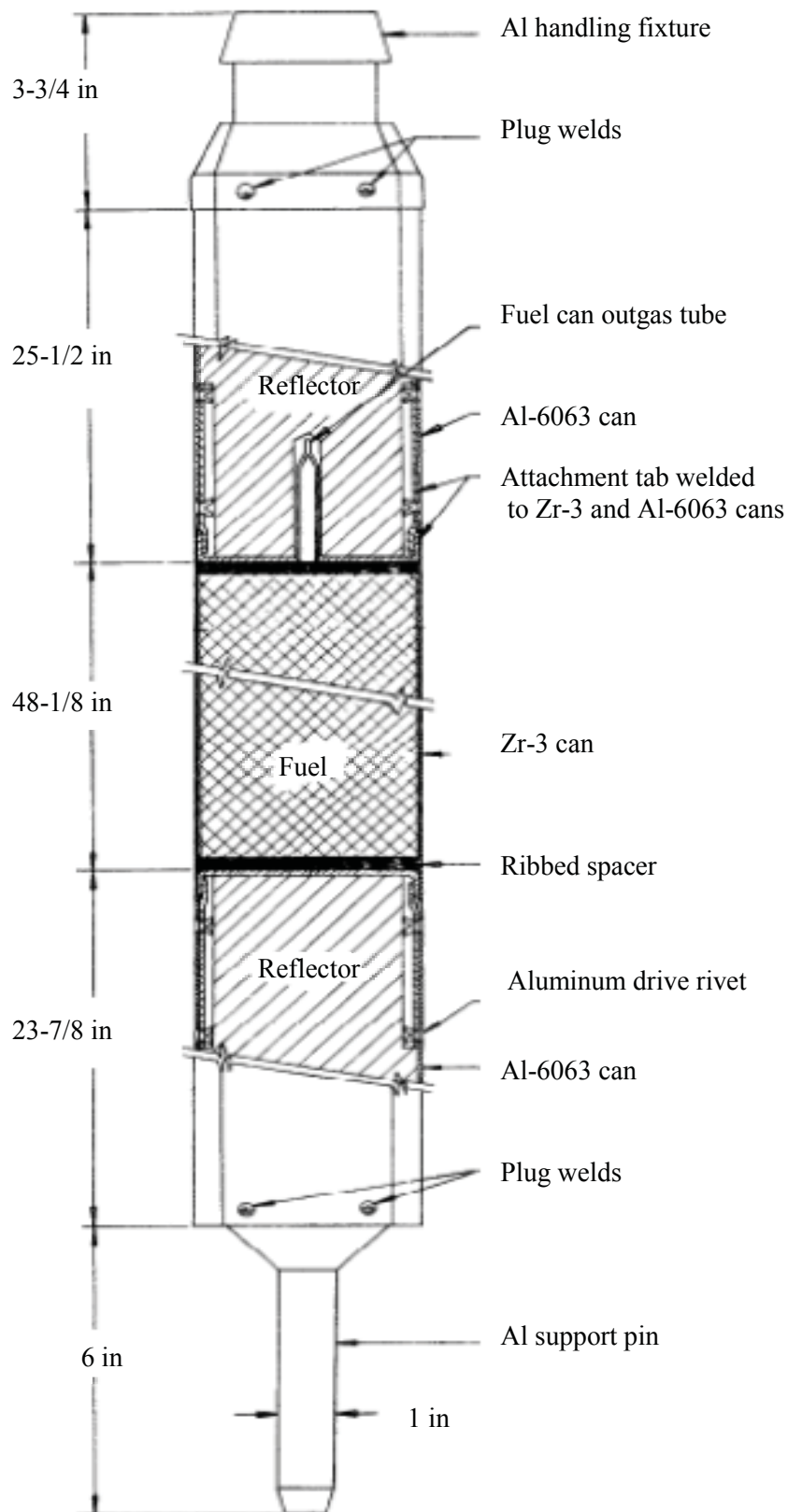


Figure 2: Axial view of a standard fuel assembly.

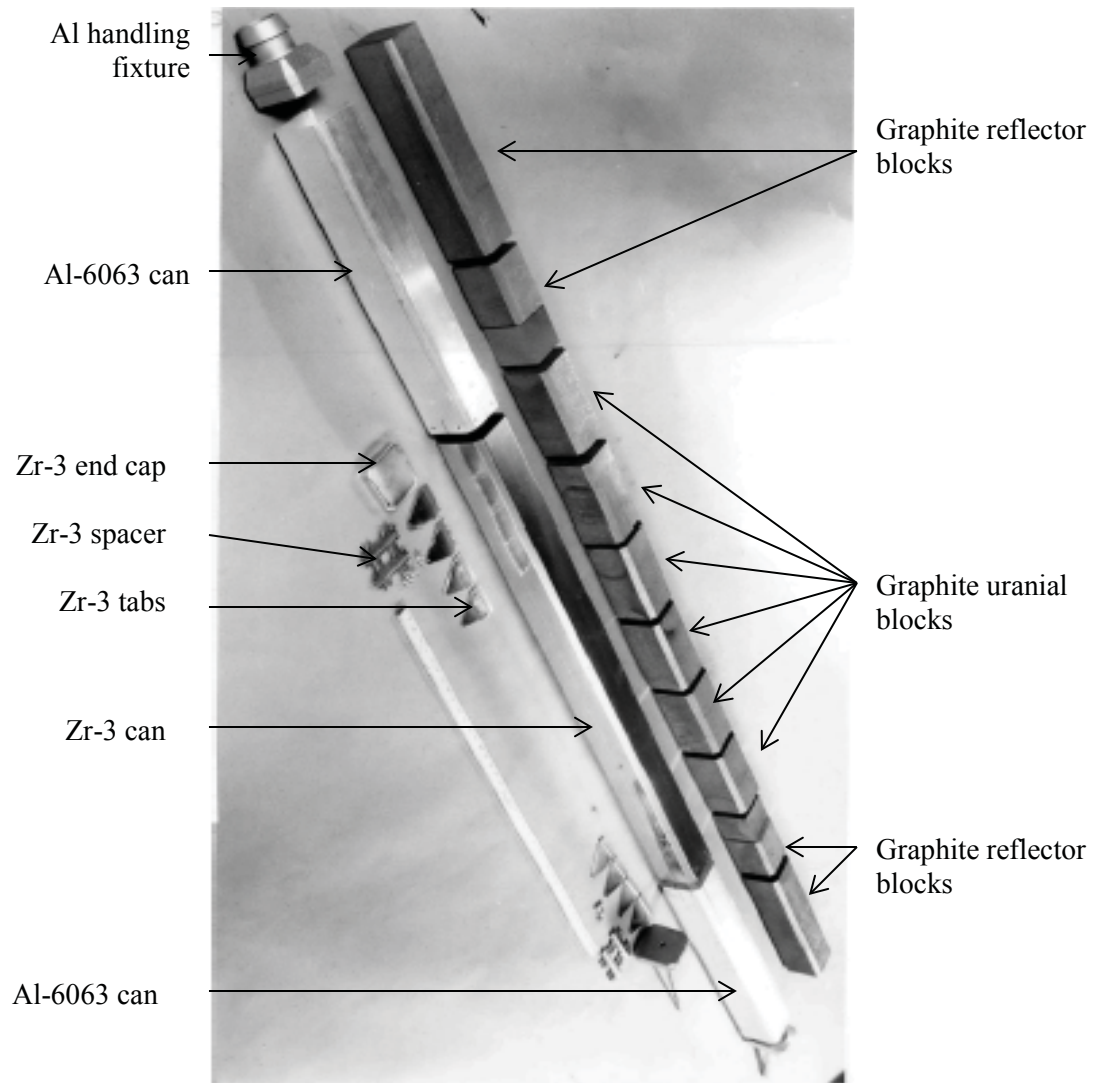


Figure 3: Standard fuel assembly components.

A 0.25 in thick Zr-3 ribbed spacer is placed on each end of the fueled section to delay heat transfer from the fuel to the reflector. The can is sealed by welding a 0.093 in thick Zr-3 cap to each end. A tube protrudes through the top cap of the Zr-3 can and is used to evacuate the can.

The top and bottom of the fuel assembly are used for reflectors and each have two graphite blocks inside aluminum-6063 (Al-6063) cans. The top and bottom long graphite blocks are 16 in and 14-3/8 in, respectively. Both short reflector blocks are 8-11/16 in

with 3-1/2 in square sections. Although the permanent reflector surrounding the core was fabricated from the dismantled Chicago Pile 2 (CP-2) reactorⁱⁱⁱ it is unclear if the reflector in the fuel assemblies was also fabricated from CP-2.

The Al-6063 cans are 0.050-in thick with a nominal gap between can and reflector of 0.030 in. The top aluminum can is 24-19/32 in and the bottom aluminum can is 23-9/32 in. The Al-6063 cans are extruded and the support pin and handling fixture are cast aluminum. The specific casting type for the handling fixture and support pin is unknown. The reflector sections are connected to the fueled section using Zr-3 tabs. The tabs are riveted to the Al-6063 cans and welded to the inside of the Zr-3 end caps. The top handling fixture and the support pin are welded in place. The Al-6063 cans are not evacuated like the Zr-3 can. Table 2 lists thermal properties of the standard fuel assembly. The fuel has a density close to graphite since the atomic ratio of carbon to uranium is near 10,000 to 1. More specific dimensions of the TREAT assembly can be found in Appendix A¹.

The drawings indicated the fuel assembly reflector is canned in aluminum-1100 (Al-1100). Al-6063 is assumed to be the correct canning material based on it being mentioned in initial design summary documentation.^[6] This is a safe assumption since the properties for Al-1100 are nearly identical to Al-6063 with the exception of thermal conductivity, which are within 5% of one another. The thermal conductivity and specific heat for the fuel are average values over the operating temperature range.

ⁱⁱⁱ The Chicago Pile 2 reactor was built from the dismantled Chicago Pile 1 reactor so the permanent reflector is graphite from the Chicago Pile 1 reactor.

Table 2: Thermal Properties for a Standard Fuel Assembly

	Density (kg/m ³)	Thermal Conductivity (W/m K)	Specific Heat (J/kg K)	Emissivity
Zr-3 ^{[7],[8]}	6533	14.4	276	0.9
Al-6063 ^[9]	2690	218	900	0.05
Fuel ^{[10],[11]}	1720	20	998	0.98
Reflector*	1720	20	998	0.98

*Properties assumed to be the same as the fuel.

Reactor Cooling

Air to cool the reactor is drawn through the core by two blowers, each with a rated capacity of 3250 cfm against a head of 1 psi at 250°F (121°C) with an intake pressure of 25 in Hg. The air enters through dampers in the roof of the reactor building and exits out the building exhaust stack. Figure 4 shows a depiction of coolant flow through the core. Approximately 500 cfm of the 6000 cfm of air flowing down through the reactor cools the permanent reflector on each side. The remaining 5500 cfm flows through 0.625 in passages^{iv} created by the fuel assemblies as shown in Figure 5. The chamfers of the fuel assemblies form 324 passages with each passage receiving 17 cfm (5500 cfm/324 passages) of air at 12.5 psi and 70 - 100°F (21-38°C). Colder inlet temperatures are not expected since during cold weather a bulk air-heating unit rated at 7500 cfm is used.

A bypass valve can be opened to allow some of the inlet air to be drawn through the subpile room in order to cool the reactor outlet air should outlet temperatures be above the 250°F rated^v components that are downstream. Reactor outlet temperatures for

^{iv} The cross-section of a fuel assembly is 3.96 in square with 0.625 in chamfers; however the top handling fixture is 4 in square with 0.625 in chamfers so the air first enters through a 0.625 in square channel rather than one with gaps in between assemblies.

^v Higher temperature components were later added with a higher rating. The bypass valve is controlled such that it is fully open once the reactor outlet temperature reaches 170°C.

steady state and post-transient conditions could not be found. Temperatures could be found in the reactor logs but since the reactor hasn't been operated in nearly twenty years they couldn't be obtained.

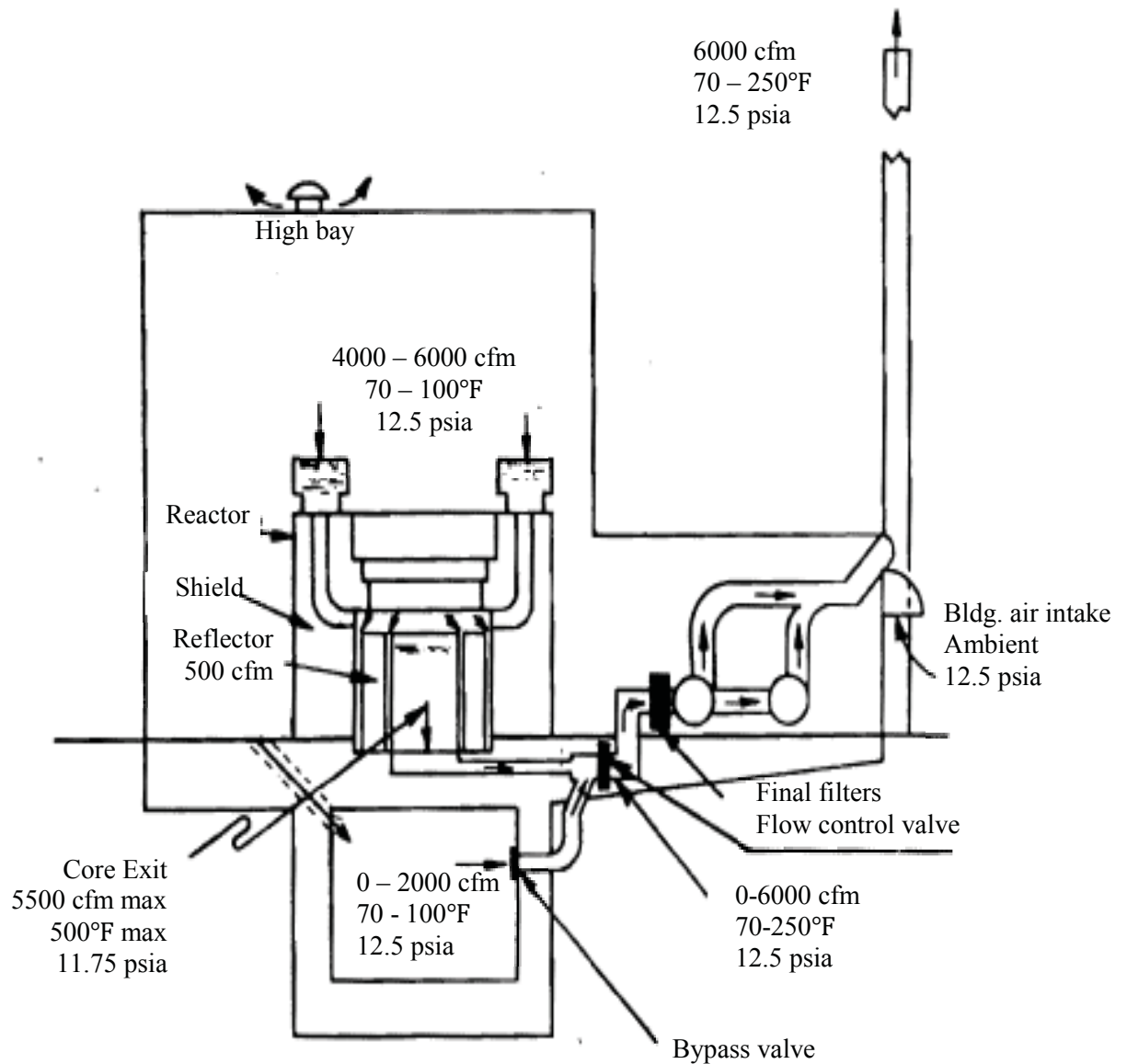


Figure 4: Schematic of the TREAT reactor cooling system.

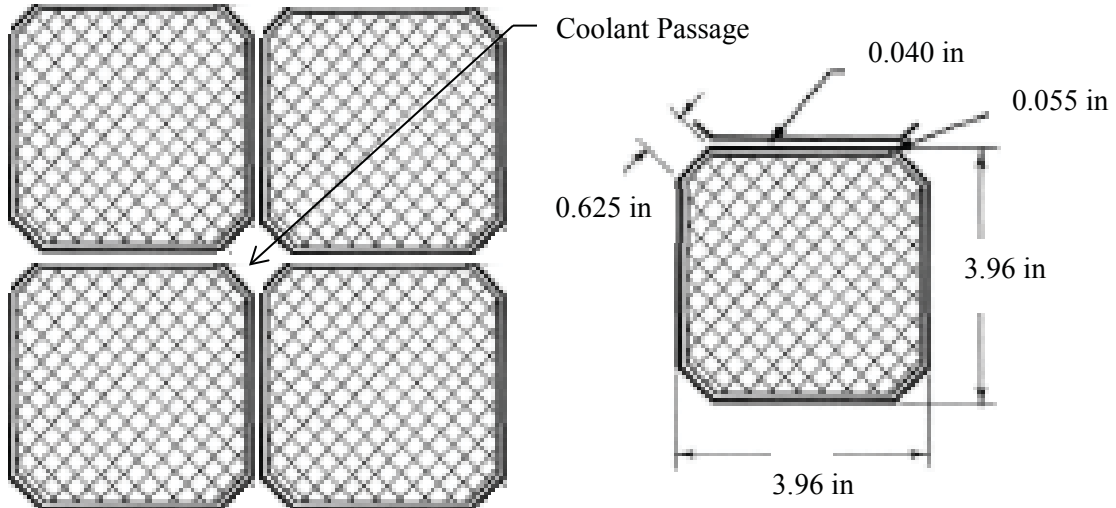


Figure 5: Four fuel elements come together to create a coolant channel.

Reference 2 states the change in temperature across the core is 118°F (48°C). Reference [6] says the temperature rise is 68°F (20°C) with a flow rate of 6500 cfm and Reference [4] says reactor outlet temperatures could reach 400°F (204°C) under accident conditions and that an alarm sounds when reactor outlet temperature reaches 345°F (174°C) and the bypass valve is fully open at 338°F (170°C). Reference [6] states that steady state power is calculated by a heat balance on reactor coolant as given by:

$$\dot{Q} = 0.1184\Delta TR \sqrt{\frac{P}{T + 273}} \quad (1)$$

where \dot{Q} is steady state power in kW, ΔT is the change in temperature in °C, T is temperature in °C, R is flow meter reading in %, and P is barometer reading with in Hg. A flow meter reading of 85% at a pressure of 25 in Hg and a temperaturer of 80°F is considered to be equal to 6000 cfm. For a steady state power of 100 kW an outlet temperature of 142°F (61°C) and a ΔT of 62°F (34°C) is found. Recall that the majority of coolant channels removing heat reside within the active core.

For a heat balance across a single flow channel instead of across the core, the following can be used:

$$\dot{Q} = \dot{m}C_p\Delta T \quad (2)$$

where \dot{m} is mass flow rate and C_p is specific heat. It is assumed that power is 556 W per assembly, inlet temperature is 80°F (27°C), C_p is 1015 J/kg-K and \dot{m} per channel is 0.008 kg/s. This gives an outlet temperature of 203°F (95°C) and a ΔT of 154°F (68°C). This assumes the core's thermal capacity has been met. There is enough thermal capacity in the fuel assembly reflectors and the permanent reflector to allow steady state operation for over 9 hours without exceeding any temperature limits. It is not required for transient cooling, but aides in operational efficiency and extends the life of the fuel assemblies by reducing oxidization at high temperature. It takes 5-7 hours to cool the core to 200°F (93°C) following a transient with air flow.

Core alignment (and gap between assemblies) is maintained by spring loaded clamping bars around the core periphery, the handling fixture of each assembly, and the grid plate that supports the core. The handling fixture measures 4 in square (slightly larger than the 3.96 in square element) with 0.625 in chamfers. Each hole in the grid plate where the support pins insert is 4 in center to center. See Figure 6 and Figure 7.

The 0.040 in gap between assemblies is nominal and is only maintained in the reflector areas of the assemblies. The Zr-3 cans are evacuated during the fabrication process to less than 0.001 in resulting in can deflection from the differential pressure between the evacuated inside and atmospheric air on the outside (local atmospheric air pressure of 12.5 psi). The deflection causes gap closure over portions of the can thus keeping the fuel centered.

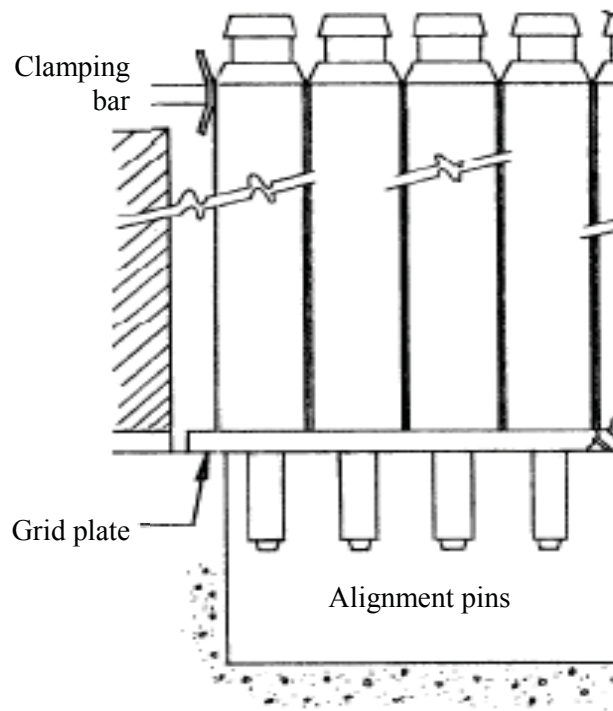


Figure 6: Core alignment is by clamping bars at the top and a grid plate at the bottom.

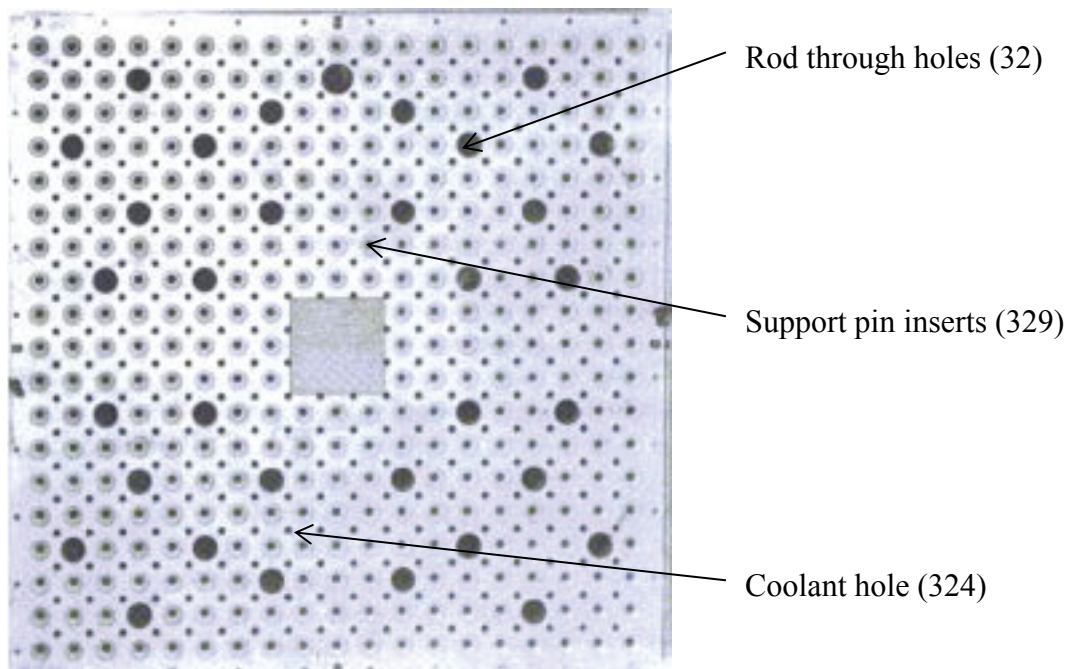


Figure 7: Grid plate for bottom alignment and core support.

Consequently, air enters the core through the 0.625 in square passages at the top of the assembly, expands slightly to fill 0.040 in gaps between assemblies, expands at the Zr-3 can due to cladding deflection, contracts back at the lower reflector, and exits through 7/8 in orifices in the grid plate. The orifices in the grid plate force 500 of the 6000 cfm of air flow around the permanent reflector as mentioned earlier.

Previous Work

Many of the reports on the TREAT's behavior involve reactor kinetics models. These models are concerned with how the nuclear behavior of the core is affected by reactor temperature, fuel loading in the core, and hold-down (control rods, shutdown rods, etc.). Reactor temperature affects the capability of the graphite to moderate neutrons, the fuel loading determines the potential energy of the core, and the hold-down is how the core's energy is held down or controlled.

Moderation is the process of slowing down (decreasing the kinetic energy) neutrons through a scattering process. Slow (low energy) neutrons are more likely to be absorbed by uranium-235 (^{235}U) and lead to fission. The TREAT reactor is an under-moderated^{vi} reactor. Similar to what exists in commercial nuclear plants under-moderated reactors have a negative temperature feedback mechanism. This inherently safe mechanism causes neutrons to leak from the reactor when higher moderator temperatures exist. When the moderator's temperature increases its density decreases. The decrease in moderator density results in fewer neutron scattering events since the number of atoms per unit volume decreases. This same thing occurs in the fuel. The coupled effect of the

^{vi} The Chernobyl Reactor was over-moderated, one of the contributing factors that led to the Chernobyl disaster in the mid 1980's. Too much moderator (over-moderated) stops neutrons (shields) from reaching adjacent fuel. If moderator is removed (by increasing temperature) the core increases in power.

decrease in fuel atoms per unit volume and slowing power of the moderator leads to neutrons leaking from the core and shutting the reactor down.

The isothermal negative temperature feedback coefficient for the TREAT was measured at $-1.8 \times 10^{-4} \Delta k/k/^\circ\text{C}$. The unit $\Delta k/k$ is a measure of reactivity (see Equation 3). In order to sustain a reaction (keep the core at steady power) k must be equal to unity. A k value greater than unity increases reactor power and less than unity is lowering reactor power or shutting the reactor down.

$$\rho = \frac{\Delta k}{k} \quad (3)$$

where ρ = reactivity, $\Delta k = k - 1$ (the change in k from $k = 1$), and k = neutron multiplication factor = the ratio of neutrons produced in the current generation to the neutrons produced in the previous generation. A reactor is safely shutdown once $\rho \cong 0.96$ so in the TREAT, once the temperature undergoes a change of 448°F (220°C), the reaction is nearly halted (assuming an initial reactivity of 1). Adding reactivity allows a greater temperature change. Reactivity can be increased by adding fuel (potential energy) or by removing hold-down.

In TREAT the transient mode is initiated by rapidly ejecting hold-down (transient rod) from the reactor. This adds initial reactivity allowing the core to undergo a power surge. The temperature feedback mechanism or control rod then adds negative reactivity and shuts the reactor down. As seen in Figure 8 and Figure 9 increasing initial reactivity causes larger power surges, which result in larger reactor temperatures.

Both temperature feedback (heat transfer from fuel to moderator) and control rod motion (computer to rod release to rod motion) take time. Time delay will allow the reactor to have slightly longer surge times; thus increasing temperature further. Reference

6 states the time delay for heat transfer from uranium oxide (UO_2) particles to graphite is 0.9 ms and the time delay for reactor SCRAM^{vii} (shutdown) to be 80 ms. The latter is designed to “clip” the transient short by removing neutrons faster than temperature feedback will alone.

Due to the impact of temperature on reactor behavior, the heat transfer effects need to be understood. Two reports on the TREAT involved heat transfer calculations on a fuel cell model and experiments^[12] on a single fuel assembly mock up. The report on the calculations is discussed first. The fuel cell model is shown in Figure 10.

The calculations were performed both by hand and programmed into an IBM-704 computer. The calculations were primarily concerned with:

- The rapidity of heat transfer from the UO_2 particles to the graphite moderator.
- The gross heat absorbing capability of the graphite.
- The rate of heat transfer across the heat barrier (spacer and end cap) between the fuel blocks and the reflector blocks.

The work was done in the early 1960’s and relies on the data given in Table 1. The rapidity of heat transfer from the UO_2 particles to the graphite moderator was determined by an equation developed by Hetrick^[13]. The result of Hetrick’s work is shown in Figure 11. The probable time lag for heat transfer between fuel and moderator was calculated to be 0.9 ms, a value considered negligible for heat transfer purposes.

In order to find the rate of heat transfer across the barrier a numerical method developed by Dusenberre was used. It involves writing heat balances for a predetermined

^{vii} SCRAM is a term that came from the mechanism used to shut down the first reactor (CP-1). It stands for Safety Control Rod Ax Man indicating that the safety control rod insertion on the first reactor was driven in by gravity. Insertion began by an individual (the ax man) cutting a rope that held the safety control rod suspended above the core. It was truly a primitive time for nuclear reactor technology.

amount of fuel and reflector segments, in this case 24. A series of equations of the following form are used:

$$T_n(t + \Delta t) = \alpha_n T_n(t) + \beta_n T_{n+1}(t) + \gamma_n T_{n-1}(t) + \delta_n [T_{c_{n-1}}(t) + T_{c_n}(t)] \quad (4)$$

where T_n is the average temperature of segment n at time t , T_{c_n} is the average temperature of the coolant in the channel adjacent to segment n at time t , and $\alpha_n, \beta_n, \gamma_n$, and δ_n are constants for segment n . The average temperature of the coolant is found from an equation of the form:

$$T_{c_n(t)} = A_n T_n(t) + (1 - A_n) T_{c_{n-1}}(t) \quad (5)$$

where A_n is a constant for segment n . The constants are functions of heat capacities and thermal resistances of fuel and coolant and were calculated by hand. The constants are not given in reference 6 so their values and how they were calculated is unknown. A radial power distribution of 1.36 (maximum to average) and an axial ratio of 1.19 were used to determine the peak-integrated power. A chopped cosine was assumed to calculate the initial axial profile. The reference core is 225 elements as mentioned in Table 1 and the volume of fuel (graphite fuel blocks) per assembly is 0.390 ft³. It was assumed that radial heat conduction between elements and heat generation in the reflector was negligible.

For radial resistance it was assumed that the gap between fuel and the Zr-3 can was filled with air at 1 atm. The total radial resistance is then the sum of the following resistances:

- Resistance between points of T_n to fuel surface
- Resistance across air gap
- Resistance across Zr-3 can

- Resistance from air film on Zr-3 can surface

The lump radial resistance is written as

$$R = \frac{\Delta T}{q} \quad (6)$$

where R is the thermal resistance per foot of coolant channel, q is the heat transfer rate, and ΔT is the temperature difference between coolant and fuel. The heat transfer coefficient was found with the following relationship for Nusselt Number developed by Evans and Sarjant^[14]:

$$Nu = h \frac{D_h}{k} = 0.020 Re_D^{0.8} \quad (7)$$

where Nu is the Nusselt Number, h is the heat transfer coefficient, D_h is the hydraulic diameter of the cell, k is the thermal conductivity of air, and Re is the Reynolds Number. Evans and Sarjant is a suitable substitute for the Dittus Boelter correlation ($Nu = 0.023 Re_D^{0.8} Pr^{0.4}$) when considering air as the fluid. Reynolds number can be calculated using the following.

$$Re_D = \frac{\rho V D_h}{\mu} \quad (8)$$

where ρ is fluid density, V is fluid velocity, and μ is the fluid's dynamic viscosity.

The axial resistance between fuel and reflector was assumed to be 1/4 in asbestos (this instead of the 1/4 in Zr-3 spacer). Asbestos was found to be comparable to the Zr-3 spacer in the experiment discussed next; however the medium in which asbestos exists in the thermal barrier is not mentioned. The calculated thermal resistance from fuel to coolant and from fuel to reflector is $0.50 \text{ } ^\circ\text{F hr ft Btu}^{-1}$ and $1.20 \text{ } ^\circ\text{F hr ft Btu}^{-1}$.

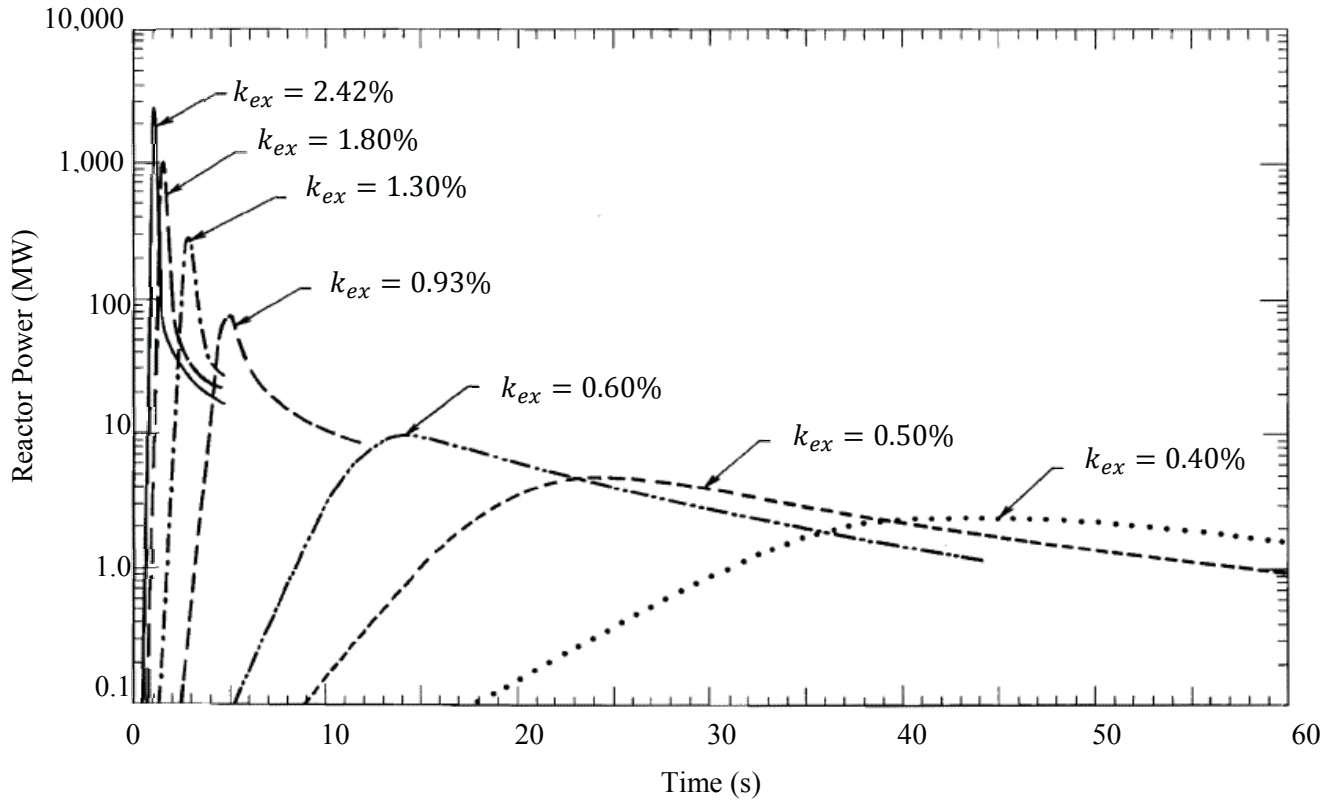


Figure 8: Reactor power vs. time for several experimental transients.^[15]

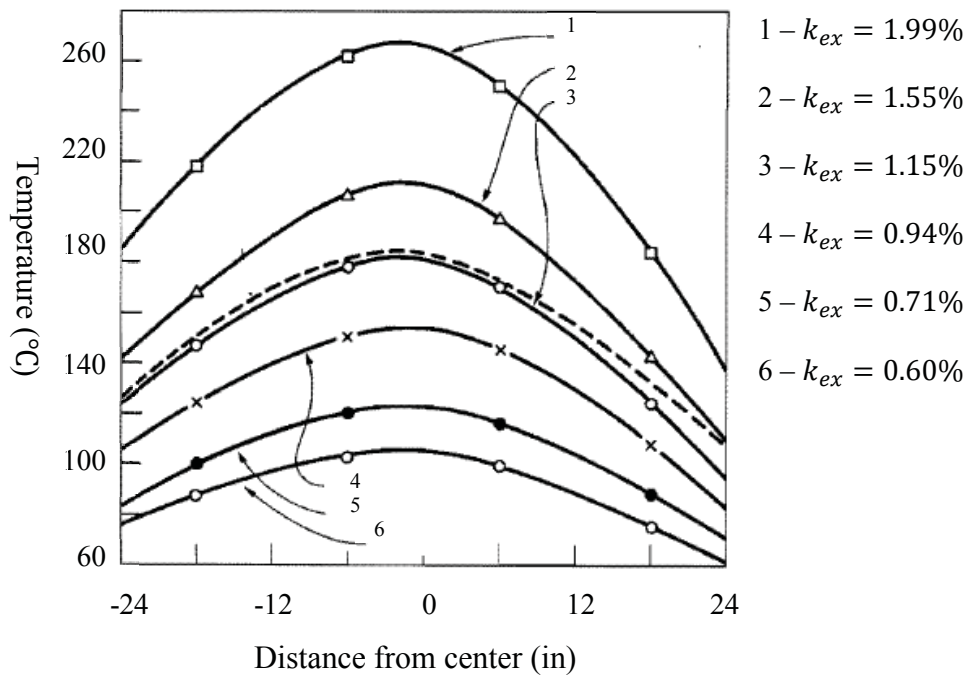


Figure 9: Axial temperature curves for several transients.^[16]

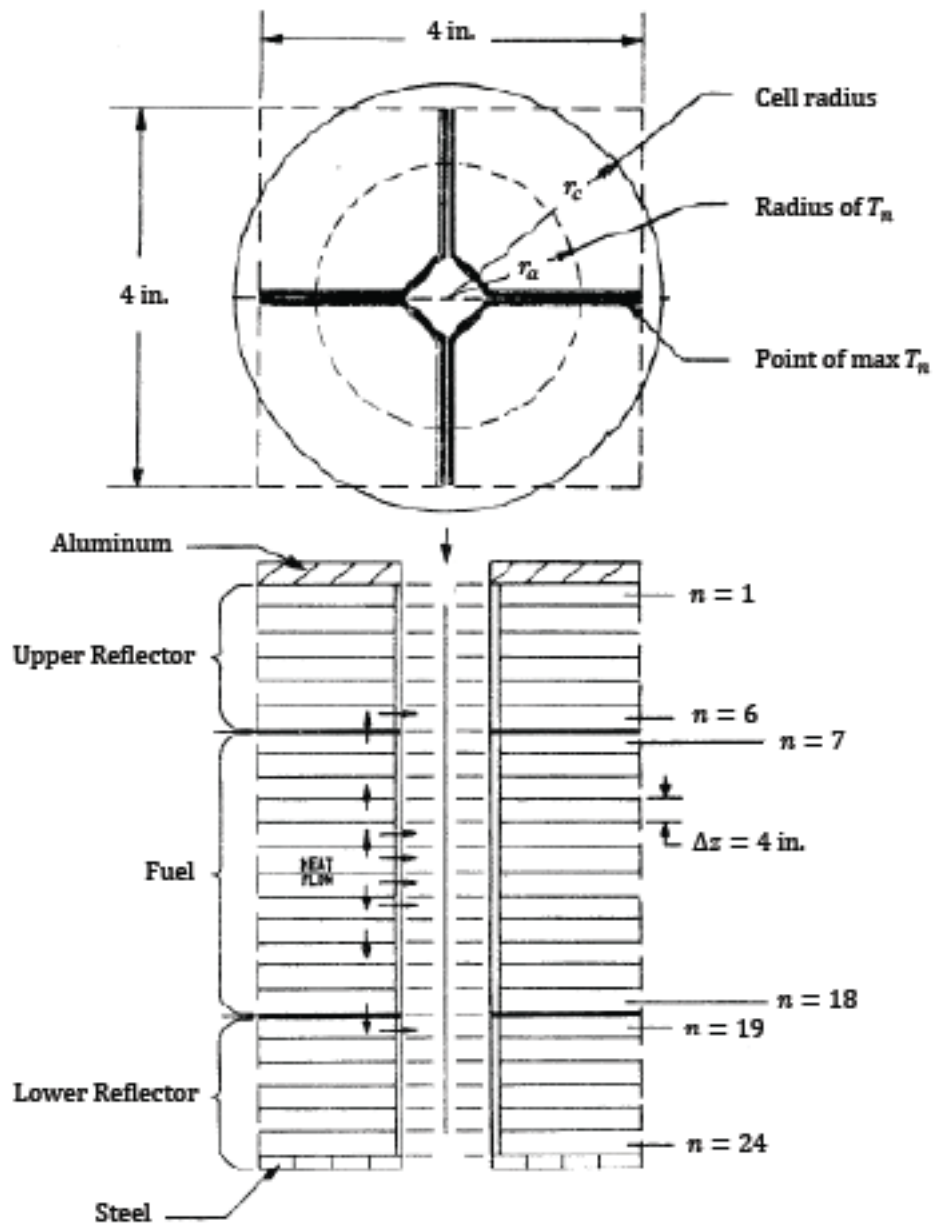


Figure 10: Model of fuel cell used in calculations.

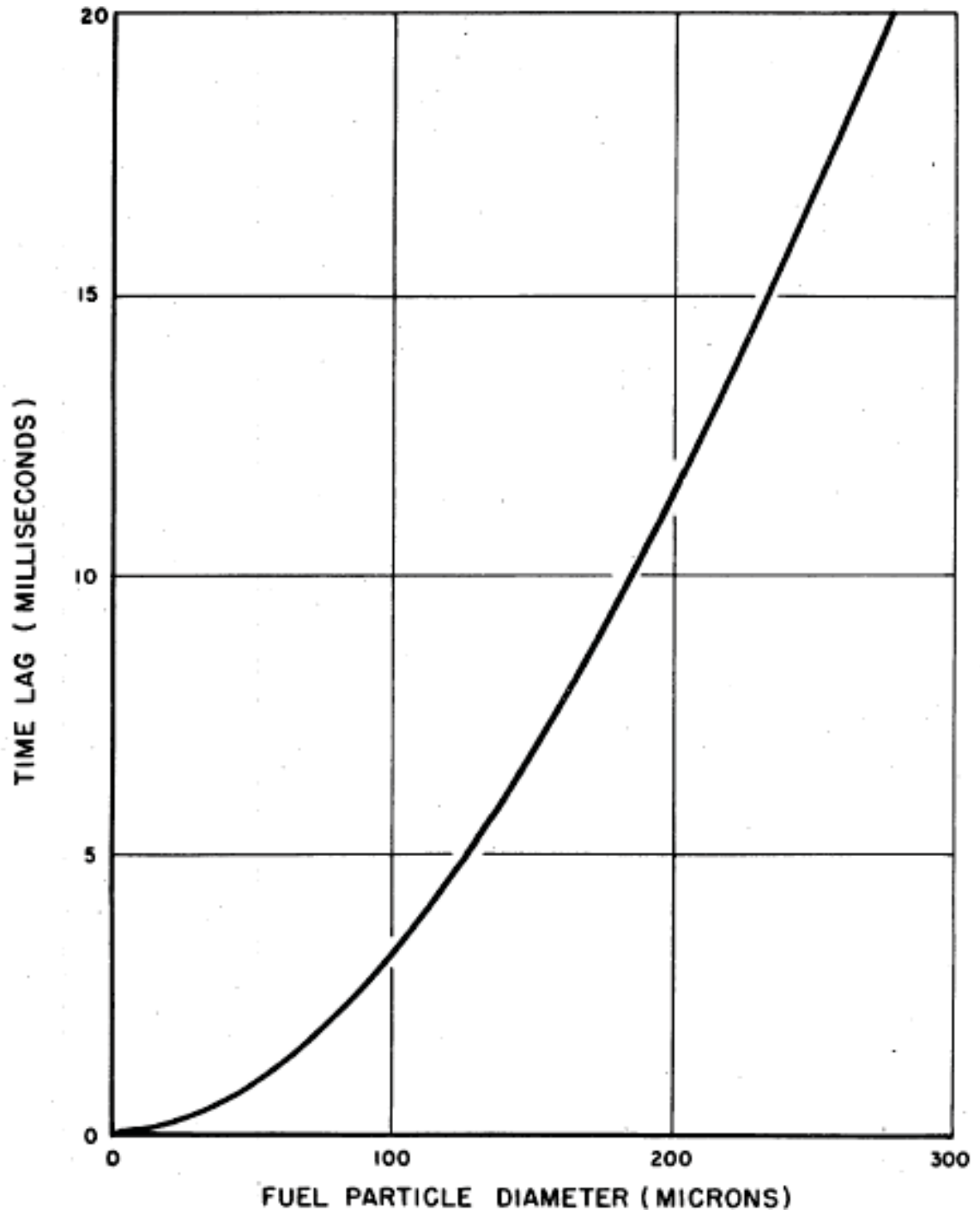


Figure 11: Time lag in heat transfer for various fuel particle sizes during initial stage and runaway. (Pile is on an 80 ms period).

Figure 12 shows the results of these calculations compared against two fuel assemblies undergoing a 445 MW-s (163 assemblies) transient conducted in the TREAT. The calculated peak temperature was 775°F (413°C) for the 1000 MWs (225 assemblies) transient. The peak temperature for the 445 MW-s transient was 506°F (263°C). The asymmetric shape of the measured profiles is typical of all transients and agrees with flux traverse data^{viii}. A maximum to average power ratio of 1.67 was calculated from temperature profiles taken from several other transients with core loadings of 160 assemblies. This ratio also compares favorably with flux traverse data.

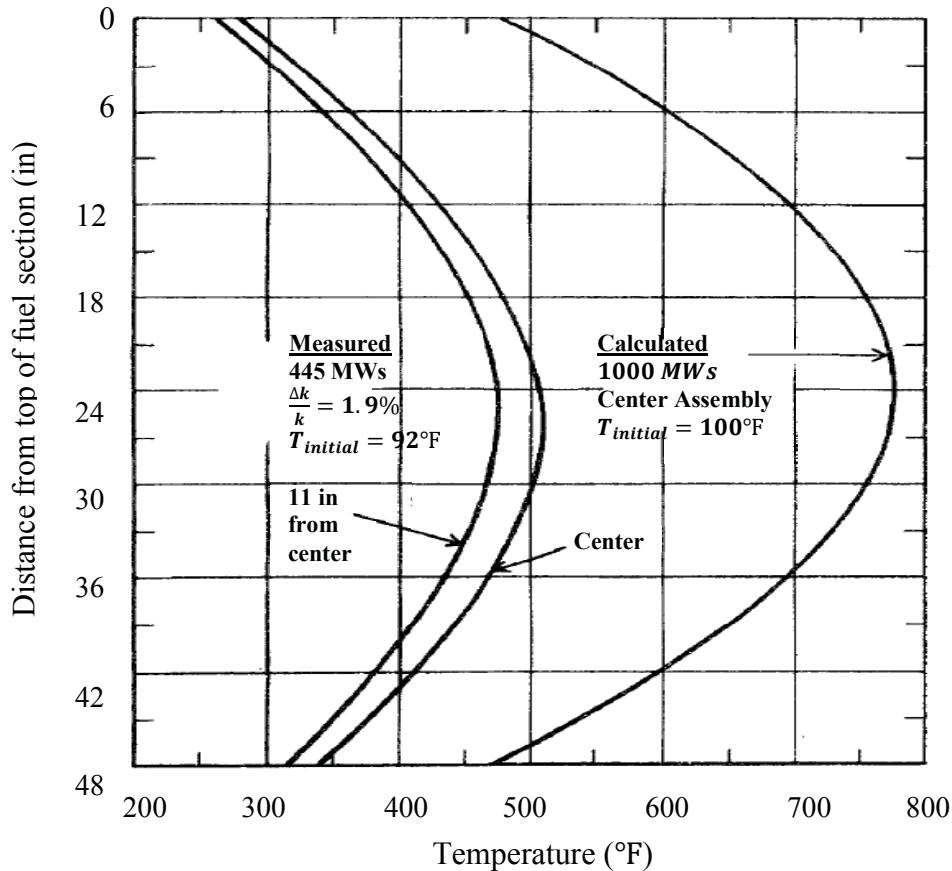


Figure 12: Measured and calculated axial temperature profiles.

^{viii} Flux traverse data is measured neutron flux across the fuel volume and is obtained by irradiating a metal foil (usually made from Au-198) and then counting the decay using a radiation detector.

For axial resistance a 2500 MW-s (worst case) transient with and without air flow is assumed. The calculated peak temperature is 1450°F (488°C). In both cases the reflector temperature was less than 400°F (204°C) during post-transient cooling (see Figure 13 compared against Figure 14). The calculated exit temperature was calculated to be 490°F hence the purpose of the bypass valve in the coolant system mentioned above.

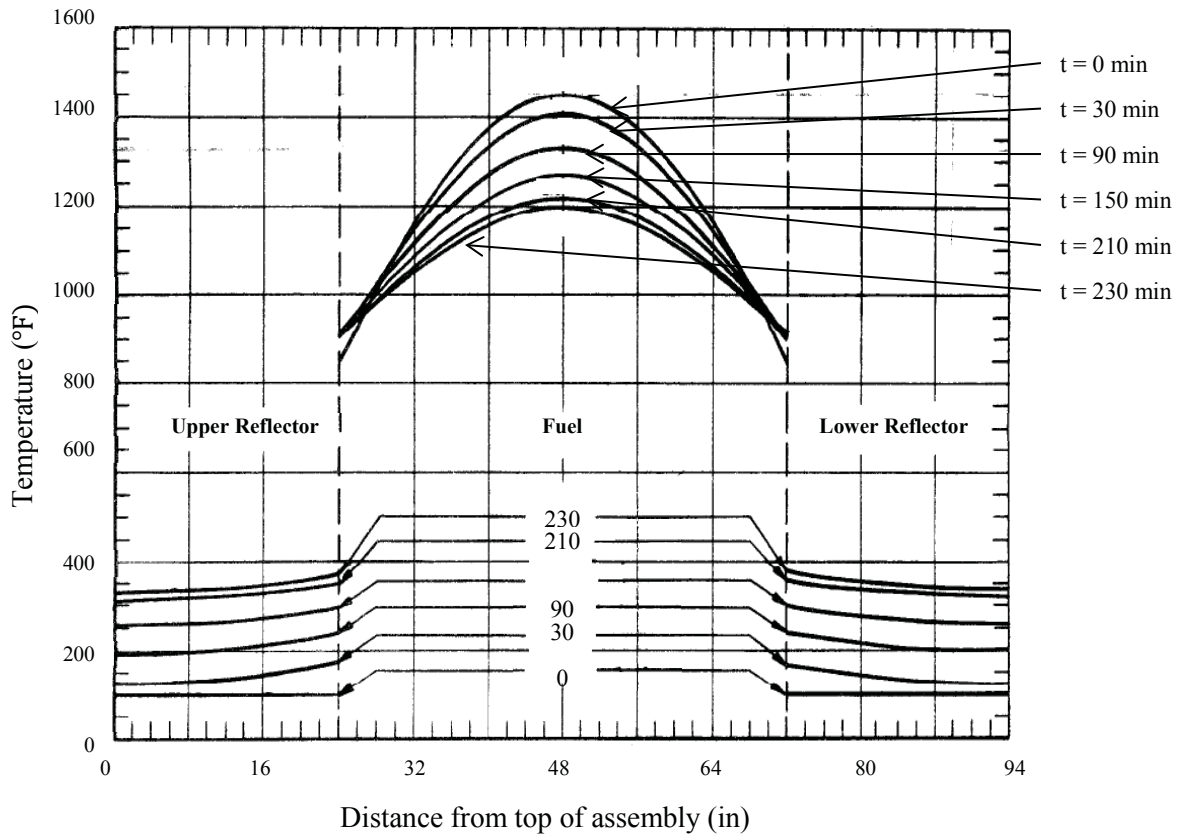


Figure 13: Calculated axial temperature profiles in center fuel assembly following a 2500 MWs transient without coolant flow.

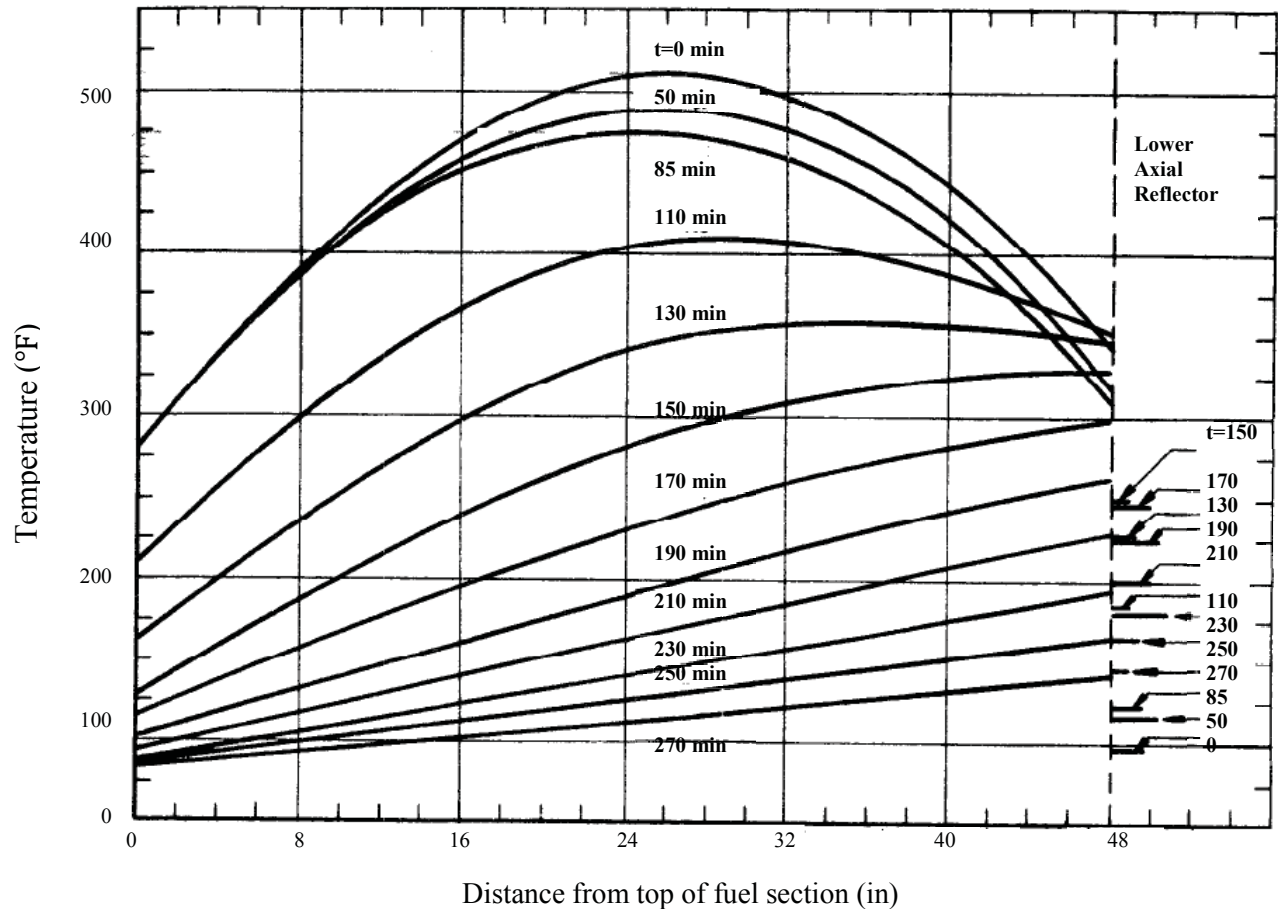


Figure 14: Measured axial temperature curves following a 800 MW-s transient. Air flow is turned on at 87 minutes at 70% flow.

Steady state calculations were performed assuming a power level of 100 kW and a flowrate of 6500 cfm. This flowrate value is slightly unrealistic since the capacity of the coolant fans is 6000 cfm. There are 180 fuel assemblies producing heat and 210 channels removing heat for this scenario. Figure 15 shows the axial temperature profile of the graphite uranium fuel, Zr-3 can, and coolant from the calculations. As fuel loading is increased (number of coolant channels increased) the curves in Figure 15 shift to the left and to the right for fuel loading decrease.

The experiment (mockup of a fuel assembly) that compliments these calculations is shown in Figure 16. The mockup was intended to model an 800 MW-s transient with

25 lbm/hr per channel coolant flow. The fuel material is identical to that used in standard fuel assemblies except it uses natural uranium ($0.0072\%^{235}\text{U}$) instead of enriched uranium ($95\%^{235}\text{U}$). The fuel blocks were drilled through to accept a heater rod with a 36 in heated length. The reflector sections were also similar except a flat plate was used instead of a handling fixture and support pin and the reflector was screwed to the Zr-3 tabs instead of riveted. Thermal couples were placed throughout the assembly at various locations both axially and radially (see Figure 17 and Figure 18).

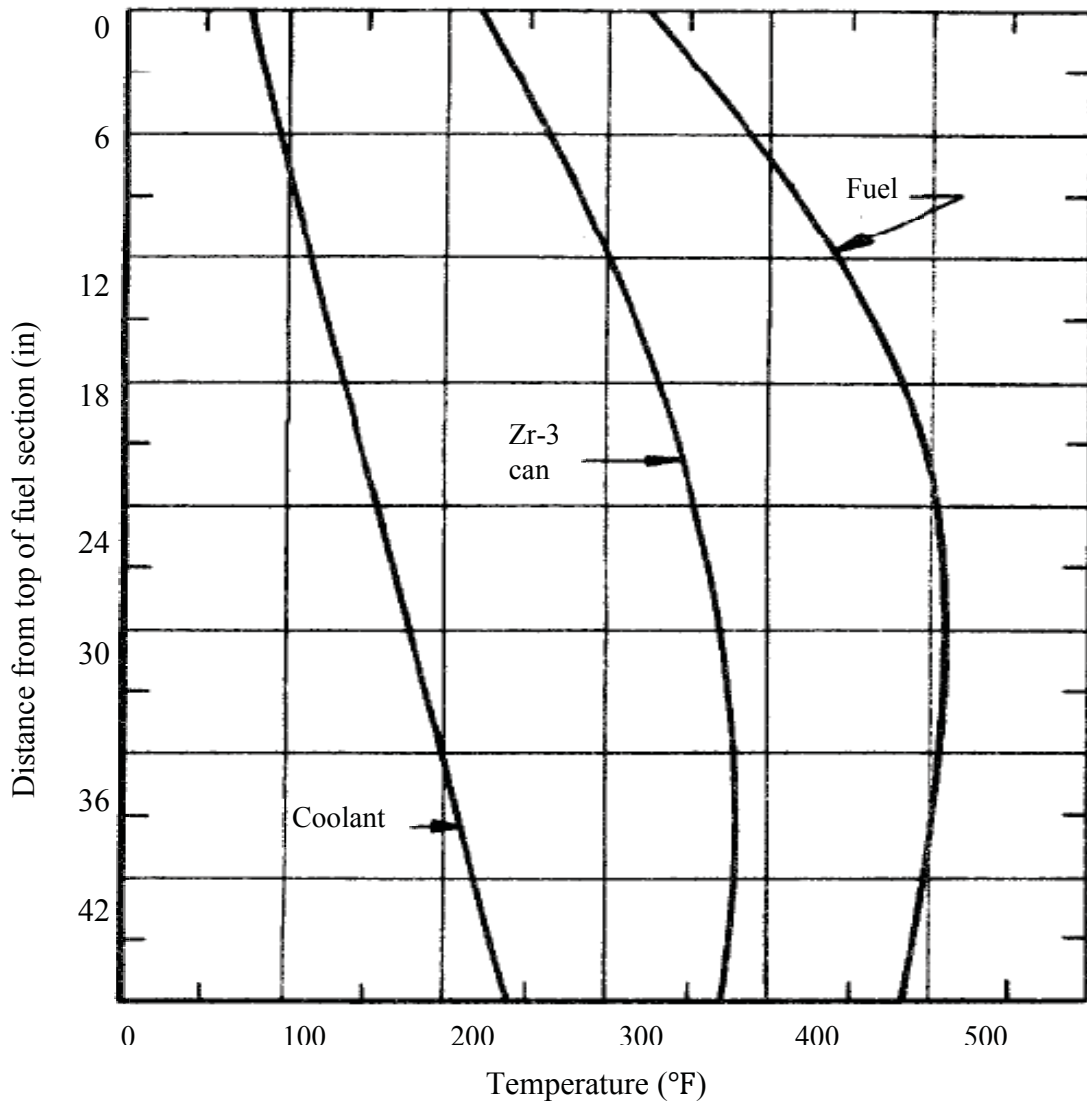


Figure 15: Calculated axial temperature profiles in coolant channel at 100 kW.

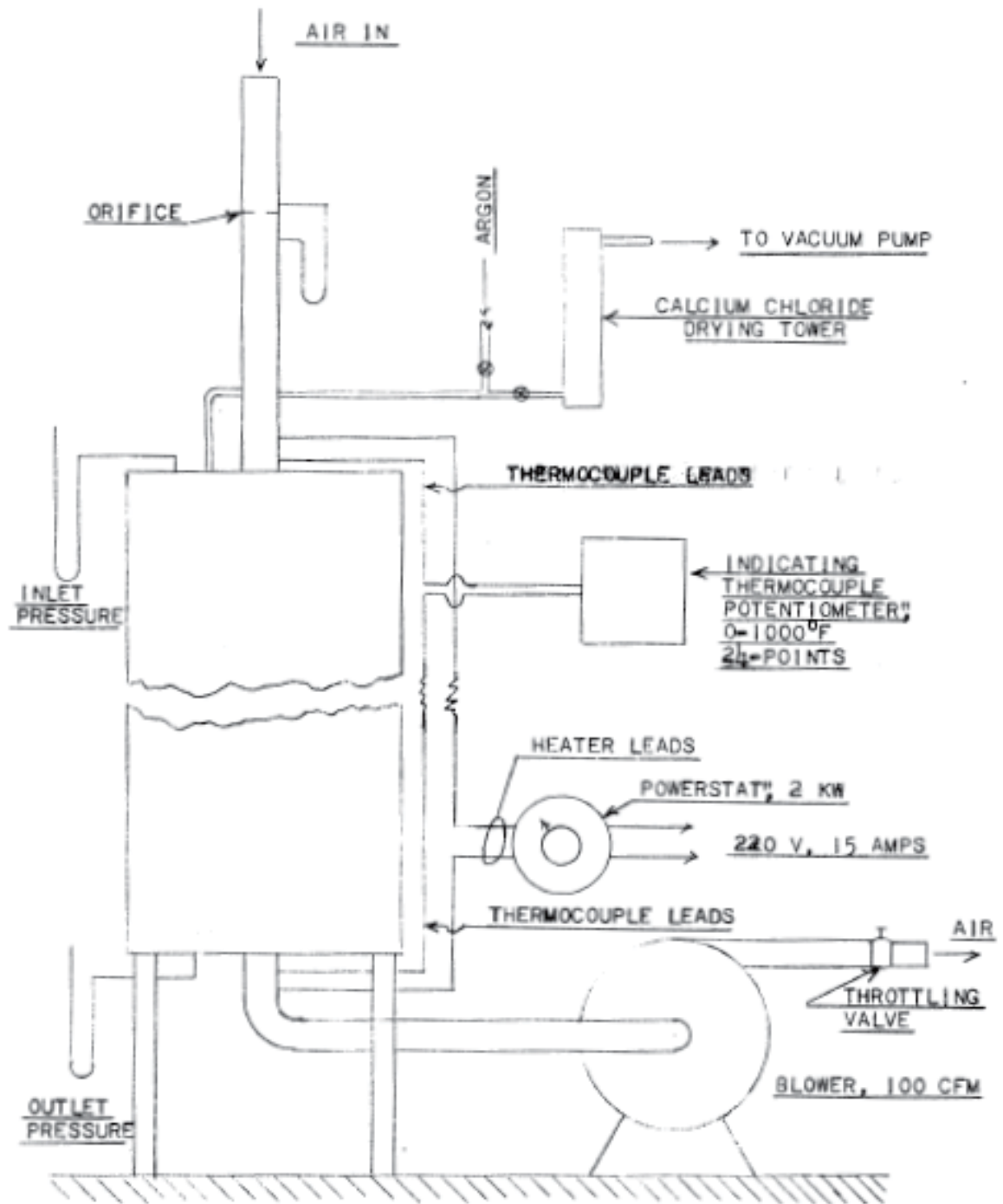


Figure 16: Apparatus used in experimental model.

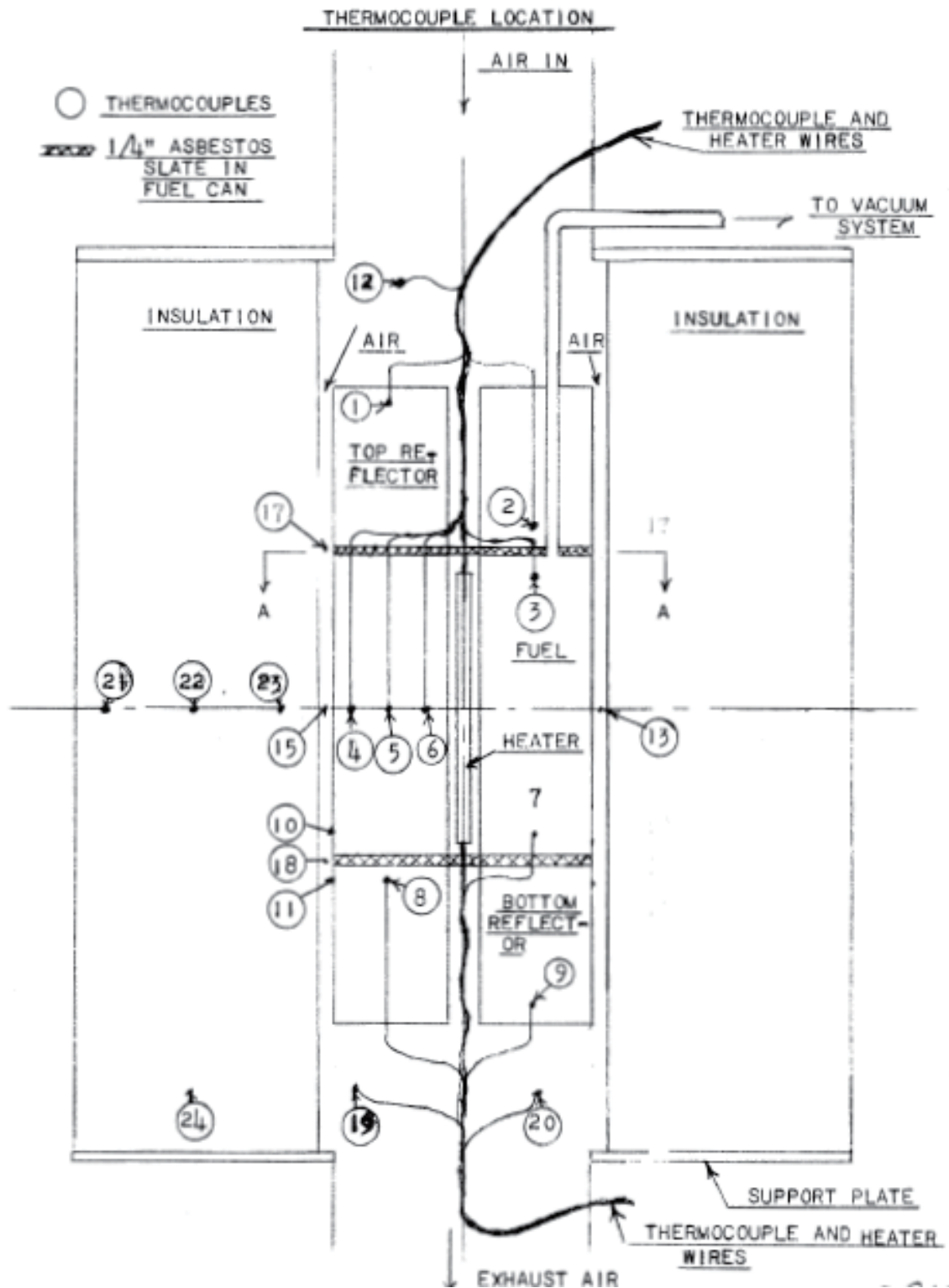


Figure 17: Axial thermocouple placement in apparatus.

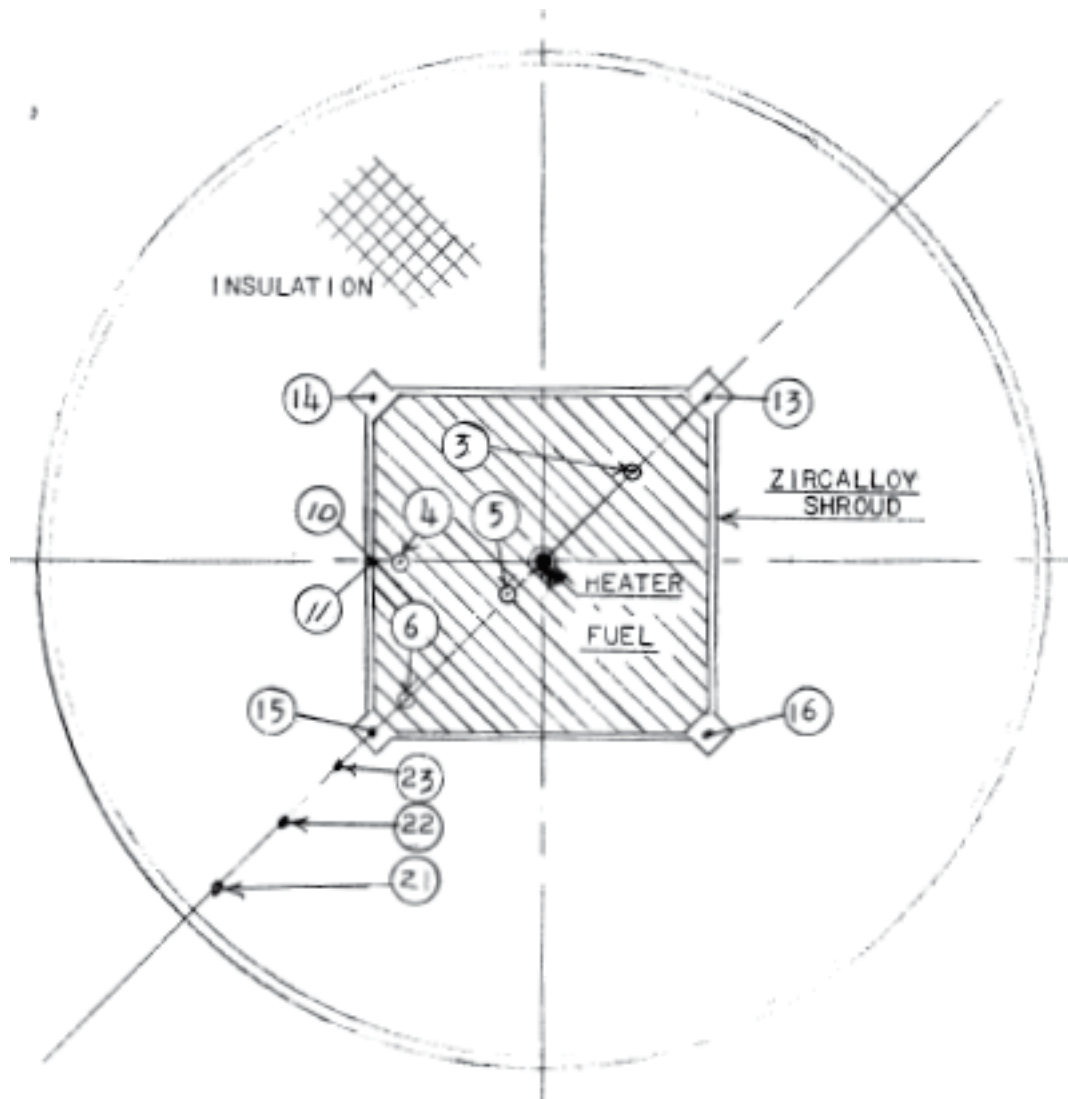


Figure 18: Radial thermocouple placement in apparatus.

The mockup was placed in an aluminum shroud with dimensions similar to those found surrounding a single fuel element in the reactor. Air was drawn through the four channels using a centrifugal blower. Flowrate was adjusted using a shudder at the fan exhaust and measured using an orifice plate at the fuel assembly air intake. Water manometers were used to measure the pressure drop across the orifice plate and across the assembly. A mercury manometer was used to measure vacuum at the air intake. A circular steel cylinder surrounded the shroud and the space in between was filled with

vermiculite thermal insulation. Thermocouples were placed in the coolant channels and the vermiculite insulation.

A total of fourteen runs were made at different power levels, flow conditions, and with different media placed between the fuel and reflector sections. Runs 1 through 8 used transite insulation, runs 10 through 13 had asbestos insulation, and run 14 had a zircaloy spacer. During run 15 the heater failed and was never completed.

The runs involved heating up the fuel assembly until a steady state condition was achieved and then turning off the heater and taking readings at 5-minute intervals for about an hour (see Figure 19 and Figure 20). In five of the runs the coolant flow was maintained. Data received from the runs included room temperature, fan inlet pressure, pressure drop across the orifice, fuel element pressure drop, heater and current voltage, and the temperatures of the thirty thermocouples placed throughout. This data was then compared against the calculations as described above.

One key difference between this experimental model and the model used in the calculation is the number of coolant channels. The experimental model has four channels surrounding a single assembly and the model used in calculations has one channel in the middle of four-quarter fuel assembly sections. In order to make flowrates the same the flowrate in the single channel model was multiplied by four.

Radial temperature distributions indicated that a large portion of the heat is transferred to the flat side of the fuel assembly rather than the chamfer (coolant channel). However this model is surrounded by insulation rather than other hot fuel elements as would be seen in the reactor. The heat rate to the sides is still larger than it should be indicating that a large portion of this heat moves to the coolant channel. This indicates the

possibility that the aluminum shroud is acting like a fin since the thermal conductivity of aluminum is significantly higher (and twice as thick) than the Zr-3 cladding.

In all cases but for the 800 MW-s transient burst the outlet coolant temperature was less than the reflector temperature. Refer to Figure 21. The cooling rate of the fuel assembly without flow in the experimental model is much higher than the fuel cell model. At the bottom plate of the fuel assembly the temperatures calculated in the fuel cell model and measured in the experimental model were nearly identical; however, at the top the experimental model temperature was considerably higher even with identical axial resistances at the top and bottom. This is likely due to the fact that in the experimental model hot air rises past the upper section (natural convection). This form of natural convection is not indicative of the TREAT core. Natural convection is from pressure differences between reactor inlet and stack outlet rather than from density gradients in the air.

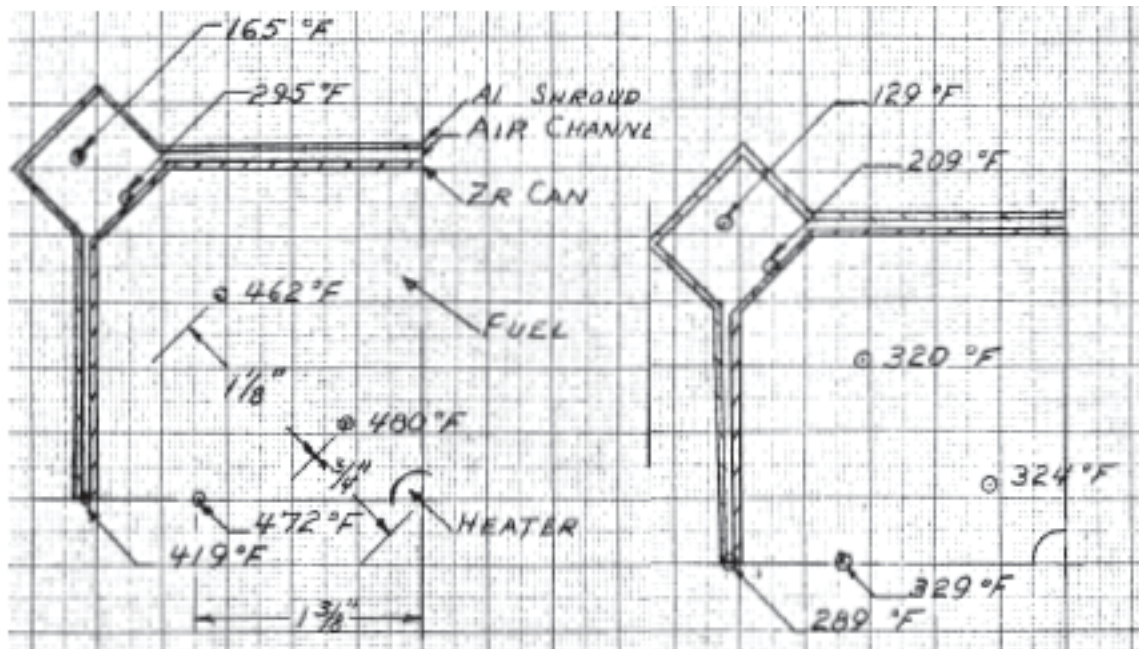


Figure 19: Axial midplane temperature distribution. Left - Steady state power of 1000 W and flow of 108 lb/hr. Right - 30 minutes after heat is turned off.

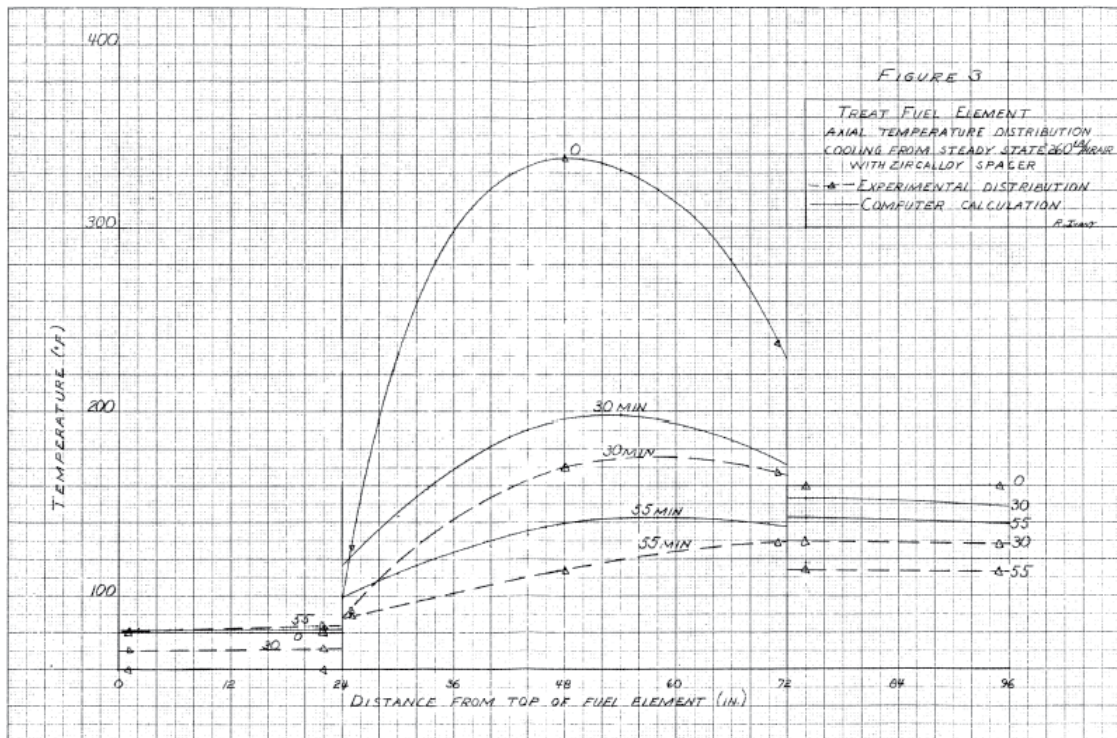


Figure 20: Axial temperature distribution for cooling from steady state power at a flowrate of 260 lbm/hr (zircaloy spacer being used).

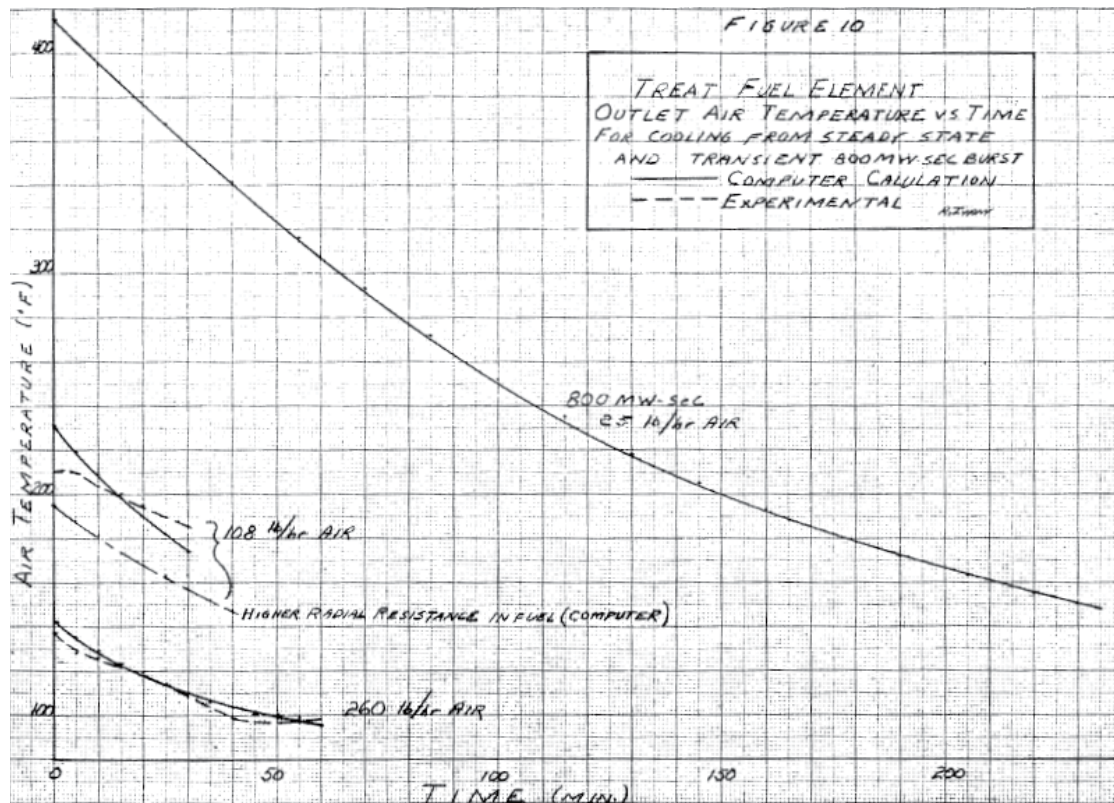


Figure 21: Outlet air temperatures for steady state and transient power.

CHAPTER 3: METHODOLOGY

Software Description

The intention of this section is to describe BISON^{[17],[18]} and other software used in model development. BISON is a modern finite element based nuclear fuel performance code that has been under development at INL since 2009. BISON is implicit (allows for large time steps), runs in parallel (allows for use of multiple processors when available), and is fully coupled (solves all unknowns simultaneously). The code is suitable to steady state and transient behavior for 1D spherical, 2D axisymmetric, and 3D geometries. BISON has been used for many fuel types including light water reactor fuel rods, tristructural isotropic (TRISO) fuel particles, and metallic fuel rods and plate geometries.

From the beginning of development BISON has implemented numerous regression tests in its models to compare against analytical and known solutions. In addition an assessment^[19] against instrumented light water reactor rods and TRISO particle benchmark cases has been completed to further the confidence in BISON's ability.

BISON models a variety of nuclear fuel behavior including fuel burnup, swelling from irradiation, irradiation induced creep, etc. The full range of nuclear behavior that BISON can model is not incorporated into the TREAT fuel assembly models. The equations from BISON that are employed in the TREAT models are applicable to heat transfer (i.e. conduction, convection, radiation) and to a lesser extent, deflection (mechanical contact between fuel and cladding).

Certainly other heat transfer codes exist; however thermally modeling of the TREAT is not the end result. The INL intends to augment these models with other behavior such as more extensive thermomechanics and neutronics^{ix} (i.e. implementing reactivity effects from hold-down and fuel loading).

The following equations implemented in BISON will demonstrate the path of heat generation in the fuel to convection by the air. Equation 9 shows the heat conduction equation.

$$\rho C_p \frac{\partial T}{\partial t} + \nabla \cdot \mathbf{q} - e_f \dot{F} = 0 \quad (9)$$

where ρ , C_p , and T are the density, specific heat, and temperature; \mathbf{q} is the heat flux described by Fourier's Law of Conduction (Equation 10), and e_f and \dot{F} are the energy released per fission and volumetric fission rate. The energy released per fission is taken as 3.2×10^{-11} J/fission.

$$\mathbf{q} = -k \nabla T \quad (10)$$

Equation 11 shows how heat is transferred across the gaps between fuel and can and fuel and reflector.

$$h_{gap} = h_g + h_s + h_r \quad (11)$$

where h_{gap} is the total conductance across the gap, h_g is the gas conductance, h_s is the increased conductance due to solid-solid contact, and h_r is the conductance due to radiant heat transfer described by Equation 12.

$$h_g = \frac{k_g(T_g)}{d_g + C_r(r_1 + r_2) + g_1 + g_2} \quad (12)$$

^{ix} Neutronics are how neutrons transport and interact within the core.

where k_g is the conductivity of the gas in the gap, d_g is the gap width, C_r is a roughness coefficient with r_1 and r_2 being the roughness of the two surfaces, and g_1 and g_2 are the jump distances at the two surfaces.

Equation 13 (Newton's Law of Cooling) describes how the air convects heat away from the cladding.

$$\mathbf{q} = h(T_s - T_\infty) \quad (13)$$

where h is the convection coefficient for air found using Equation 7, T_s is the surface temperature, and T_∞ is the free stream temperature.

BISON requires two files to run. One is a mesh file with a .e extension. The software used to generate mesh files for the TREAT models was CUBIT. The other file is an input file that can be generated in any general text editor capable of producing a .i file extension. Once BISON runs the results can be viewed in ParaView for post-processing.

CUBIT^[20] is a full-featured software toolkit for robust generation of 2D and 3D finite element meshes and geometry preparation developed by Sandia National Laboratories. CUBIT can be run as a GUI or by command line (preferable). The CUBIT version used was 14.0. The text editor used to generate input files was Text Wrangler. Text Wrangler is a generic open source text editor that can be downloaded from the Internet. The Text Wrangler version used was 4.5.5. ParaView^[21] is an open-source, multi-platform data analysis and visualization package. ParaView can run on supercomputers to analyze datasets of exascale size or on laptops for smaller data. The version of Paraview that was used is 3.14.1.

Assumptions

Some assumptions are necessary to fill in information that could not be obtained and to simplify the model. A list of assumptions is given below:

- Model does not have kinetics/neutronics (not observing neutron behavior).
- Fuel assembly is radially symmetric.
- Inlet conditions are assumed known.
- Initial temperature profile of core is uniform and equal to the ambient temperature.
- Model does not contain pressure changes in the coolant.
- Model does not have fuel burnup and fission product generation.
- Model does not have irradiation effects (gamma heating, creep, fuel and cladding swelling, evolving properties, etc.).
- No oxidation layers on cladding.
- No air in Zr-3 can so that only radiative heat transfer exists from fuel to Zr-3 can.
- Air in Al-6063 cans is at local atmospheric pressure (12.5 psi).
- Model excludes rivets, welds, tabs, vacuum tube, handling fixture, and support pin.
- No time lag for heat transfer between UO_2 particles and graphite moderator.
- The fueled portion of the element is a single block
 - Neglects contact resistance between fuel blocks.
- The reflector portion of the element contains merged blocks.
 - Neglects contact resistance between reflector blocks.
- Cladding is merged at Zr-3 and Al-6063 can interface.

- Neglects contact resistance between Al-6063 and Zr-3 cans.
- Constant uniform heat generation for steady state.
 - Assumes reactor power is 100 kW.
- Transients last one second and discharges 1000 MW.
- Zr-3 spacer is a gas gap with the thermal conductivity of asbestos.
- Steady state mode is with full coolant flow.
- Transient mode is without coolant flow.

Parametrics and Model Development

A benchmark model is built first and is closest to a fuel assembly in the TREAT. Throughout the parametrics the geometry is held constant and only property values have variance. New LEU fuel would have an identical or nearly identical geometry to the existing fuel but different material properties. Changing the material properties gives the indication of how they affect core temperature at some arbitrary point in time. The model doesn't observe a change in every property and doesn't allow multiple properties to change at the same time (except two cases). The variation magnitude is arbitrary and can be seen in Table 3. If larger property variations are desired this can be accomplished by simply modifying the input file. This gives INL a general idea of how material selection and associated properties affect thermal characteristics of new fuel and allows them to change the input file based on a specific material of interest.

The parameter of interest for steady state power is the steady state temperature, and the parameters of interest for transient surges are the temperature immediately following the transient and the temperature after seven hours of adiabatic cooling (all

heat is dissipated into the assembly). Waiting seven hours gives an indication of how much heat the axial reflectors will absorb with no flow.

Table 3: Parametrics

Input File*	Property	Variation
Run0.i/RunT0.i	Benchmark	N/A
Run1.i/RunT1.i	Fuel C_p	20%
Run2.i/RunT2.i	Fuel C_p	-20%
Run3.i/RunT3.i	Fuel k	20%
Run4.i/RunT4.i	Fuel k	-20%
Run5.i/RunT5.i	Fuel ρ	20%
Run6.i/RunT6.i	Fuel ρ	-20%
Run7.i/RunT7.i	Fuel emissivity (ε)	0.05
Run8.i/RunT8.i	Fuel ε	0.96
Run9.i/RunT9.i	Zr-3 can C_p	20%
Run10.i/RunT10.i	Zr-3 can C_p	-20%
Run11.i/RunT11.i	Zr-3 can k	20%
Run12.i/RunT12.i	Zr-3 can k	-20%
Run13.i/RunT13.i	Zr-3 can ρ	20%
Run14.i/RunT14.i	Zr-3 can ρ	-20%
Run15.i/RunT15.i	Zr-3 can ε	1
Run16.i/RunT16.i	Zr-3 can ε	0.8
Run17.i/RunT17.i	Spacer k	20%
Run18.i/RunT18.i	Spacer k	-20%
Run19.i/RunT19.i	Al-6063 can to Zr-3 can	N/A
Run20.i/RunT20.i	Zr-3 can to Al-6063	N/A

*T attached to an input file indicates it is a transient case.

The geometry chosen for the model is an octant of the fuel assembly. Figure 22 shows an axial view of the fuel assembly before its divided into an octant and Figure 23 shows a cross-sectional view of the octant fuel assembly at the fueled region. The octant takes advantage of symmetry and decreases computer run-time. The Zr-3 cladding is built deflected in CUBIT (it is not a result of BISON solving an elastic problem). Building deflection into the cladding reduces computer run-time significantly since elastic modeling requires a fine mesh; however it also neglects contact resistance between the

cladding and the fuel where gap closure exists. The amount of gap closure along the fuel assembly was based off a 2D model that compared built deflection against the elastic model BISON solves. Figure 24 shows the comparison.

As mentioned earlier the mesh file is created in CUBIT. The mesh file defines the geometry of the model and the meshing interval over the geometry. Small intervals present more accuracy in the answer but also take increasing computational time to solve, especially in a 3D model. CUBIT also identifies the portions of the fuel assembly that will be designated for each material (e.g. fuel, reflector, and cladding) and designates geometrical faces of the fuel assembly for boundary condition inputs. The journal file used to create the mesh can be found in Appendix B: Mesh file.

The input file for the benchmark model can be found in Appendix C. It includes:

- Coordinate system (Cartesian x, y, z in this case).
- Mesh file with .e file extension (.e for Exodus).
- Material properties for each material (density, specific heat, thermal conductivity, etc.).
- Volumetric heat generation rate (volumetric fission rate).
- Initial and boundary conditions (temperature, convection coefficient, etc.).
- Run time length and time steps.
- Tolerance on the residual (the point where BISONs answer is close enough to the actual answer).
- Values to observe in post-processing (fuel temperature, cladding temperature, rod power, etc.)

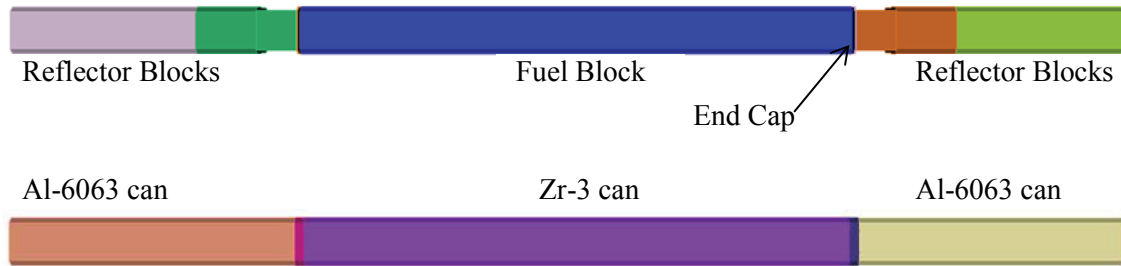


Figure 22: Axial view of TREAT fuel assembly showing components.

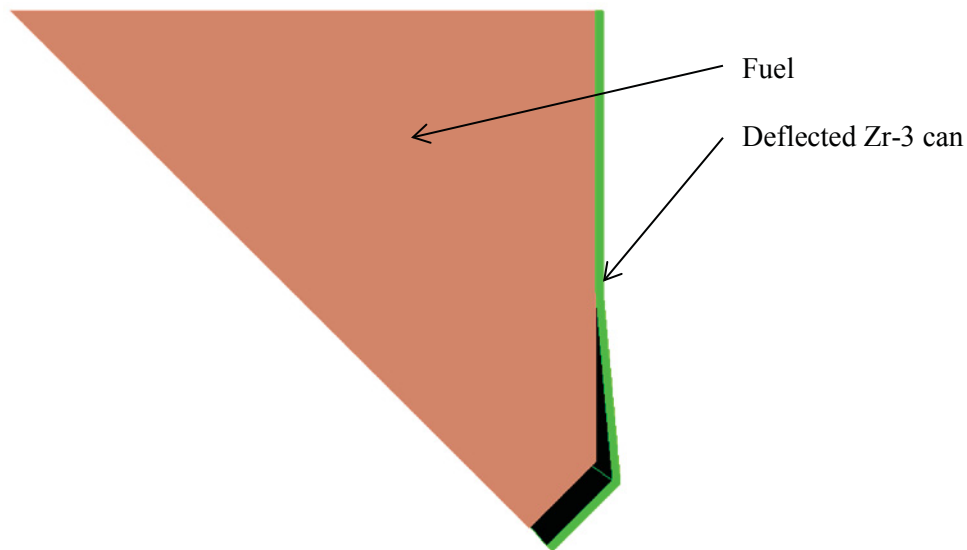


Figure 23: Cross-sectional view of the octant and the fueled region.



Figure 24: Built-in deflection compared against the elastic model BISON solves. The model on the left does not have pressure applied to cladding.

The coordinate system in BISON is taken from what is referenced in CUBIT. The z-axis is the axial length with $z = 0$ being the bottom of the fuel element. Material properties are taken from the literature as seen in Table 1. The reflector is assumed to

have the same properties as the fuel. Volumetric heat generation rate was calculated using the volume of the active core, the power (steady state) or energy (transient) deposited into the core, and the energy per fission. The fuel volume of each element is 0.39 ft^3 . For steady state and transients the active core size is 180 and 225 assemblies, respectively, which results in active core sizes of 70.3 ft^3 (1.988 m^3) and 87.6 ft^3 (2.48 m^3). Power is 100 kW for steady state and 1000 MW-s for transient. The energy per fission is given as $3.2 \times 10^{-11} \text{ J}$ (based of 200 MeV per fission). Using Equation 14 the volumetric heat generation rate for steady state is:

$$e_f \dot{F} = \left(\frac{1 \text{ fission}}{3.2 \times 10^{-11} \text{ J}} \right) \left(100 \frac{\text{kW}}{\text{core}} \right) \left(1000 \frac{\text{J}}{\text{s kW}} \right) \left(\frac{1 \text{ core}}{1.988 \text{ m}^3} \right) = 1.57 \times 10^{15} \frac{\text{fissions}}{\text{m}^3} \quad (14)$$

The transient case is found similarly but considering the shape of transient.

Recall the assumption that transients were 1000 MW and lasted 1 second. Since the heat generation takes place over a short period of time the time step is adjusted to observe the fission rate at 0, 0.9, and 1 second. The shape of the heat generation curve is assumed to be linear as seen in Figure 25.

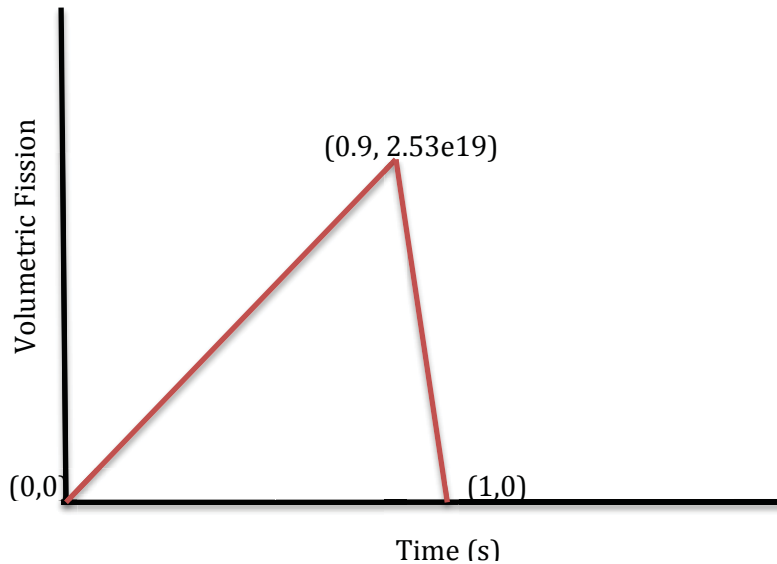


Figure 25: Heat generation curve as a function of time for the transient mode.

The heat generation rate can be found using the area under the curve or for a triangle $0.5(\text{base})(\text{height})$. The resulting volumetric heat generation rate is 2.51×10^{19} fissions/m³. The steady state fission rate is input as a constant value while the transient fission rate is input as a piecewise linear function.

The initial condition and far-field temperature were both taken to be 80°F (300K). The convection coefficient is found using Reynolds number, Nusselt number, the hydraulic diameter made by 4 fuel assemblies coming together, and the properties of air averaged over the temperature range (see Table 4). The Reynolds number shown in Equation 15 uses mass flowrate since it can be taken as constant across the fuel assembly by taking into account conservation of mass in a steady state process. The mass flow rate is calculated from a flow rate per channel of 17 cfm and the density of air at the entrance.

$$Re = \frac{\dot{m}D_h}{A_{cs}\mu} \quad (15)$$

The mass flow rate is held constant and D_h , A_{cs} , and μ are allowed to fluctuate over the length of the assembly. Table 4 shows the results. From Table 4 the Nusselt number and convection coefficient is calculated. The Nusselt number used for the model is calculated using Equation 7 and the convection coefficient using Equation 16. This Nusselt number was chosen since it is the same correlation used in the calculation from reference 6. For comparison, additional Nusselt numbers and convection coefficients are given in Table 5 with accompanying equations is Table 6. The friction factor assumes turbulent flow through a smooth tube.

$$h = \frac{Nuk}{D_h} \quad (16)$$

Table 4: Reynolds Numbers by Axial Position

	Temperature (K)	D_h (in)	A_{cs} (in ²)	Ratio	Re
Top fixture	300	0.625	0.391	1.600	27637
Top Al can	300	0.170	0.635	0.267	4617
Zr can	350	0.251	0.966	0.260	3995
Bottom Al can	400	0.170	0.635	0.267	3711
Grid plate	400	0.875	0.601	1.455	20201

The run time for steady state was chosen based on the time it takes to reach steady state temperature conditions which was found to be $\sim 300,000$ s using a trial and error method. The run time for transient was based on the cooling time to ambient (5-7 hours with full flow) following a transient. Time steps are adaptive (BISON controls the time step based on the residual) for each case with a max time step of 10,000 s for steady state and 1,000 s for transients. For transient cases the time step is controlled at 0, 0.9, and 1 seconds to account for the piecewise linear function on volumetric fission rate.

The residual tolerance is 0.008 based off an example developed by the Fuels Modeling and Simulation Department at INL for light water reactor fuel rods. Values of interest in post-processing are the element average temperature of the fuel, reflector, Zr-3 can, Al-6063 can, and the magnitude of rod total power.

Table 5: Nusselt Numbers and Convection Coefficients by Axial Location

Axial Location	Nusselt Numbers			
	Evans-Sarjant	Dittus-Boelter	Colburn	Gnielinski
Top fixture	71	72	74	67
Top Al can	17	17	18	16
Zr can	15	15	16	14
Bottom Al can	14	14	15	13
Grid plate	56	56	58	53
Axial Location	Convection Coefficients ($\text{W m}^{-2} \text{K}^{-1}$)			
	Evans-Sarjant	Dittus-Boelter	Colburn	Gnielinski
Top fixture	117	118	121	110
Top Al can	103	104	106	94
Zr can	70	70	72	63
Bottom Al can	109	109	112	96
Grid plate	82	82	84	77

Table 6: Equations for Nusselt Numbers

Evans-Sarjant	$0.020Re^{0.8}$
Dittus-Boelter ^[22]	$0.023Re^{0.8}Pr^{0.4}$
*Chilton-Colburn ²²	$0.125fRePr^{1/3}$
**Gnielinski	$\frac{(f/8)(Re - 1000)Pr}{1 + 12.7(f/8)^{0.5}(Pr^{2/3} - 1)}$
* $f = 0.184Re^{-0.2}$	
** $f = (0.790 \ln Re - 1.64)^{-2}$	

Analytical Comparison to BISON

Before a 3D model is ran with BISON simple analytical models are created to build trust in BISON's results. For steady state runs we look at two models. A circular 2D model and a 2D axial model seen in Figure 26. For the circular model a radius is chosen that would give the same fuel volume found in the TREAT fuel element with the same gap and cladding thicknesses. The 2D axial model is what would be seen looking at only the fuel in the TREAT element.

For the circular problem the governing equation (Equation 17) for steady state 1D conduction is:

$$\frac{1}{r} \frac{\partial}{\partial r} (kr) \frac{\partial T}{\partial r} = -e_f \dot{F} \quad (17)$$

where r is the radius of the circle. Each region (fuel, gap, and cladding) is analyzed separately in which case thermal conductivity and fission rate can be assumed constant. Transforming the partial differential equation into an ordinary differential equation for each region is given in Equations 18 – 20.

$$\frac{1}{r} \frac{d}{dr} r \frac{dT_f}{dr} = -\frac{e_f \dot{F}}{k_f} \quad (18)$$

$$\frac{d}{dr} r \frac{dT_g}{dr} = 0 \quad (19)$$

$$\frac{d}{dr} r \frac{dT_c}{dr} = 0 \quad (20)$$

Where the subscript on thermal conductivity represents the fuel, gap, and cladding. The boundary conditions for Equations 18 - 20 are shown in Equations 21 - 26.

$$\left. \frac{dT_f}{dr} \right|_{r=0} = 0 \quad (21)$$

$$k_f \left. \frac{dT_f}{dr} \right|_{r=r_f} = k_g \left. \frac{dT_g}{dr} \right|_{r=r_f} \quad (22)$$

$$k_g \left. \frac{dT_g}{dr} \right|_{r=r_g} = k_c \left. \frac{dT_c}{dr} \right|_{r=r_g} \quad (23)$$

$$-k_c \left. \frac{dT_c}{dr} \right|_{r=r_c} = h[T_c(r = r_c) - T_\infty] \quad (24)$$

$$T_f(r_f) = T_g(r_f) \quad (25)$$

$$T_g(r_g) = T_c(r_g) \quad (26)$$

The solution for T_f , T_g , and T_c can be readily found to be:

$$T_f(r) = \frac{e_f \dot{F} r_f^2}{2} \left(\frac{\ln r_g}{k_g} - \frac{\ln r_f}{k_g} + \frac{\ln r_c}{k_c} - \frac{\ln r_g}{k_c} + \frac{1}{2k_f} + \frac{1}{r_c h} - \frac{1}{2k_f} \frac{r^2}{r_f^2} \right) + T_\infty \quad (27)$$

$$T_g(r) = \frac{e_f \dot{F} r_f^2}{2} \left(-\frac{\ln r}{k_g} - \frac{\ln r_g}{k_c} + \frac{\ln r_g}{k_g} + \frac{1}{hr_c} + \frac{\ln r_c}{k_c} \right) + T_\infty \quad (28)$$

$$T_c(r) = \frac{e_f \dot{F} r_f^2}{2hr} + T_\infty \quad (29)$$

Maximum temperature ($T_f(0)$) and temperature at the surface of the cladding ($T_c(r_c)$) are the properties used for comparison. Plugging in the values of $r = 0$ m into Equation 27 and $r = 0.056134$ m into Equation 29 gives a $T_f = 413$ K (284°F) and $T_c = 369$ K (205°F). This is nearly the same result as with BISON. Doing similarly with an axial model gives the results seen in Equations 30 - 32.

$$T_f(x) = e_f \dot{F} x_f \left(\frac{x_c}{k_c} - \frac{x_g}{k_c} + \frac{x_g}{k_g} - \frac{x_f}{k_g} + \frac{x_f}{2k_f} - \frac{x}{2k_f} + \frac{1}{h} \right) + T_\infty \quad (30)$$

$$T_g(x) = e_f \dot{F} x_f \left(\frac{x_g}{k_g} - \frac{x}{k_g} - \frac{x_g}{k_c} + \frac{1}{h} + \frac{x_c}{k_c} \right) + T_\infty \quad (31)$$

$$T_c(x) = e_f \dot{F} x_f \left(\frac{x_g}{k_c} - \frac{x}{k_c} + \frac{1}{h} \right) + T_\infty \quad (32)$$

The temperature results for the 2D axial model are higher at $T_f = 465$ K (377°F) and $T_c = 386$ K (235°F), but still agrees with the BISON result. One key difference in these models is radiation heat transfer between the fuel and cladding is removed and replaced with an air gap at local atmospheric pressure. For comparison with the 3D model the gas conductivity can be made infinitely large or removed.

For a transient case we can solve an adiabatic case of the 3D model. In an adiabatic case all the energy is deposited in the element. Since the transient is short (1 second), assume all the energy is deposited only in the fuel (see Equation 33). Following the transient the energy disperses throughout the element (see Equation 34). Basically observing the thermal capacity of the fuel element rather than the ability to transfer heat throughout the element.

$$T_{max} = \frac{e_f \dot{F} \Delta t}{(\rho \forall C_p)_{fuel}} \quad (33)$$

$$T_{min} = \frac{e_f \dot{F} \Delta t}{\sum (\rho_i \forall_i C_{p_i})_{element}} \quad (34)$$

For a 1000 MW-s transient $T_{max} = 595$ K (611°F) and $T_{min} = 440$ K (332°F).

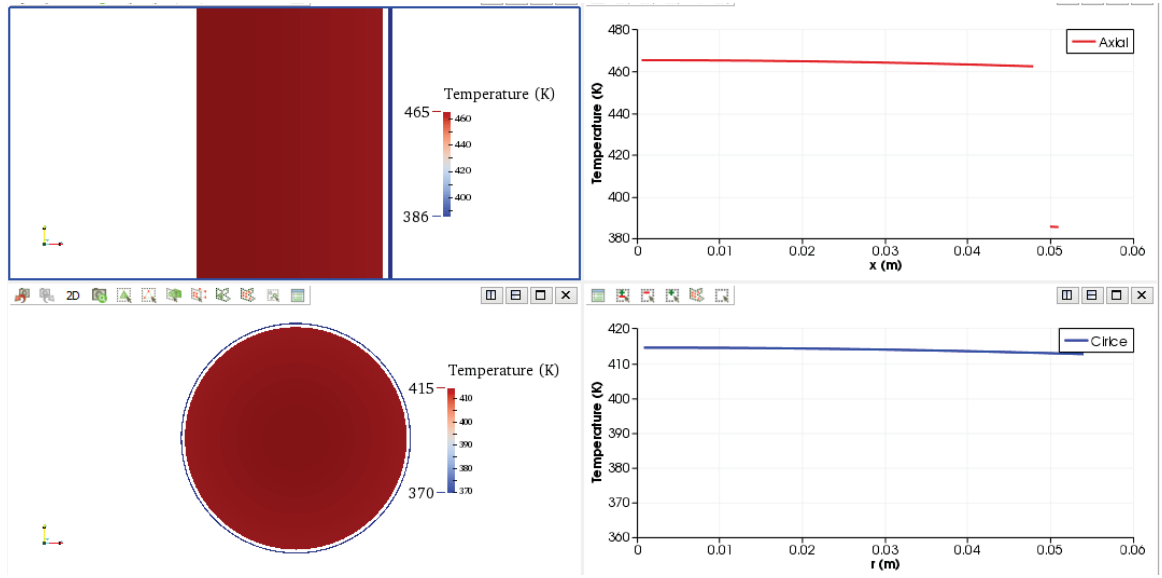


Figure 26: BISON 2D models to compare against analytical solution (100 kW and 300,000 s).

CHAPTER 4: RESULTS

Property Variation

Table 7 gives a quick summary of the resulting hot spot temperature in the octant fuel assembly.

Table 7: Hot Spot Temperatures

Input File	Steady State Temperature Final (K)	Transient Temperature Initial (K)	Transient Temperature Final (K)
Run0.i/RunT0.i	516	642	577
Run1.i/RunT1.i	516	599	549
Run2.i/RunT2.i	516	704	615
Run3.i/RunT3.i	514	641	573
Run4.i/RunT4.i	518	644	583
Run5.i/RunT5.i	516	599	551
Run6.i/RunT6.i	516	704	612
Run7.i/RunT7.i	544	642	578
Run8.i/RunT8.i	516	639	577
Run9.i/RunT9.i	516	644	577
Run10.i/RunT10.i	516	641	578
Run11.i/RunT11.i	509	643	575
Run12.i/RunT12.i	524	642	580
Run13.i/RunT13.i	516	644	577
Run14.i/RunT14.i	516	641	578
Run15.i/RunT15.i	514	642	577
Run16.i/RunT16.i	518	642	577
Run17.i/RunT17.i	515	642	574
Run18.i/RunT18.i	516	642	581
Run19.i/RunT19.i	537	642	585
Run20.i/RunT20.i	456	656	537

The hottest temperature for steady state power was 544 K (520°F) caused by lowering fuel emissivity to 0.05. Lowering emissivity inhibits the ability of the fuel to

emit heat from the periphery thereby increasing the delta on temperature across the fuel. The lowest temperature for steady state was 456 K (361°F) caused by changing the Zr-3 cladding to Al-6063 cladding. Although the emissivity for the Al-6063 cladding is also 0.05 the temperature is driven by the larger thermal conductivity of the Al-6063 (218 W/m-K vs 14.4 W/m-K). The higher thermal conductivity allow the heat to dissipate from the fuel to the coolant quicker. The hottest temperature for transient power was 704 K (807°F) caused by an increase in decrease in fuel density and fuel specific heat and vice versa for the lowest temperature of 537 K (507°F). See the section on transients below for more information. Table 8 provides a comparison against the literature for steady state operational mode. The results are within what was calculated and measured.

Table 8: Steady State BISON results compared against literature.

390 °F	1000 W, unknown spacer type
470 °F	1000 W, Asbestos 108 lb/hr flowrate
340 °F	1000 W, Zr spacer 260 lb/hr flowrate
510 °F	100 kW calculated, 6500 cfm, 180 elements
475 °F	50 kW measured, 50% flow, 157 elements
405 °F	100 kW measured, 84% flow, 203 elements
469 °F	BISON with gap closure, 6000 cfm
511 °F	BISON w/o gap closure, 6000 cfm

The plots below provide more detail on the effects. What is shown is the axial temperature distribution with the axis running down the center of the fuel assembly. The

plots parametrics are compared against the benchmark on a single plot and then broken down for readability and to better ascertain impacts on temperature from each parameter change. Steady state power temperature distributions are displayed first (see Figure 27 – 32) followed by transient power temperature distributions. The magnitude of the resulting temperature change from each parameter change can be understood by observing Equation 35 which is a modified version of Equation 9 created by substituting for $\nabla \cdot \mathbf{q}$.

$$\rho C_p \frac{\partial T}{\partial t} = \frac{\partial}{\partial x} \left(k \frac{\partial T}{\partial x} \right) + \frac{\partial}{\partial y} \left(k \frac{\partial T}{\partial y} \right) + \frac{\partial}{\partial z} \left(k \frac{\partial T}{\partial z} \right) + e_f \dot{V} \quad (35)$$

When the fuel assembly reaches steady state temperature conditions $\frac{\partial T}{\partial t} \rightarrow 0$ and the only term that has an impact on the temperature is thermal conductivity. It is interesting that an equal change in thermal conductivity on the Zr-3 can has a greater effect on temperature than for fuel thermal conductivity. This is because the heat has to travel through the cladding to a greater extent than it does for the fuel. Recall the heat generation in the fuel was uniform. For the cladding the heat has to impinge on the inner side, travel through the cladding, and then be convected away. If the heat generation came from a point source than fuel thermal conductivity would have a greater effect on hot spot temperature since the heat would have to propagate a greater distance. choosing a material (fuel or can) with low emissivity increases radial resistance therefore increasing temperature.

Displayed with the steady state plots is a 3D rendering of the benchmark octant fuel assembly observed in the post processing tool ParaView (see Figure 33 – 36). The purpose is to give the reader an illustration of the problem results in addition to the axial profile plots.

Steady State

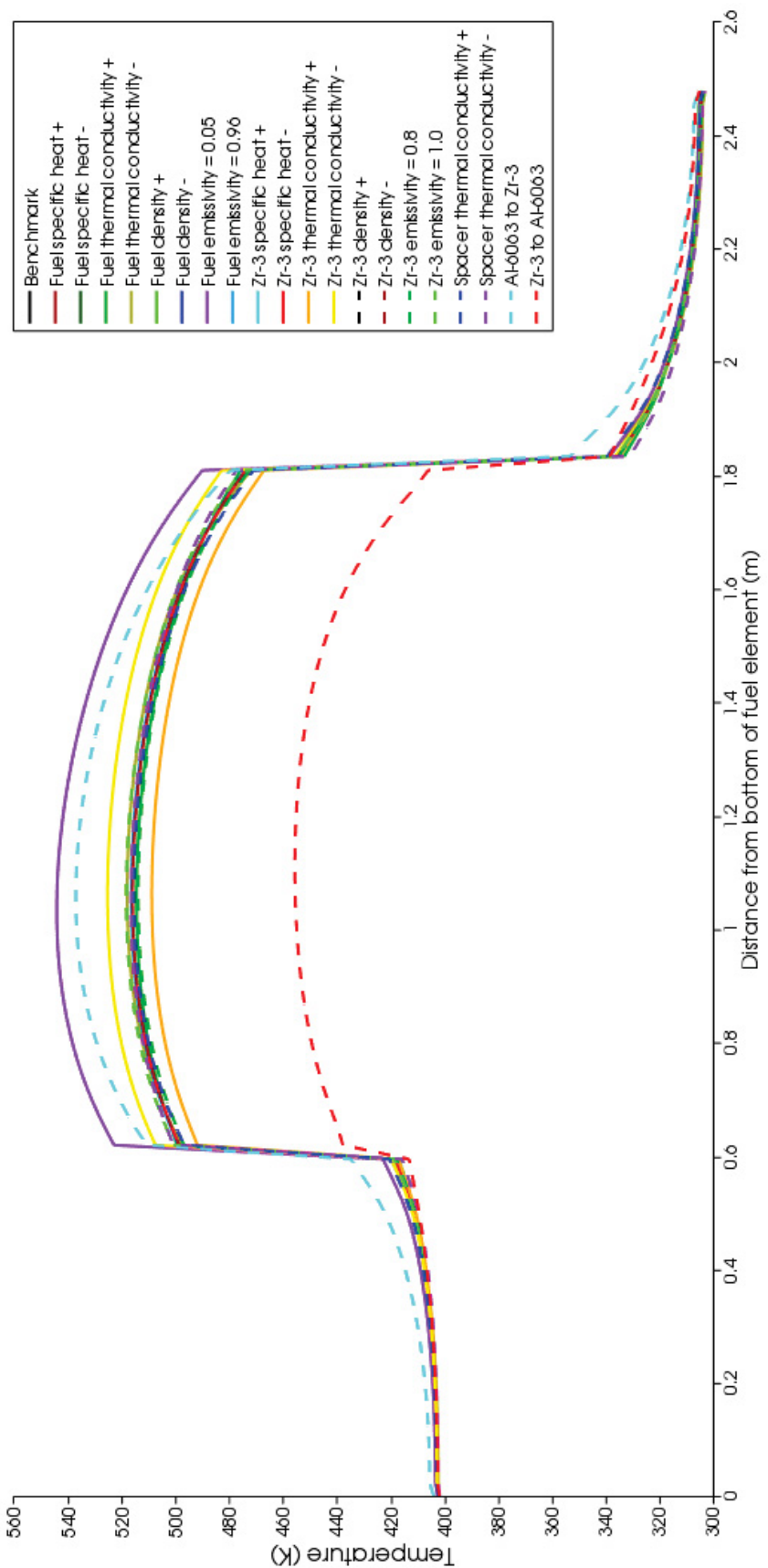


Figure 27: Axial temperature distribution for a steady state power of 100 kW at 300,000 s.

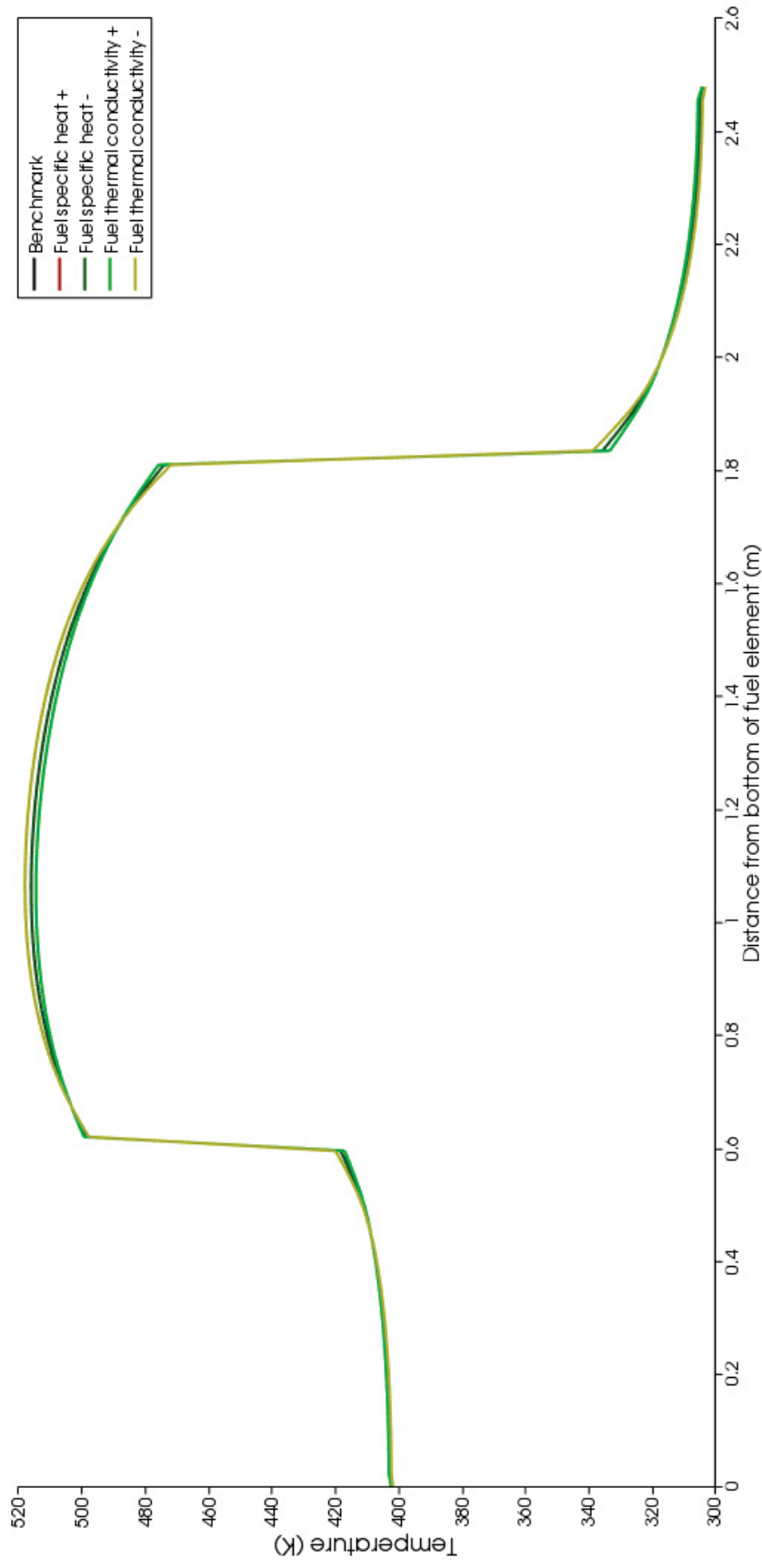


Figure 28: Steady State Benchmark –vs- fuel specific heat and thermal conductivity.

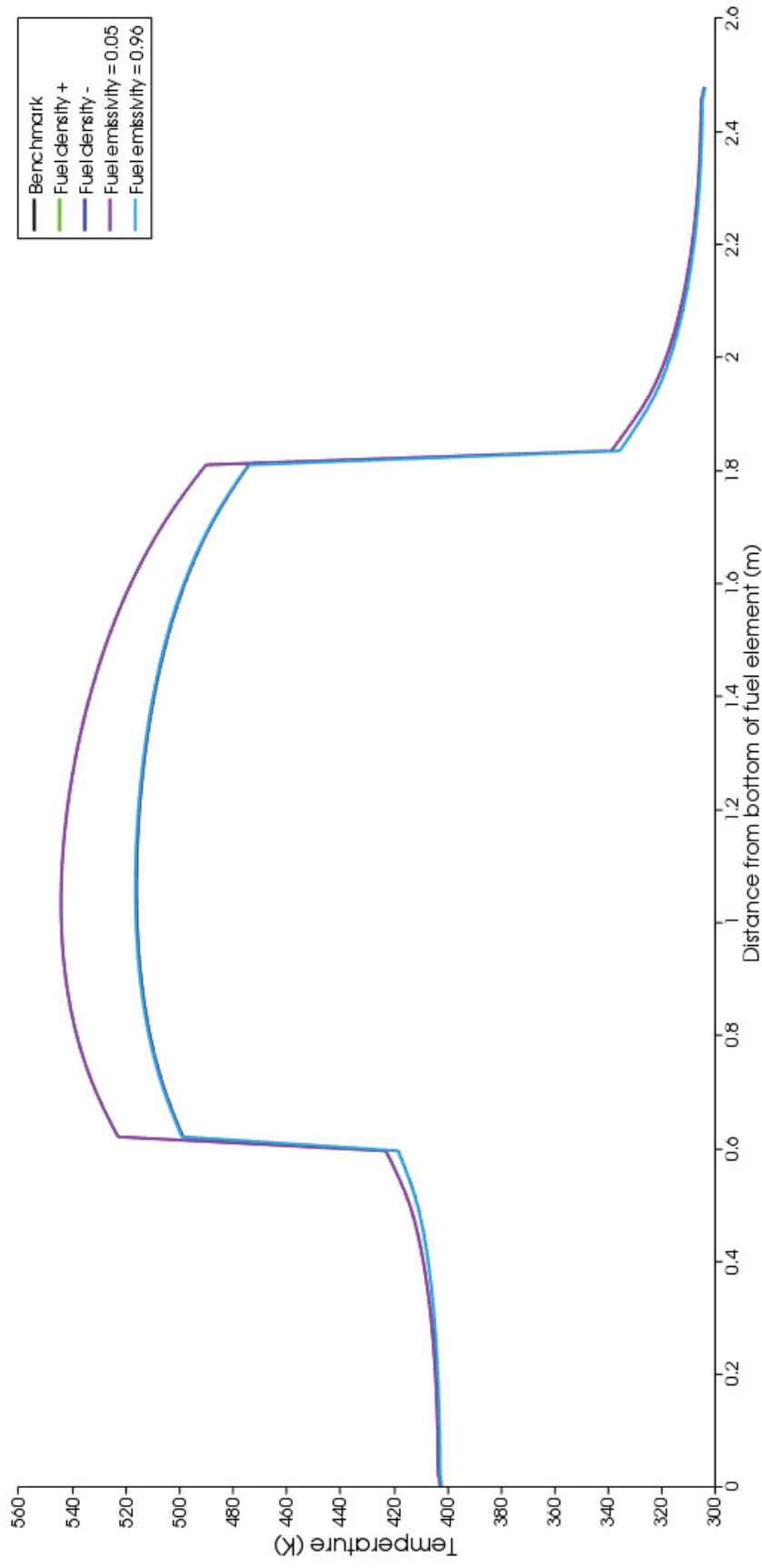


Figure 29: Steady State Benchmark -vs- fuel density and fuel emissivity.

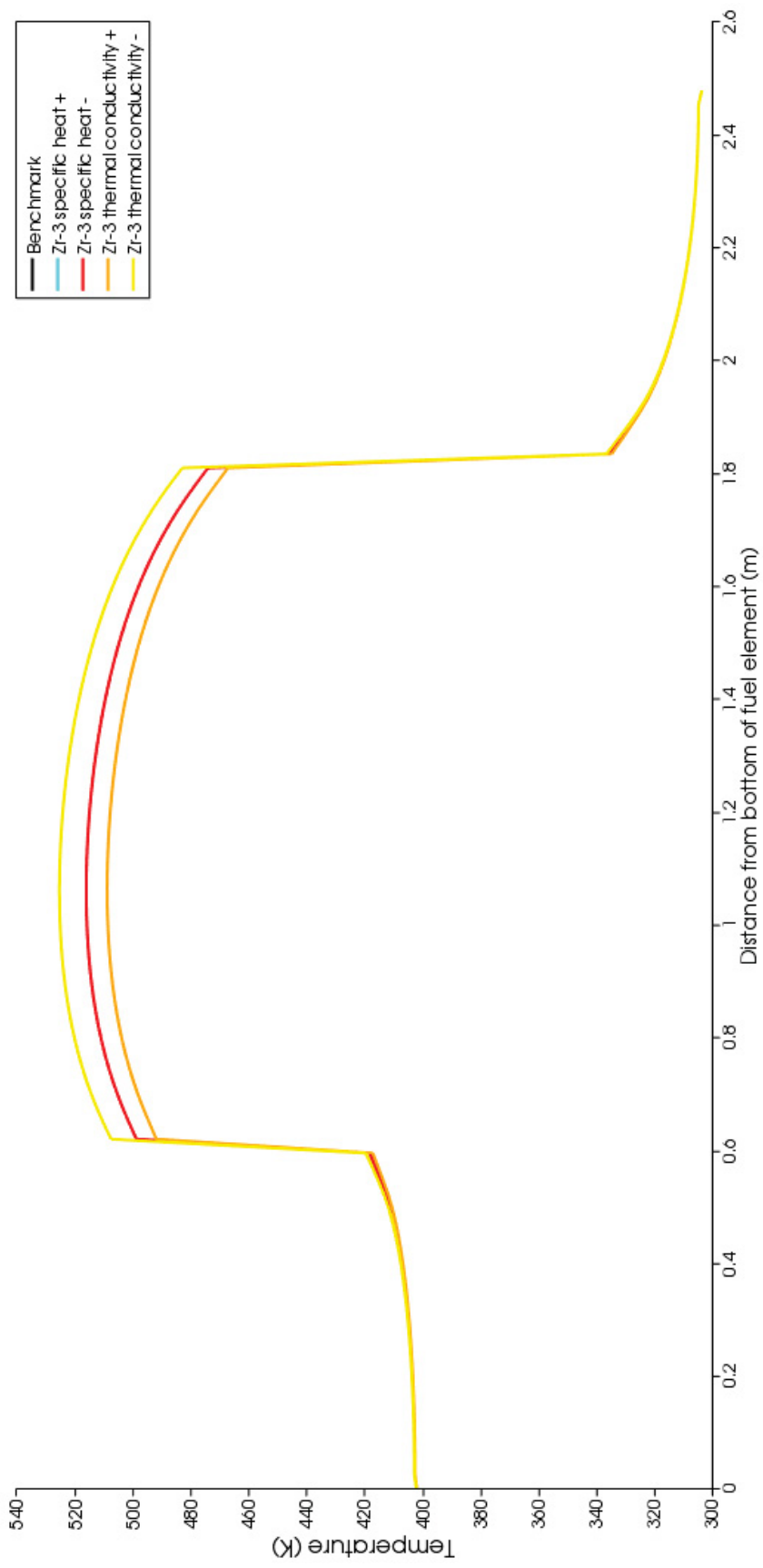


Figure 30: Steady State Benchmark -vs- Zr-3 specific heat and thermal conductivity.

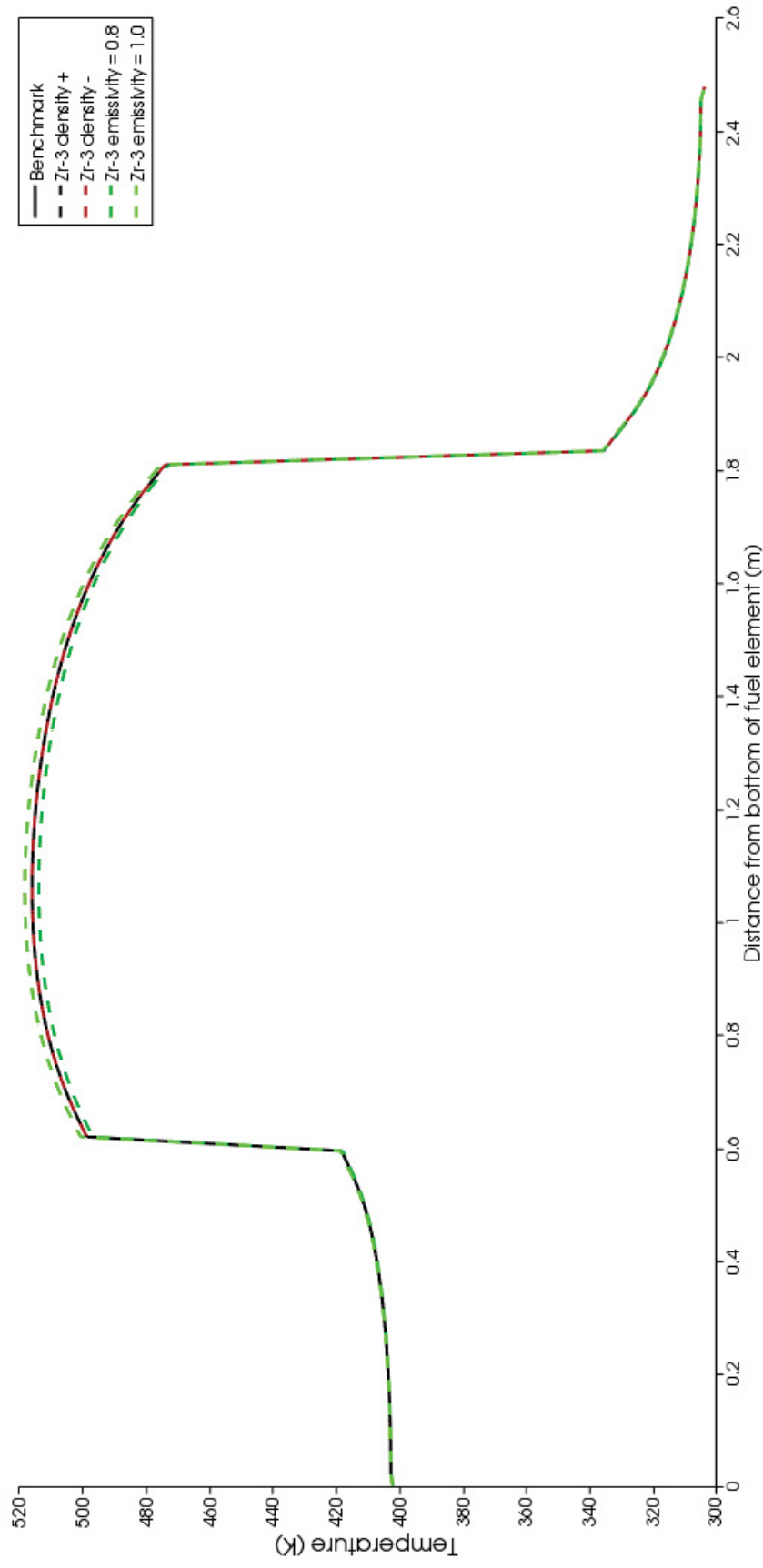


Figure 31: Steady State Benchmark -vs- Zr-3 density and emissivity.

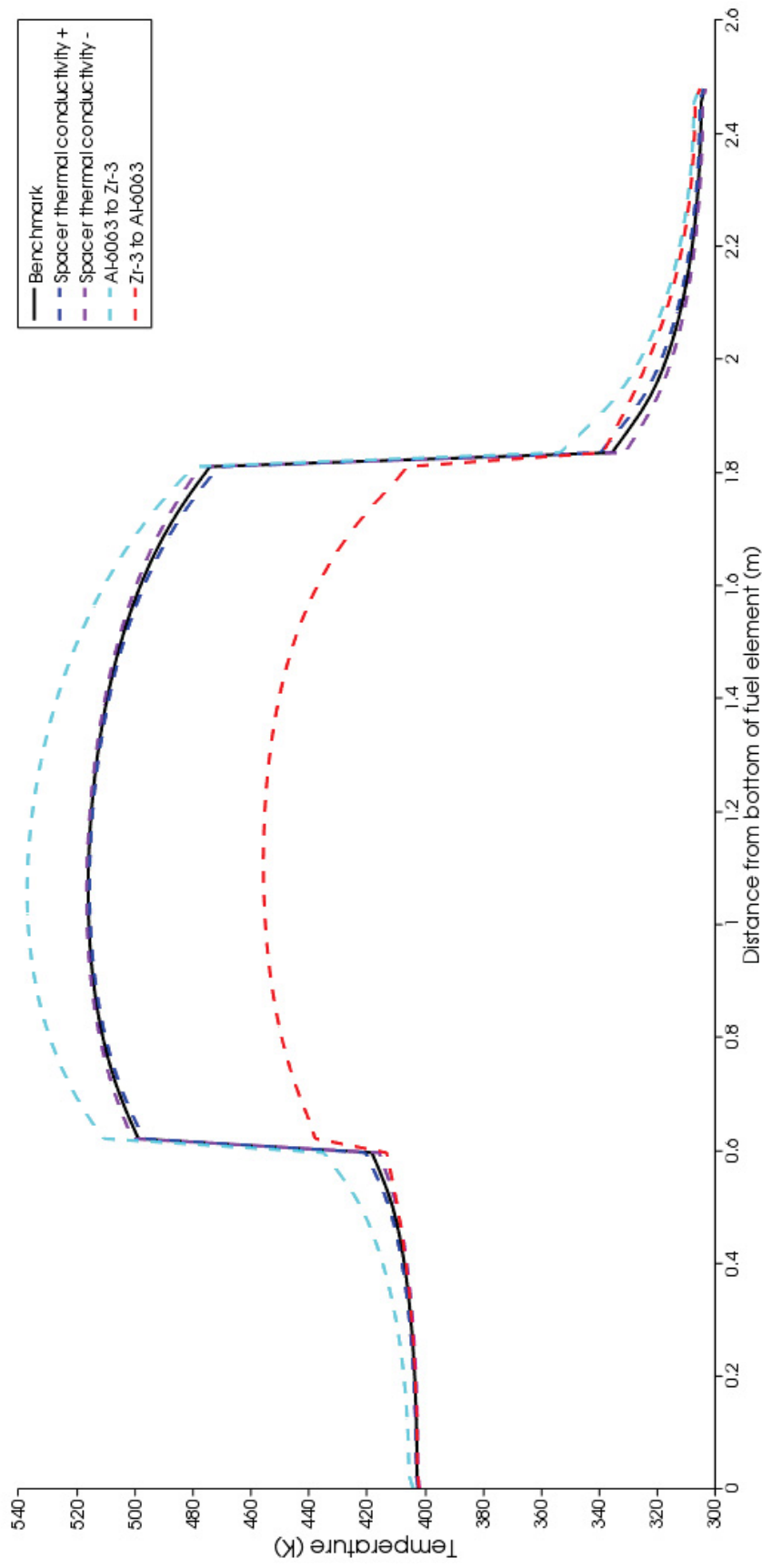


Figure 32: Steady State Benchmark -vs- spacer thermal conductivity and canning material type.

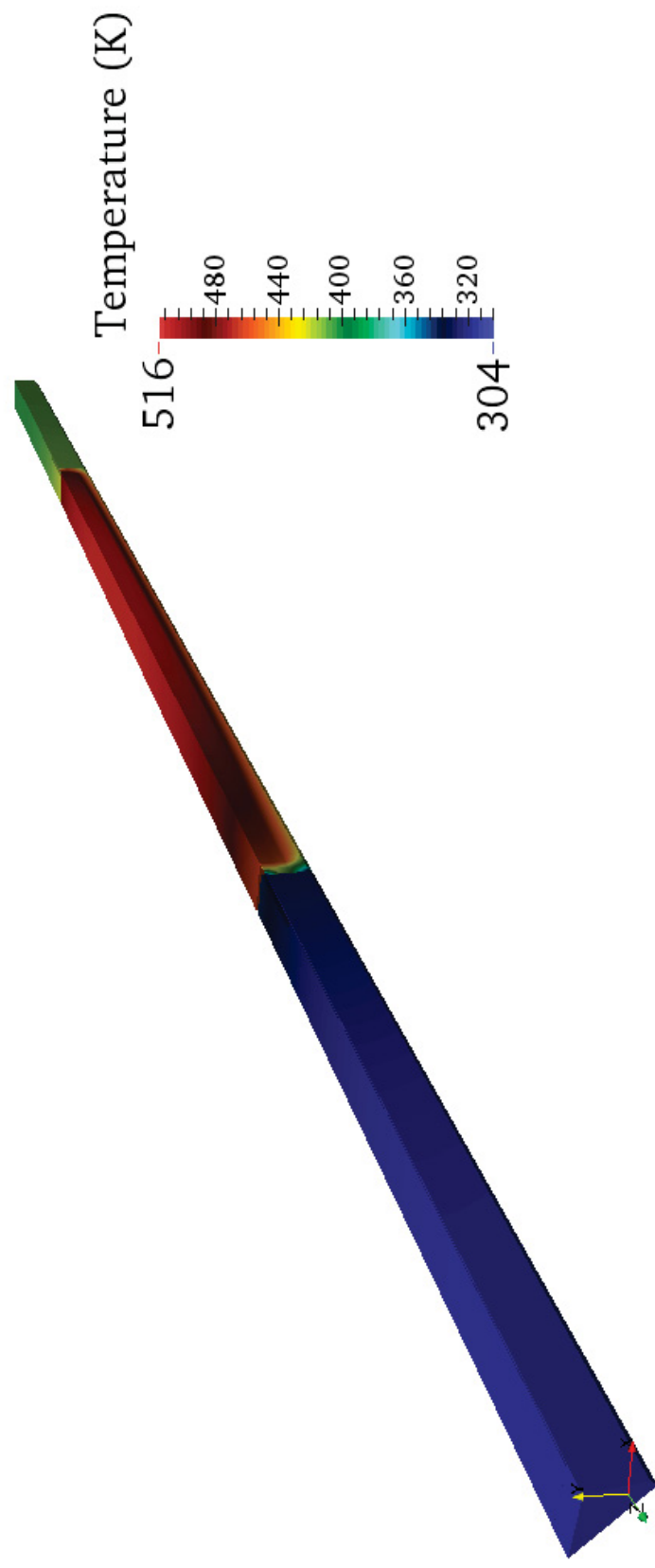


Figure 33: Temperature distribution of a TREAT fuel assembly at a power of 100 kW and 300,000 s. Shown is an octant of the assembly.

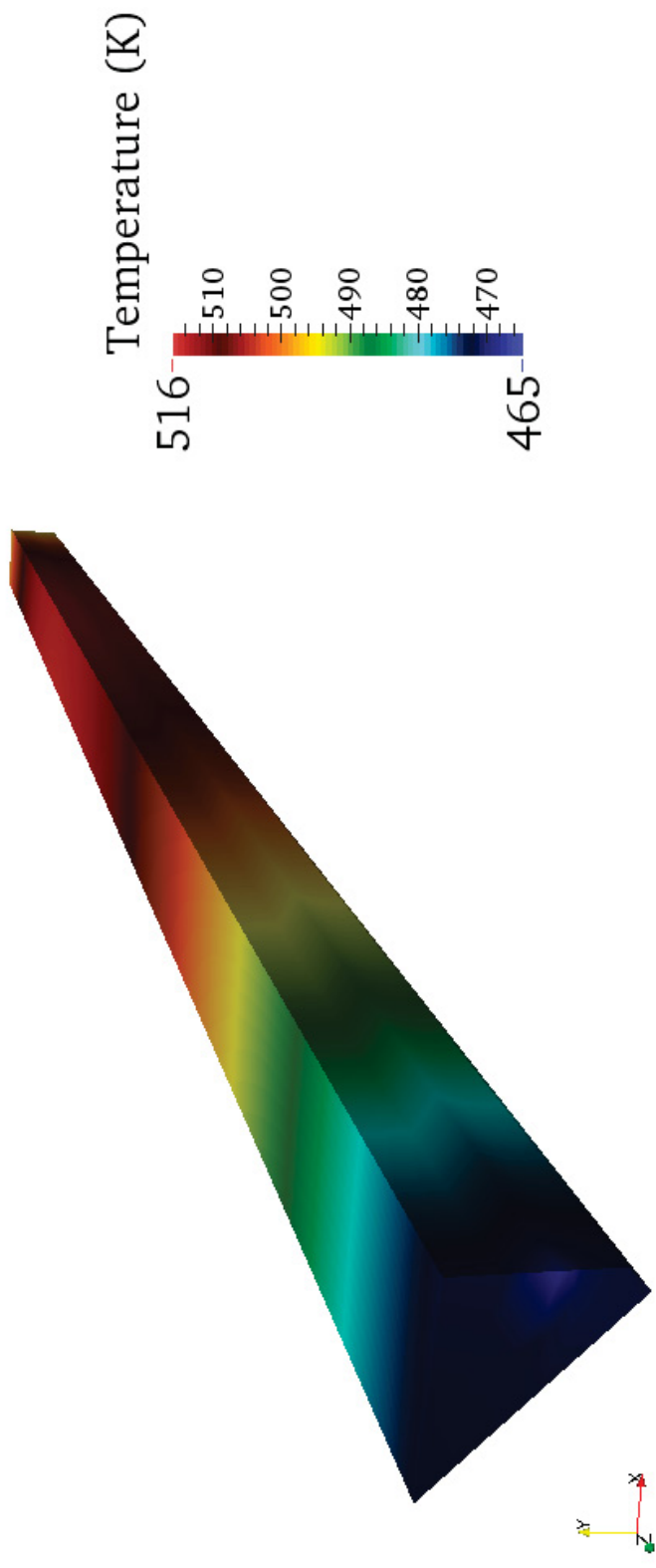


Figure 34: Temperature distribution of the fuel. The top of the fuel is coolest as is expected for air that flows downward.

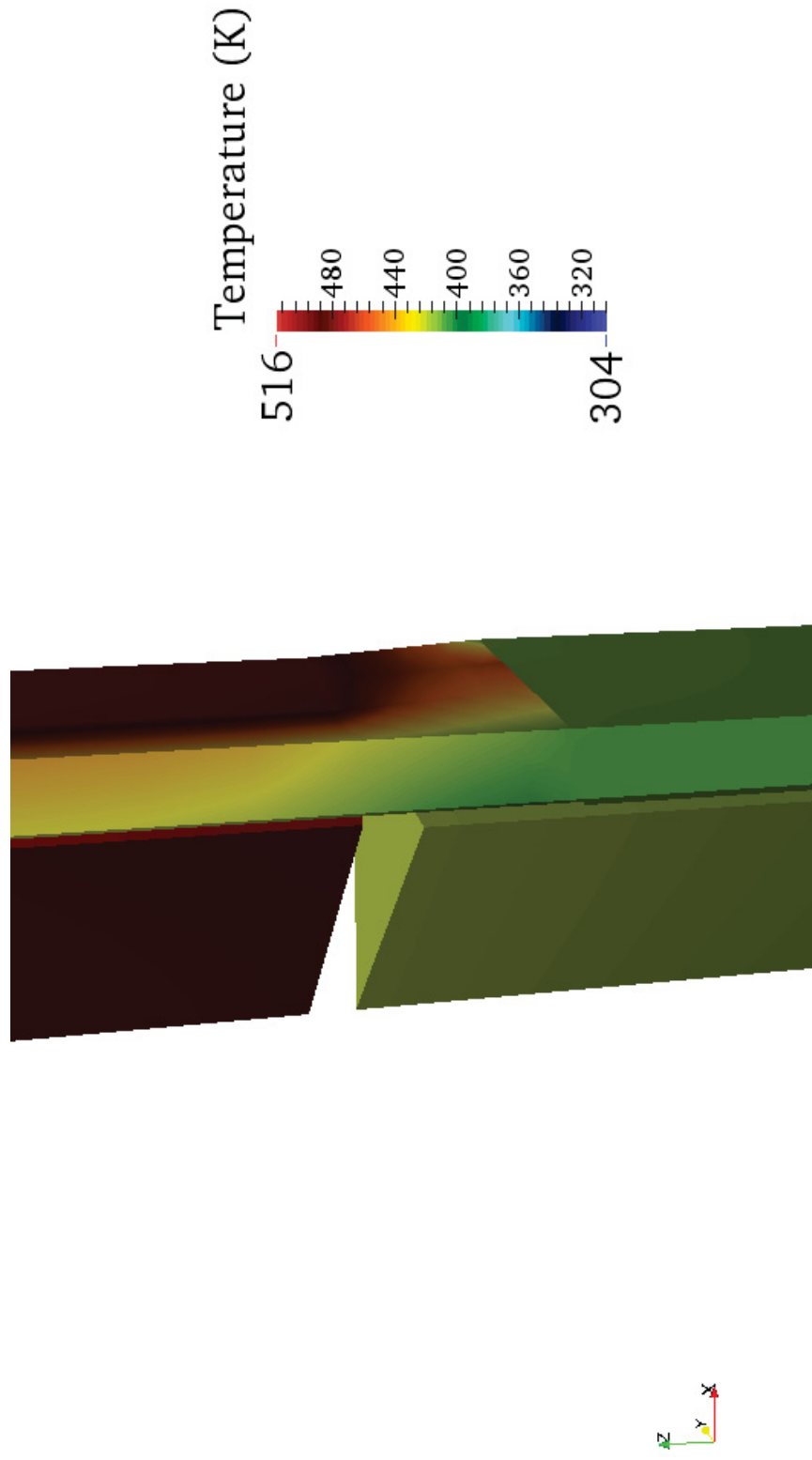


Figure 35: Interface for Zr-3 and Al-6063 cans and interface for fuel and reflector blocks. Observable is the effect the spacer has on delaying heat transfer.



Figure 36: Radial temperature distribution across the fuel showing the cooling takes place primarily where the cladding makes contact.

Transients

At the termination the transient fuel thermal conductivity and density are the only thing affecting temperature. Since the transient only lasts 1 second there is not significant time for heat transfer to take place. Thermal capacity of the fuel is driving the temperature ($\Delta T = Q/mC_p$). For an analogy consider a light bulb. The light bulb would not feel hot to the touch one second after turning it on because there has not been sufficient time for the heat to transfer from the filament to the light bulb surface. The initial effects of fuel thermal conductivity and fuel density are seen through the remainder the cooling period since they act more like an initial condition. The end of the transient cooling period is similar to the steady state cases with the effects of cladding thermal conductivity becoming observable. Table 9 provides a comparison against what was found in the literature.

Table 9: Transient BISON results compared against the literature.

620 °F	800 MW-s experiment
775 °F	1000 MW-s calculated
510 °F	445 MW-s measured
1450 °F	2500 MW-s calculated
696 °F	1000 MW-s BISON triangle transient shape
504 °F	1000 MW-s analytical
500 °F	1000 MW-s BISON square transient shape

The reported temperature using a triangle transient shape is inaccurate for uniform heat generation (see square transient shape and analytical solution) but has viability in the real reactor where temperature profiles are parabolic in the both the radial and axial direction.

Plots immediately following the transient can be seen in Figures 37 – 39. The 3D renderings at 1.0 s can be seen in Figures 40 – 44. As mentioned previously only fuel specific heat and fuel density have effects. Since they are both on the same side of the equation (Equation 35) multiplying either one by +/- 20% results in equal effects. Parameter changes in non-fuel materials have negligible effects until later on in the cooling period (see Figures 45 – 53). As the fuel cools the temperature in the fuel as a function of position changes axially and radially causing thermal conductivity and other material properties to have a greater effect on fuel temperature. Changing Zr-3 to Al-6063 dominates temperature at the end of the cooling period. The resulting reflector temperature is likely inaccurate. What is likely happening is the heat is transferring from the fuel to the fuel can to the reflector can to the reflector rather than from the fuel to the reflector. In other words the can is heating the reflector faster than the fuel can. This result would only be likely in a vacuum environment.

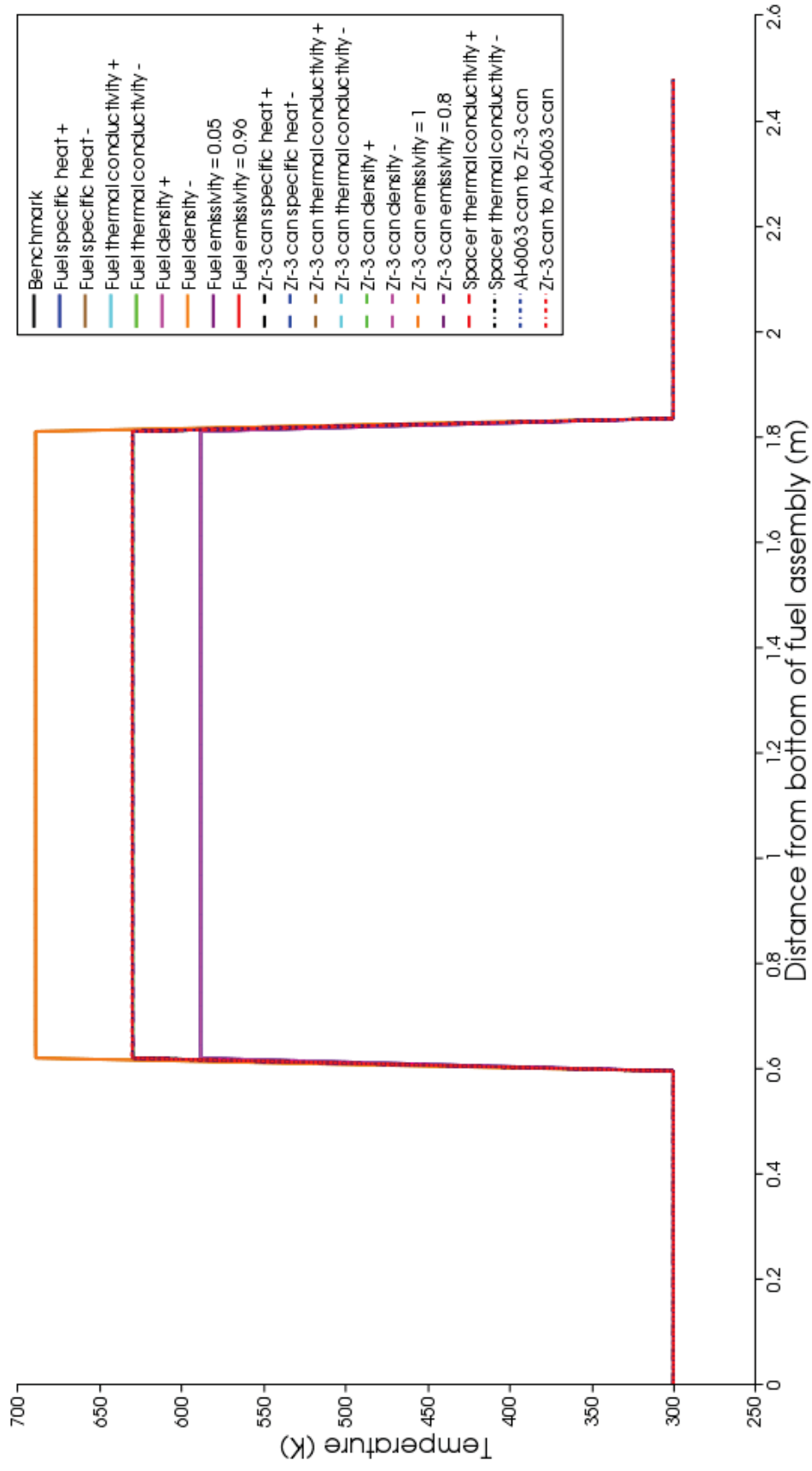


Figure 37: Axial temperature distribution for a transient of 1000 MJ at 0.9 s.

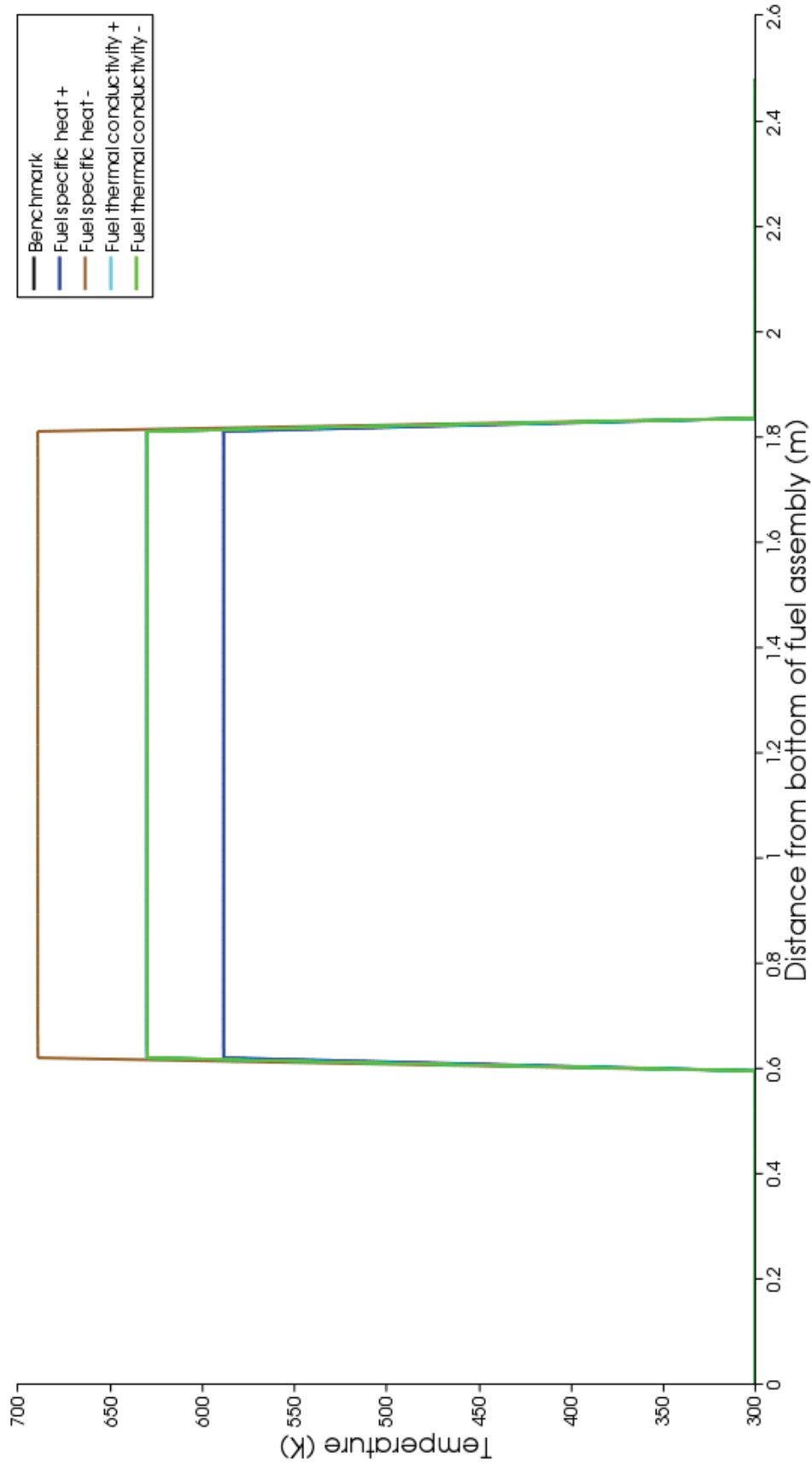


Figure 38: Benchmark compared against C_p and k . Fuel k has negligible effects on temperature.

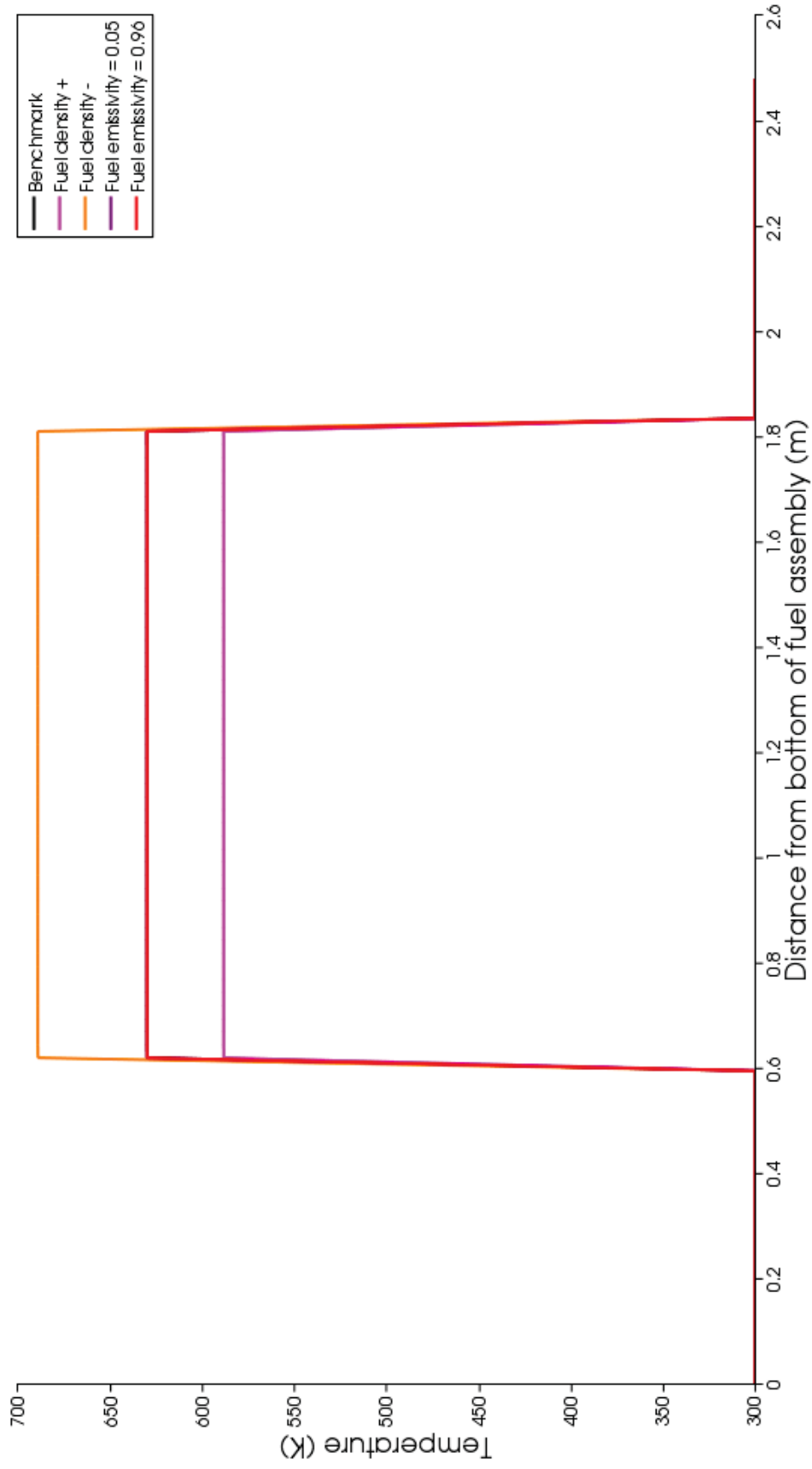


Figure 39: Benchmark compared against fuel ρ and ϵ . Fuel ϵ has negligible effects on temperature.

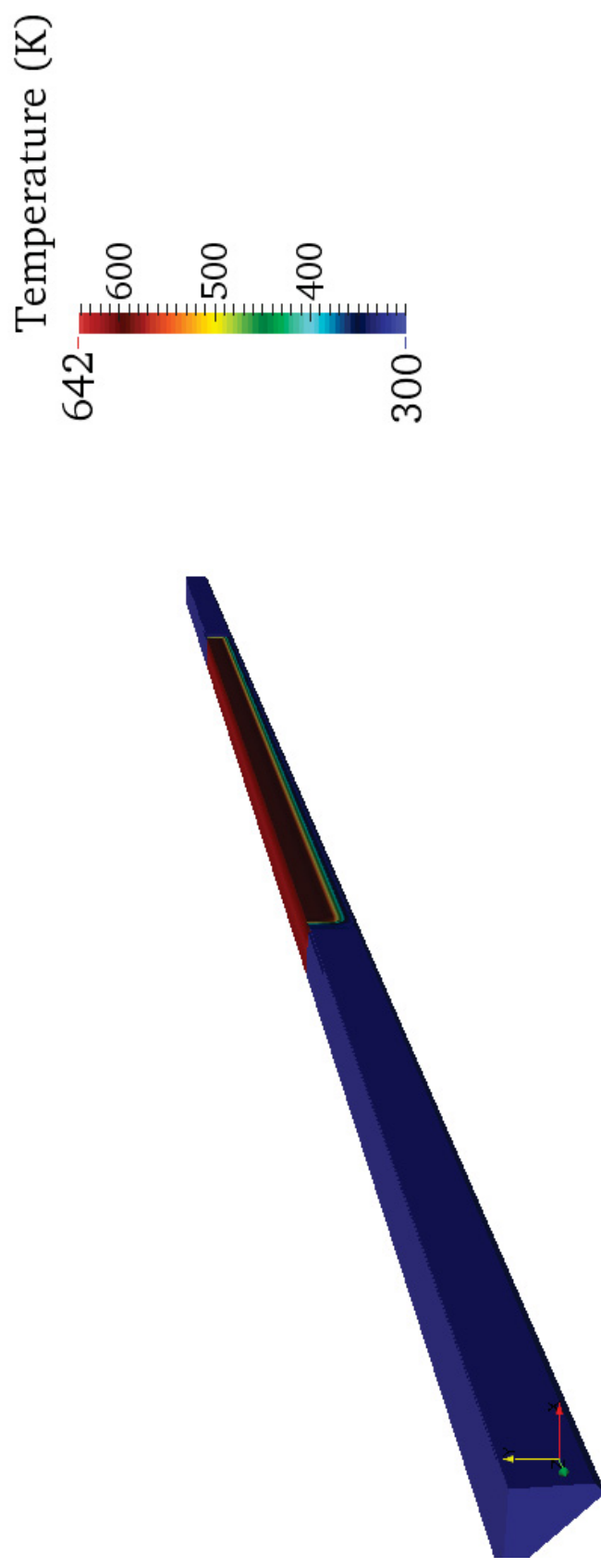


Figure 40: Temperature distribution at 1000 MJ and 0.9 s. Shown is an octant of the assembly.

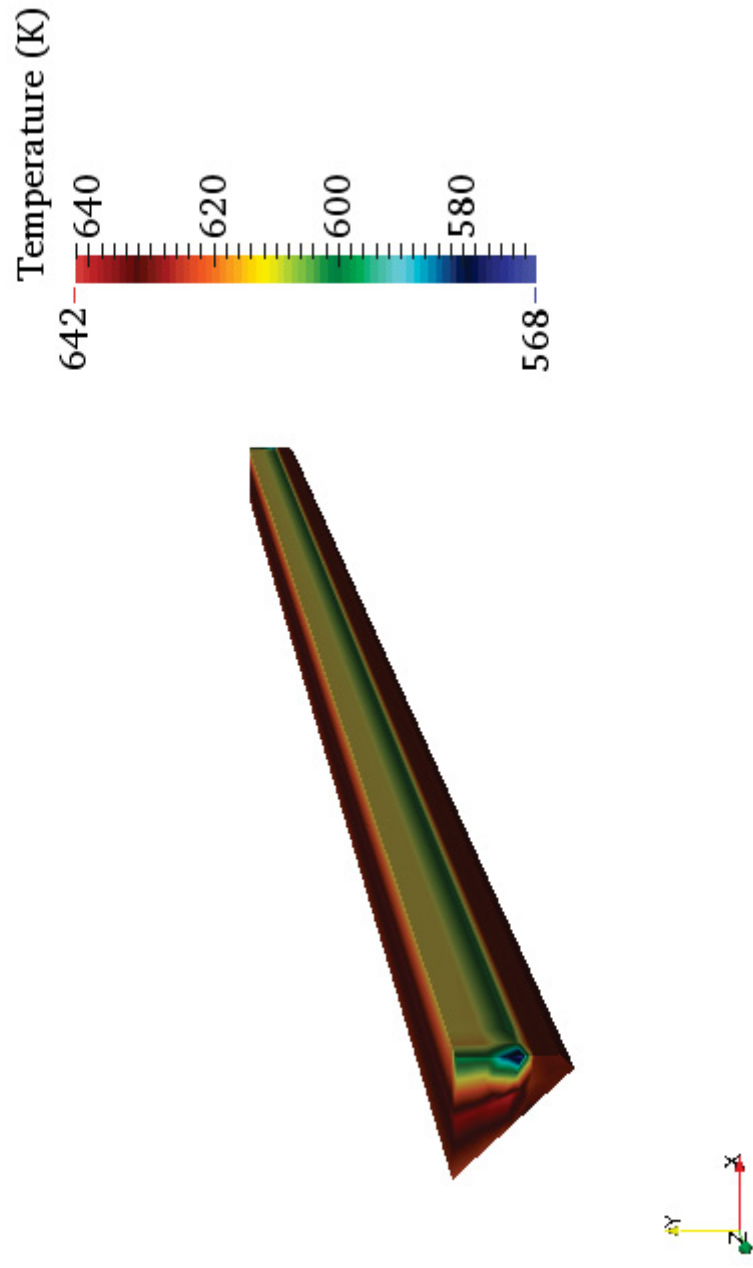


Figure 41: Temperature distribution of the fuel. The outside of the fuel is cooler since it is in contact with the Zr-3 can allowing some of the heat to dissipate there.

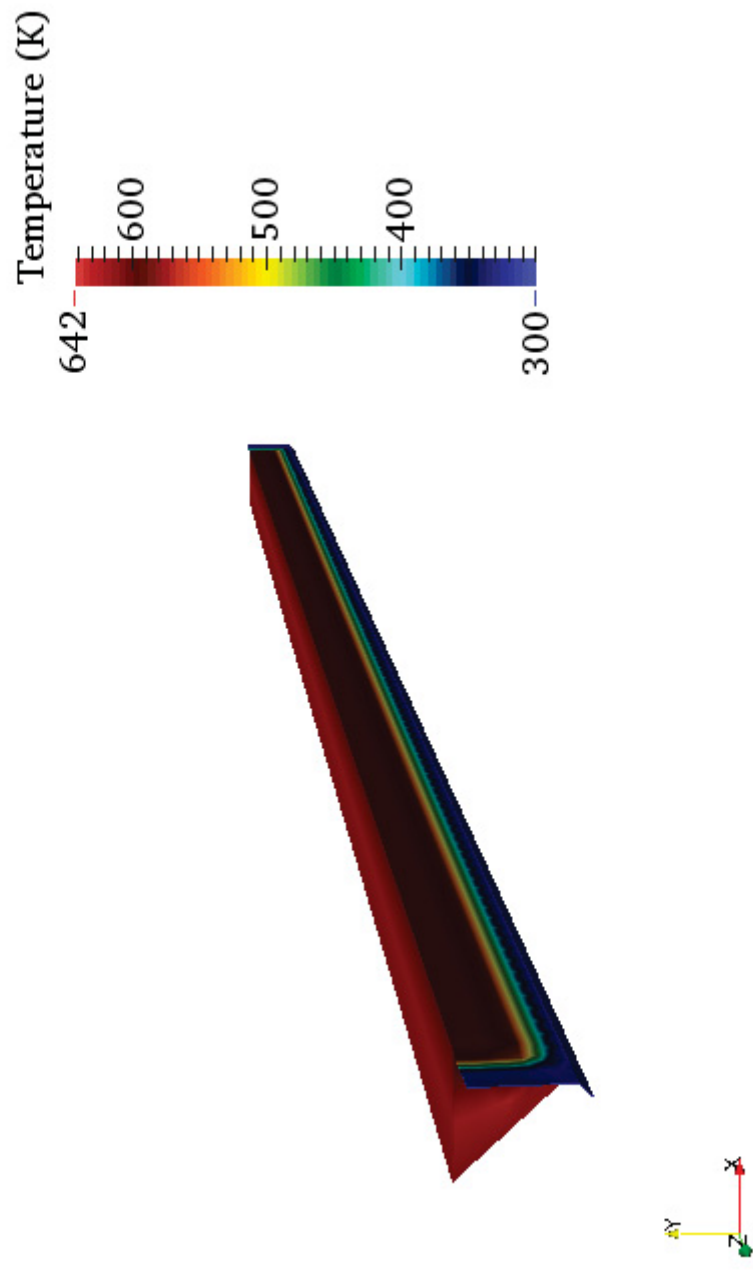


Figure 42: Zr-3 can temperature distribution. The hotter spots on the can are in contact with the fuel.

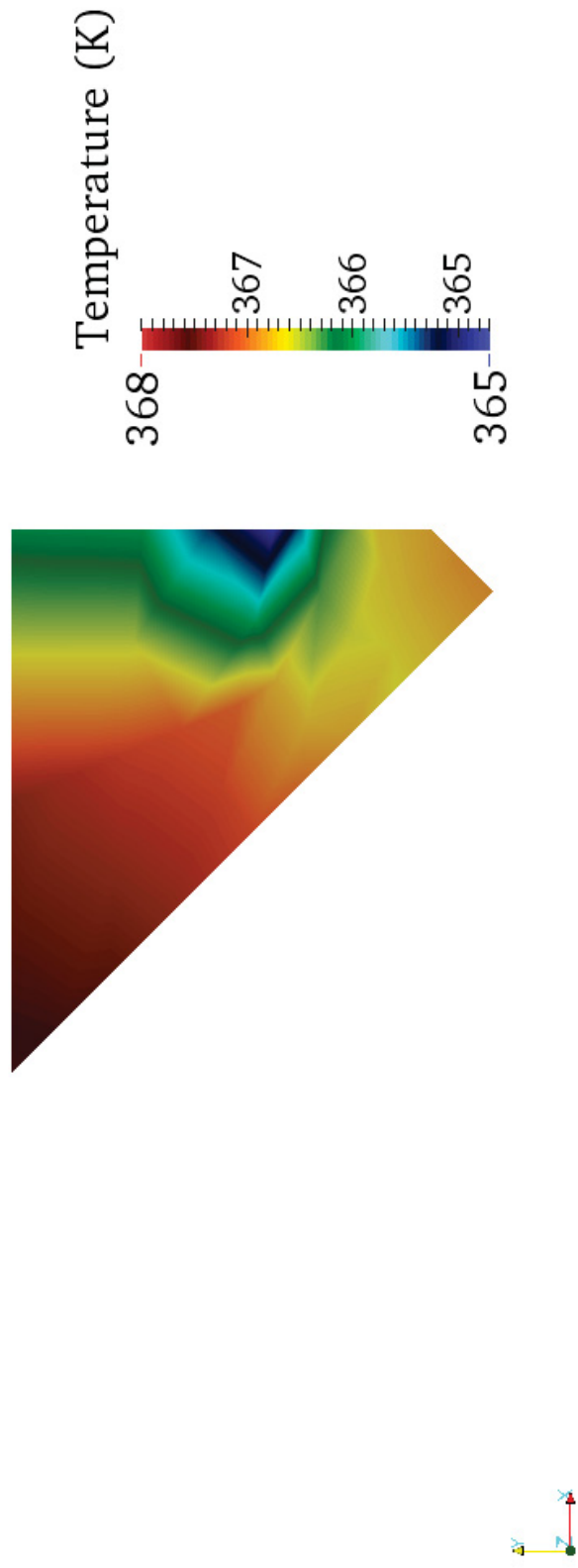


Figure 43: Radial distribution of the fuel. The side is cooler than the chamfer because the fuel is in contact with the Zr-3 can.

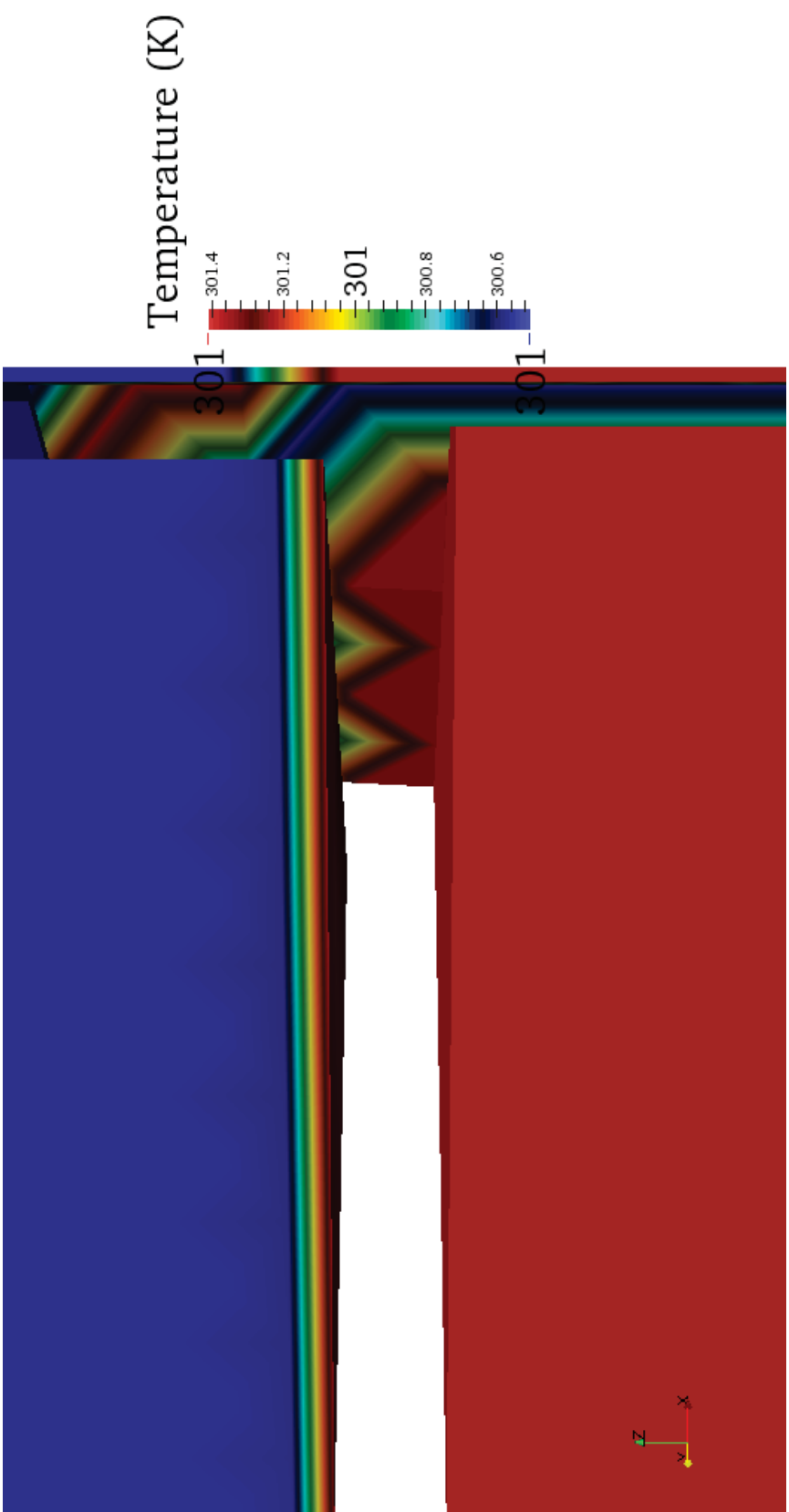


Figure 44: Delayed heat transfer from spacer.

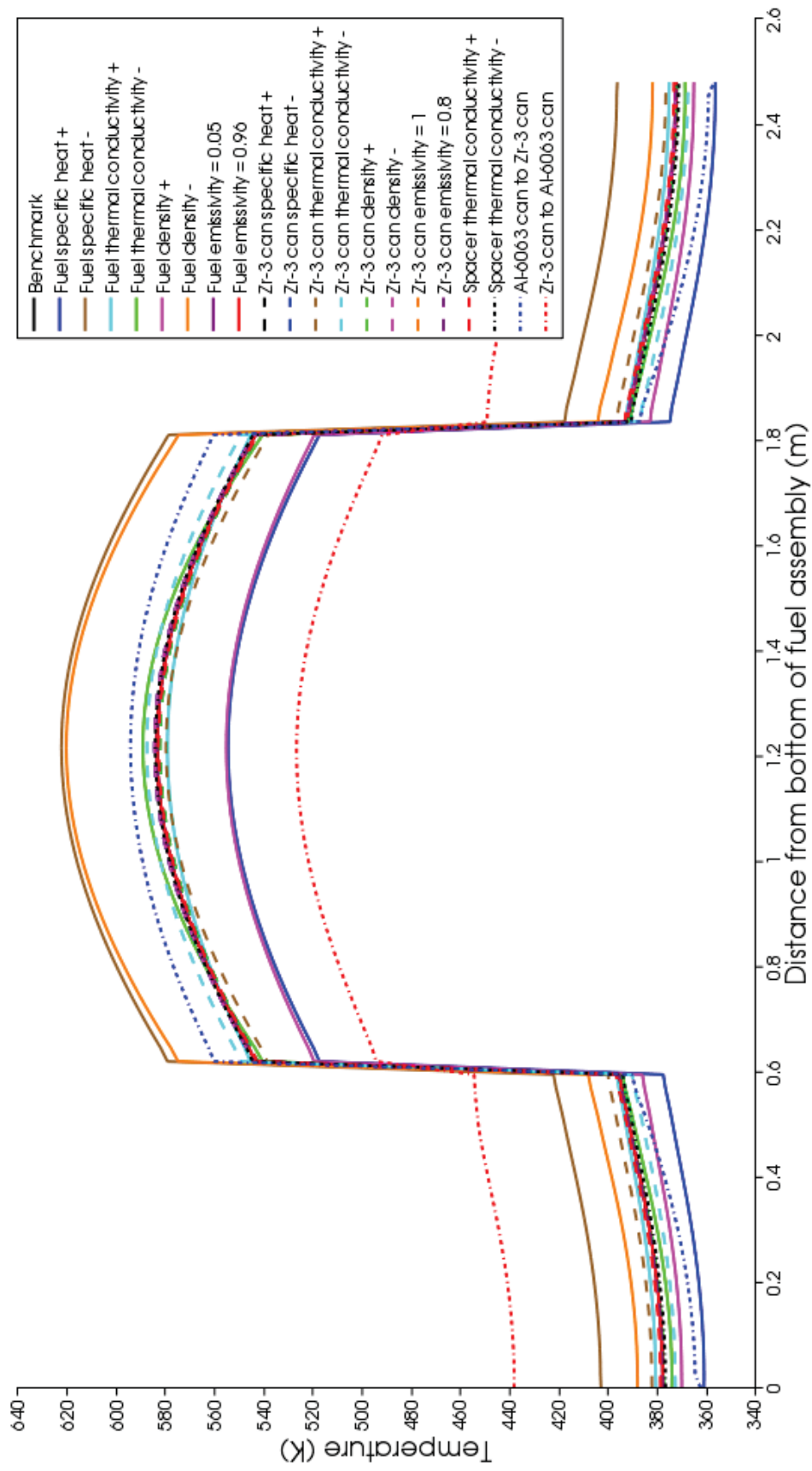


Figure 45: Axial temperature distribution 25,000 s after a 1000 MW-s transient.

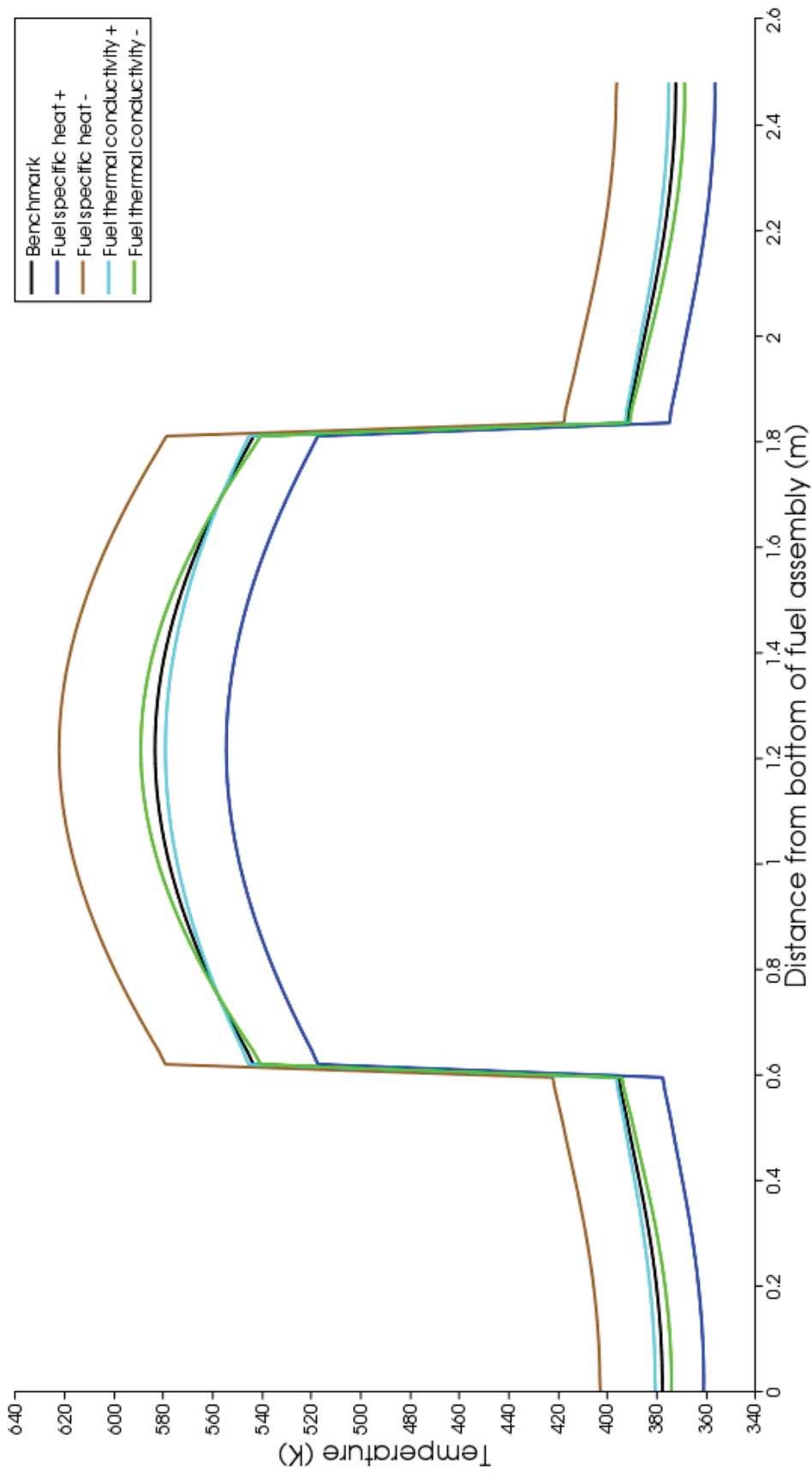


Figure 46: Benchmark compared against C_p and k . Both these properties affect temperature, however C_p has a greater effect.

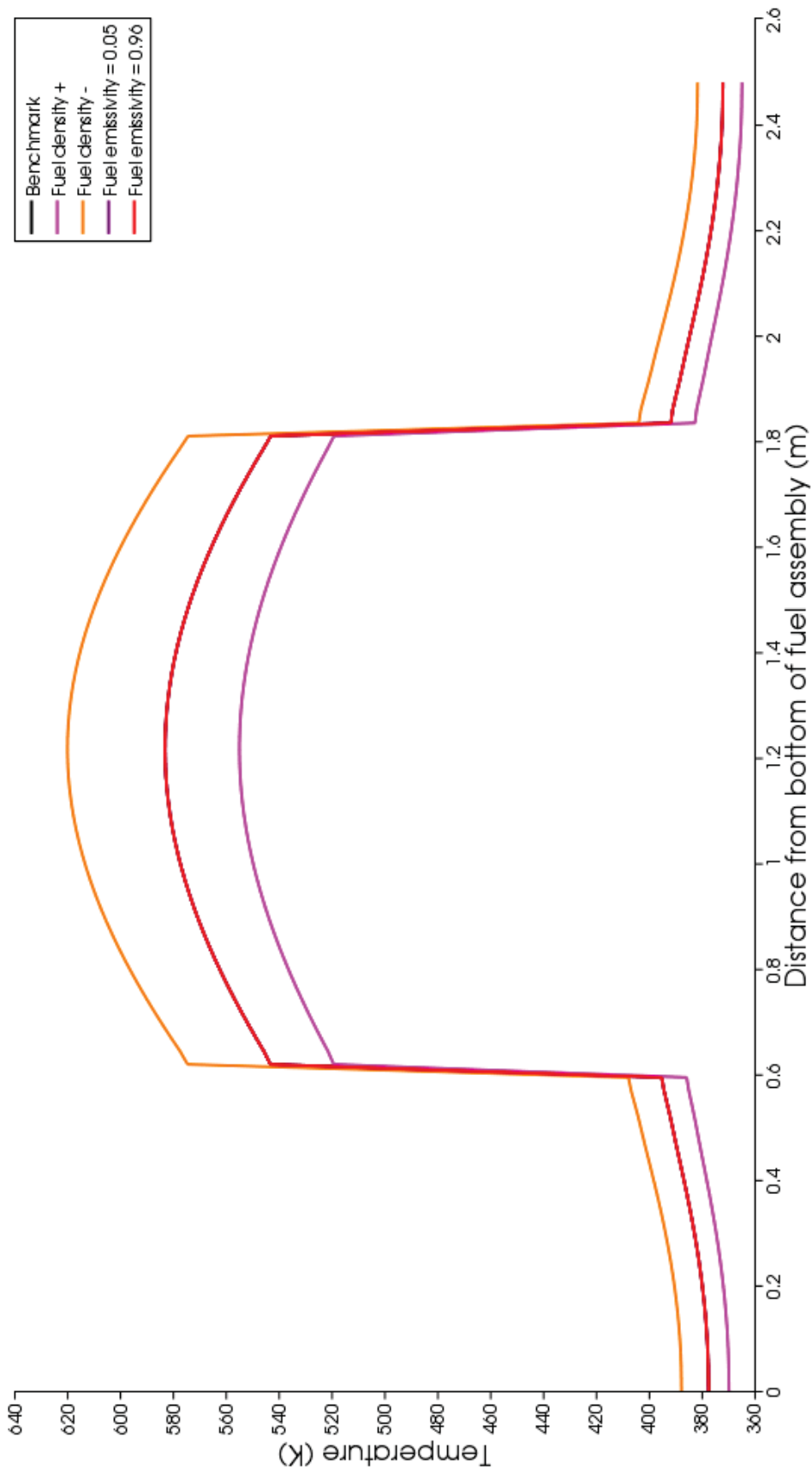


Figure 47: Benchmark compared against fuel ρ and ϵ . Fuel ϵ has negligible effects on temperature.

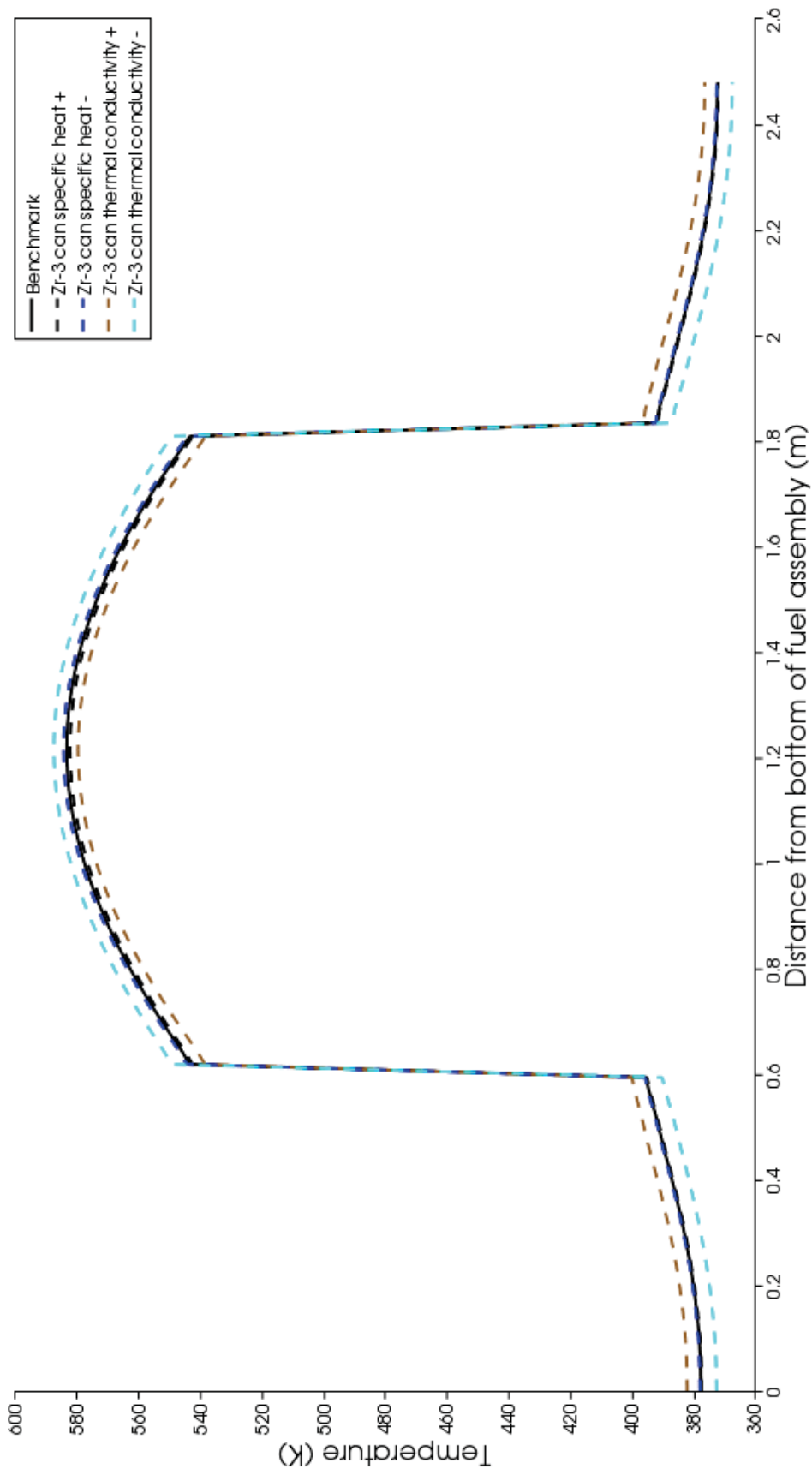


Figure 48: Benchmark compared against Zr-3 can C_p and k . Zr-3 C_p has negligible effects on temperature.

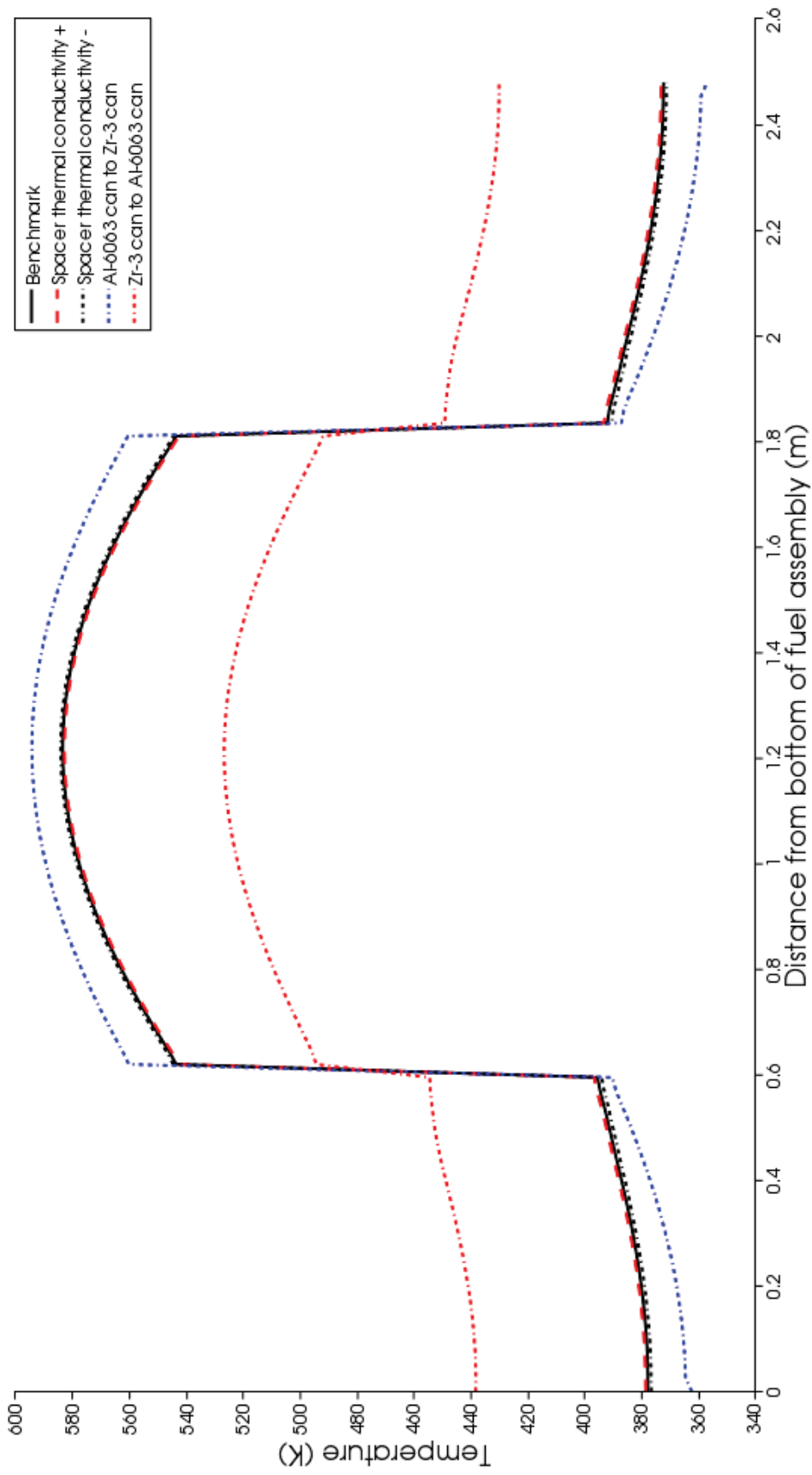


Figure 49: Benchmark compared against spacer k and canning material.

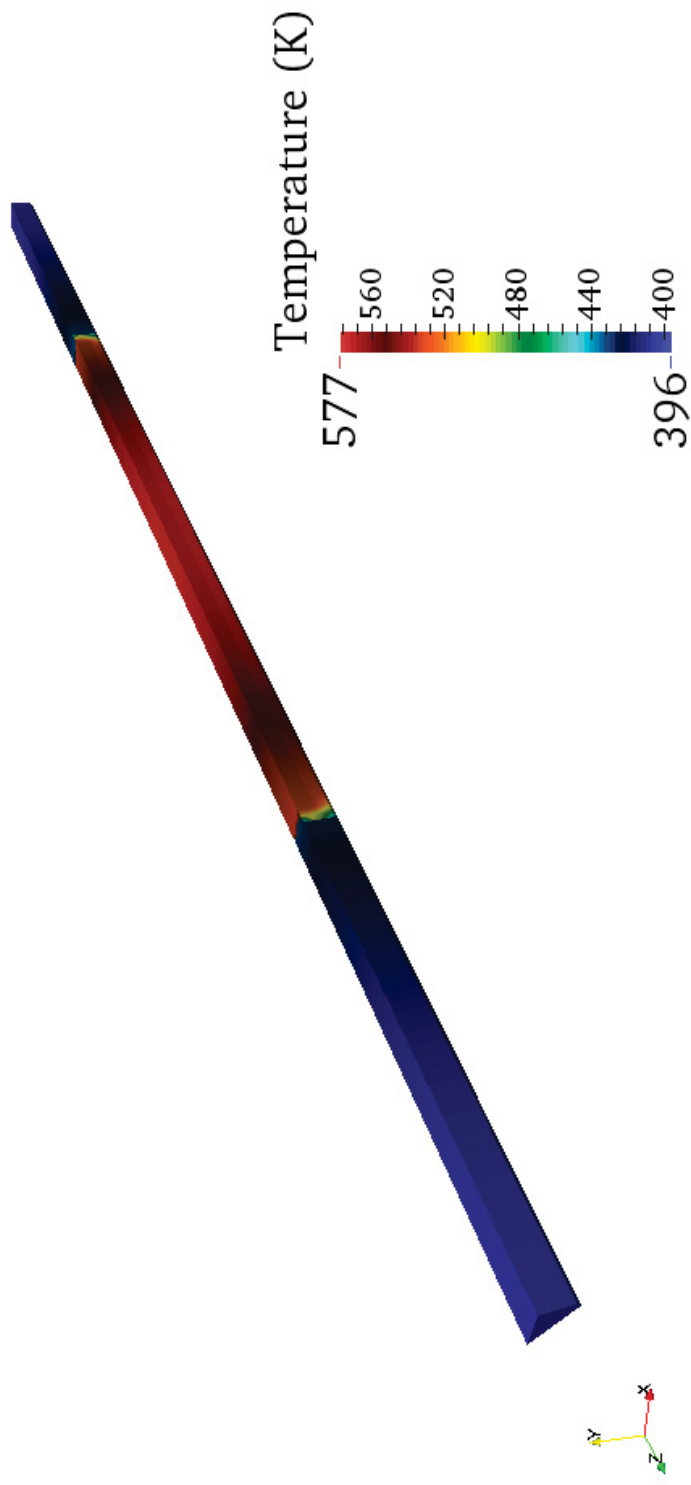


Figure 50: Temperature distribution 25,000 s after a 1000 MW-s transient. Shown is an octant of the fuel assembly.

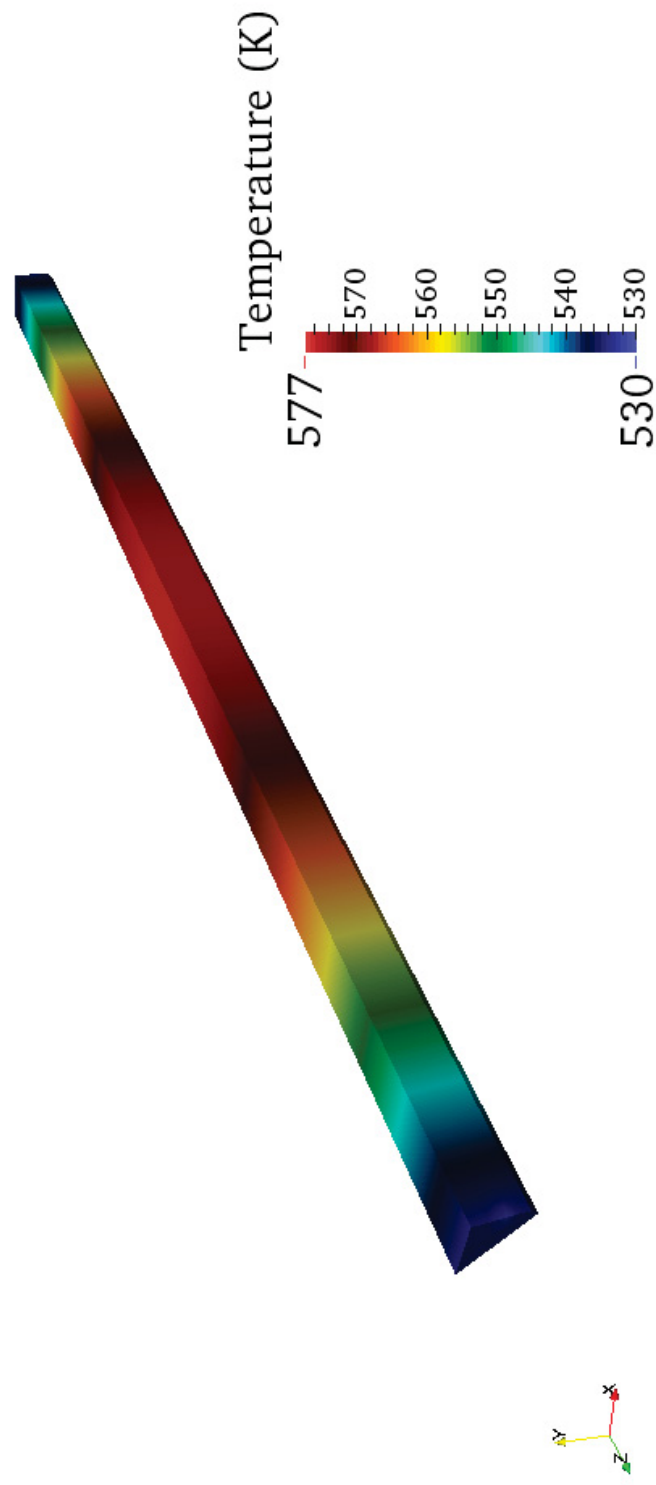


Figure 51: Axial temperature distribution of the fuel section.

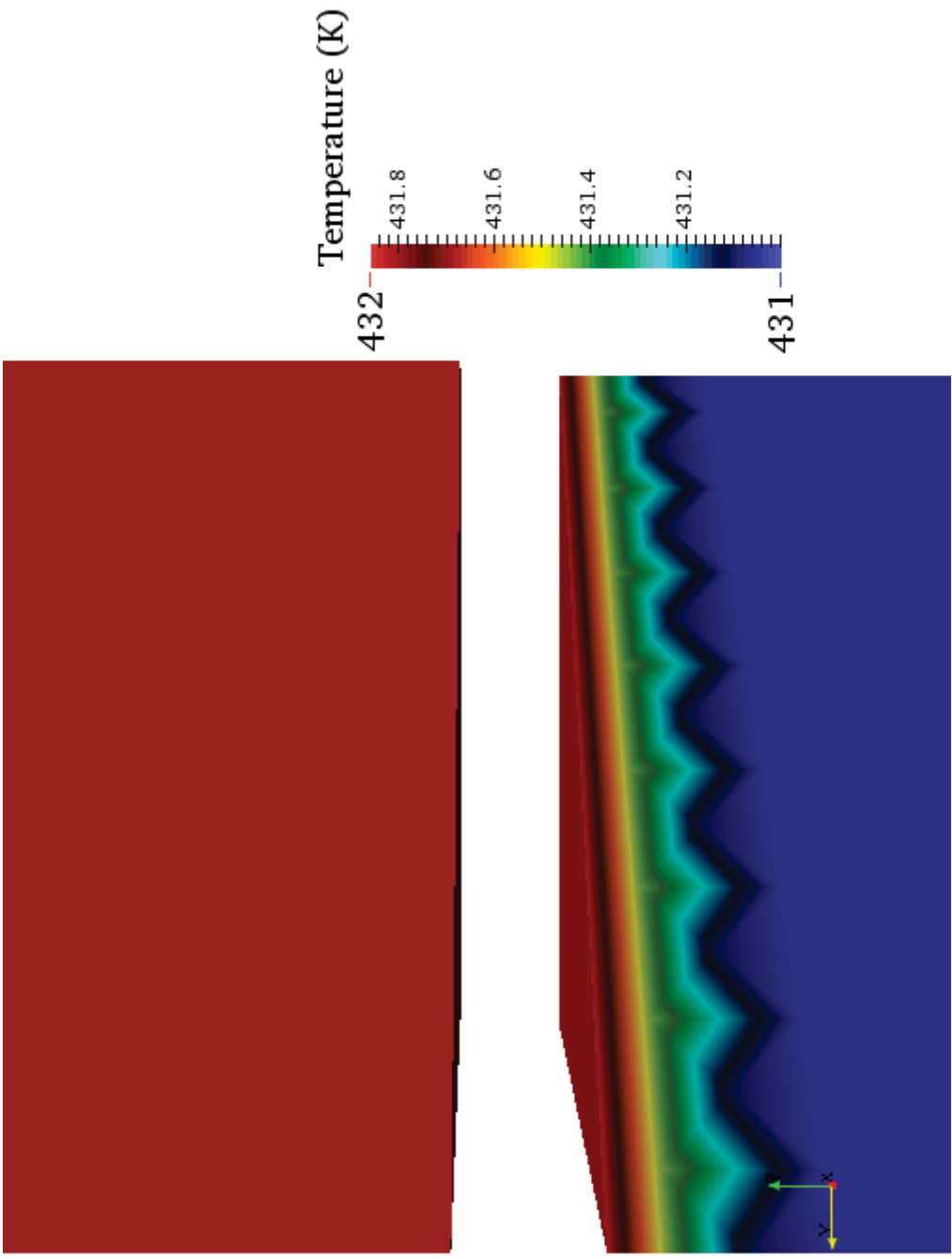


Figure 52: Fuel transferring heat across spacer to reflector.

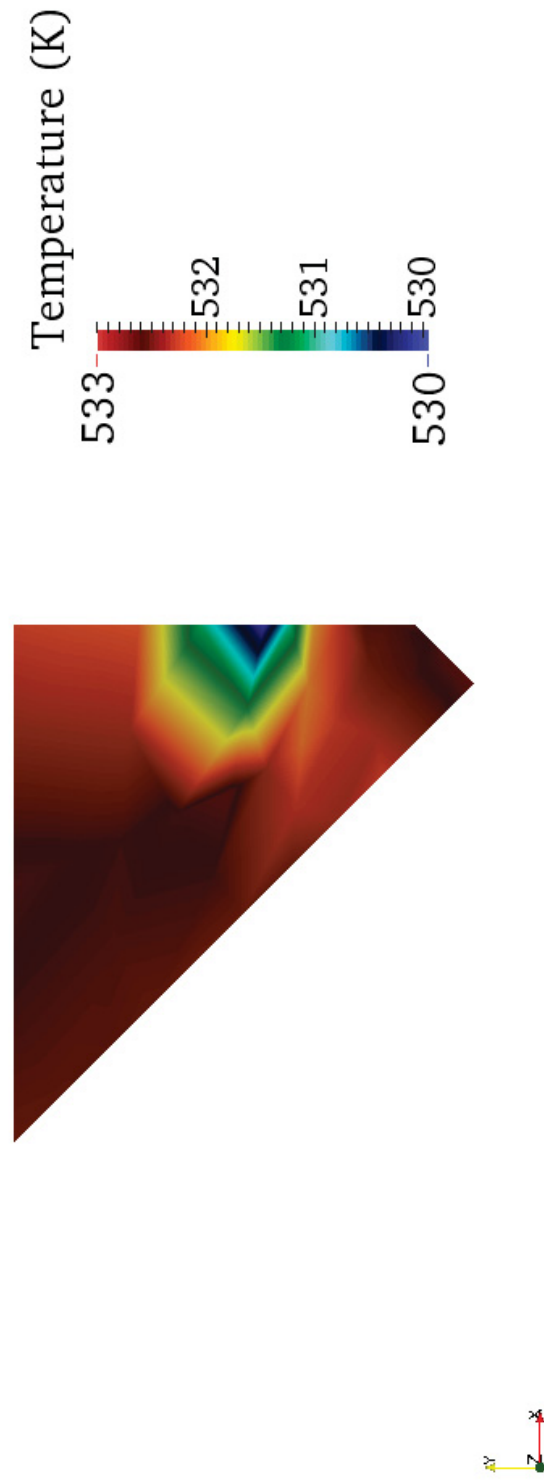


Figure 53: Radial temperature distribution of the fuel. Similar the steady state case the cooler spots where the Zr-3 can makes contact.

CHAPTER 5: CONCLUSION

A description of TREAT and its operating parameters was given. The method to developing the fuel assembly in BISON and associated computational tools was explained. An octant of a TREAT fuel assembly was modeled to best known conditions and then parametric studies were performed to understand the impacts.

BISON's ability to predict thermal behavior of the TREAT fuel assembly compares well to previously performed calculations and experimental data. For steady state the parameter that has the greatest effect is thermal conductivity. The changes in material properties were small and reflect material choices that would be similar to what exists in TREAT now. For simplification the effects of changing properties are reflected on each side of Equation 35. For steady state:

$$e_f \dot{F} = \nabla \cdot \mathbf{q} \quad (36)$$

For transients:

$$e_f \dot{F} = \rho C_p \frac{\partial T}{\partial t} \quad (37)$$

Or post transient:

$$0 = \nabla \cdot \mathbf{q} \quad (38)$$

Choosing a material with a high thermal conductivity has little effect at the termination of a transient (i.e. Zr-3 can to Al-6063 can) since heat transfer has not had sufficient time to take place (thermal capacity of the fuel dominates). Conversely density and specific heat have little effect on steady state scenarios but have significant effects on transients. In the steady state case thermal capacity of the fuel has been reached and temperature equilibrium has occurred so specific heat and density no longer contribute. Also seen in

Chapter 4 the changes in a material's emissivity have no significant effects on temperature. This is primarily because the cladding is in contact with the fuel.

From a thermal perspective in regard to protecting the fuel from temperature failure the best material choice would be one that has high thermal conductivity, high density, and high specific heat. A balance is needed to ensure the desired effect is obtained on the experiment in core (i.e. experimental fuel/material meltdown).

Still needed is a neutronics model that can be coupled to the thermal model. As seen in the plots generated in ParaView, assuming the fission rate is uniform throughout the fuel isn't realistic and may lead to discrepancies in parametric effects where temperature would be a stronger function of position in the fueled region. A neutronics model also gives greater confidence in material choice by ensuring the desired thermal and nuclear behavior coincides.

BISON currently has the ability to model energy deposition into a coolant channel containing water. The ability to also model an air-cooled channel would be beneficial to getting a more accurate temperature distribution. Obtaining outlet temperature readings from previously logs and flow rates are needed for comparison against such a model. Any measurable flow rate from natural convection would also help determine how much heat is removed from the core without coolant flow from the blower(s).

Gap closure was calculated using BISON's elastic model. Other documents mentioned there was gap closure as well, however, the extent of the closure is not known. Validating the calculations from BISON by measuring the real world fuel assembly's Zr-3 can deflection could prove useful.

The models developed were based off the original design of the TREAT. An understanding of the effects of increased safety limits and various operating conditions and transient types on the fuel model is needed.

REFERENCES

- [1] Argonne National Laboratory, TREAT Operations, Engineering Physics Division. (1992). Treat baseline description document (Z0003-0004-OJ-12)
- [2] MacFarlane, D. R., Freund, G. A., & Boland, J. F. Argonne National Laboratory, Reactor Engineering Division. (1958). Hazards summary report on the transient reactor test facility (treat) (ANL-5923)
- [3] Wolfensberger. Argonne National Laboratory, (1991). Treat reactor pictorial (DR Z0720-0424-EE-00)
- [4] Idaho National Laboratory, (2009). Transient reactor test facility (treat) final safety analysis report (S3942-0001-YT)
- [5] Bean, C. H., McCuaig, F. D., & Handwerk, J. H. Argonne National Laboratory, (1959). The fabrication of the fuel elements for the transient reactor test (ANL-FGF-162)
- [6] Freund, G. A., Elias, P., MacFarlane, D. R., Geier, J. D., & Boland, J. F. Argonne National Laboratory, Reactor Engineering Division. (1960). Design summary report on the transient reactor test facility (treat) (ANL-6034)
- [7] (2002). Engineering alloys digest. Zircaloy-3 (Corrosion and Heat Resistant Alloy), May(1969).
- [8] Ainscough, J. B. Organization for Economic Co-operation and Development, Nuclear Energy Agency. (1982). Gap conductance in zircaloy-clad lwr fuel rods (CSNI Report No. 72)
- [9] Properties of wrought aluminum and aluminum alloys. In (1990). ASM Handbook: Properties and Selection: Nonferrous Alloys and Special-Purpose Materials (Vol. 2, pp. 62-122).
- [10] Handwerk, J. H., & Lied, R. C. Argonne National Laboratory, Metallurgy and Ceramics. (1960). The manufacture of the graphite-urania fuel matrix for treat (ANL-5963)
- [11] Infrared Services Inc. (2014, Febuary 15). Emissivity values for common materials. Retrieved from www.infrared-thermography.com/material-1.htm
- [12] Ivany, R. Argonne National Laboratory, Reactor Engineering Division. (1959). Treat experimental heat transfer

- [13] Hetrick, D. L. Atomic Energy Commission, Atomic Energy Research Department. (1952). The effect of fuel particle size on the transient behavior of a homogeneous graphite reactor (NAA-SR-210)
- [14] Annaratone, D. (2010). Engineering heat transfer. (p. 93). Heidelberg Dordrecht London New York: Springer.
- [15] Dickerman, C. E., Johnson, R. D., & Gasidlo, J. Argonne National Laboratory, (1962). Kinetics of treat used as a test reactor (ANL-6458)
- [16] Kirtland, F., Boland, J., Lawroski, H., & Cook, R. Argonne National Laboratory, (1960). Reactor physics measurements in treat (ANL-6173)
- [17] Hales, J. D., Novascone, S. R., Pastore, G., Perez, D. M., Spencer, B. W., & Williamson, R. L. Idaho National Laboratory, Fuel Modeling and Simulation Department. (2013). Bison theory manual
- [18] Hales, J. D., Novascone, S. R., Pastore, G., Perez, D. M., Spencer, B. W., & Williamson, R. L. Idaho National Laboratory, Fuel Modeling and Simulation Department. (2013). Bison users manual
- [19] Perez, D. M., Williamson, R. L., Novascone, S. R., Pastore, G., Hales, J. D., Spencer, B. W., Idaho National Laboratory, Fuel Modeling and Simulation Department. (2013). Assessment of bison: a nuclear fuel performance analysis code
- [20] CUBIT Support. (2013, December 20). Cubit. Retrieved from <https://cubit.sandia.gov>
- [21] (2013, December 20). Paraview. Retrieved from www.paraview.org
- [22] Cengel, Y. A., & Ghajar, A. J. (2011). Heat and mass transfer. (4th ed., pp. 488-489). New York: McGraw Hill.

APPENDIX A: DRAWINGS

The drawings contained in Appendix A come from reference [1] Appendix B Volume 1 which is titled “TREAT Reactor Drawings”. The drawings were used to create the geometry in CUBIT. Table A-1 lists the drawings as seen in the following pages.

Table A-1: List of Drawings for a TREAT Fuel Assembly

Drawing Number	Description	Figure
RE-1-21094-D	TREAT Fuel Assembly	A1
RE-1-21578-A	Fuel Block	A2
RE-1-21768-A	Plug Long	A3
RE-1-22739-A	Plug- Plain Short	A4
RE-1-21767-A	Plug-Short	A5
RE-1-22736-B	End Tube	A6
RE-1-21717-C	Fuel Section	A7
RE-1-22699-B	Tab	A8
RE-1-24160-B	Spacer	A9
RE-1-21880-B	Fitting - Top Fuel	A10
RE-1-21881-B	Fitting - Bottom Fuel	A11

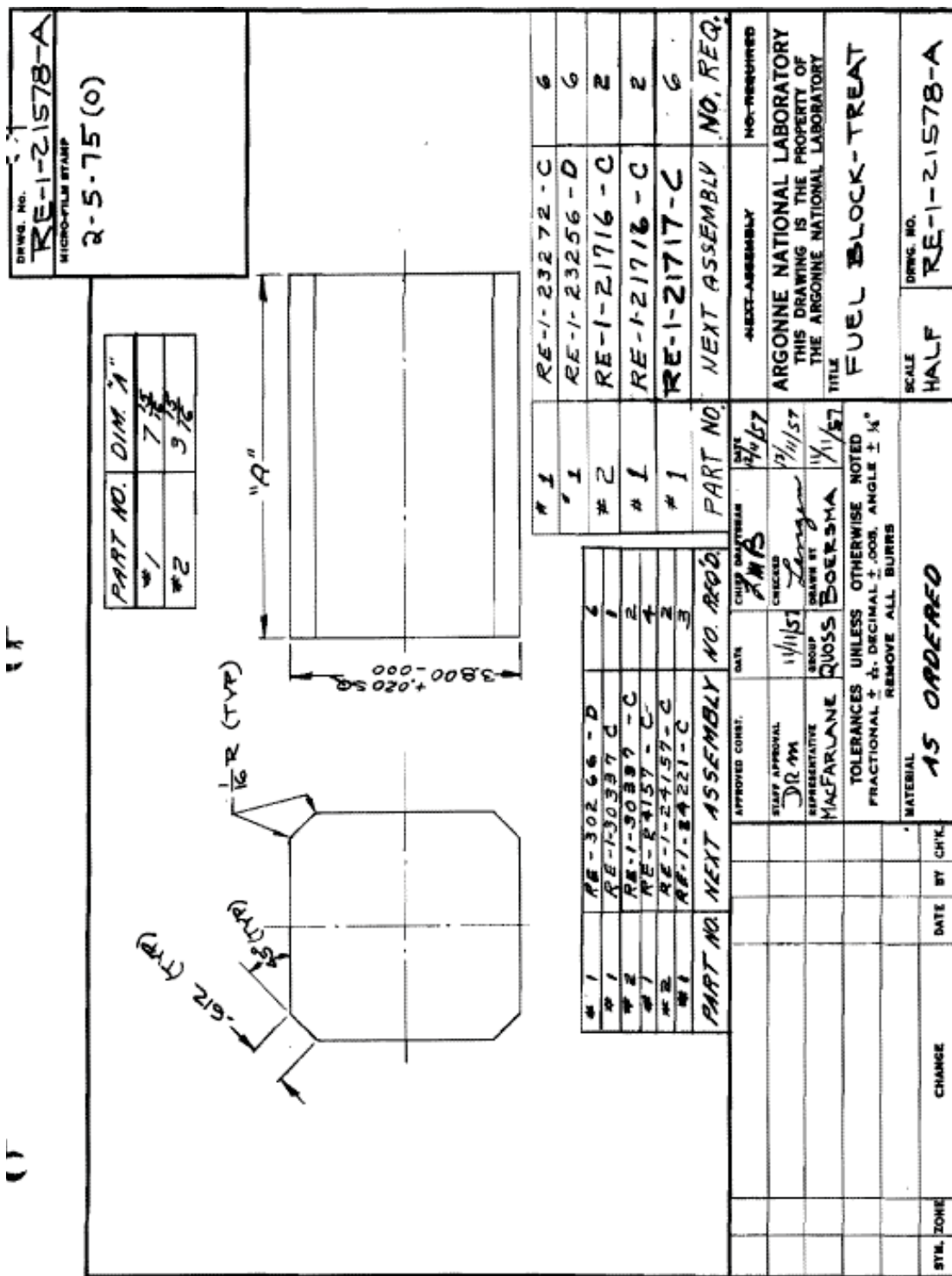


Figure A2: TREAT Fuel Assembly Fuel Block.

(1)

(1)

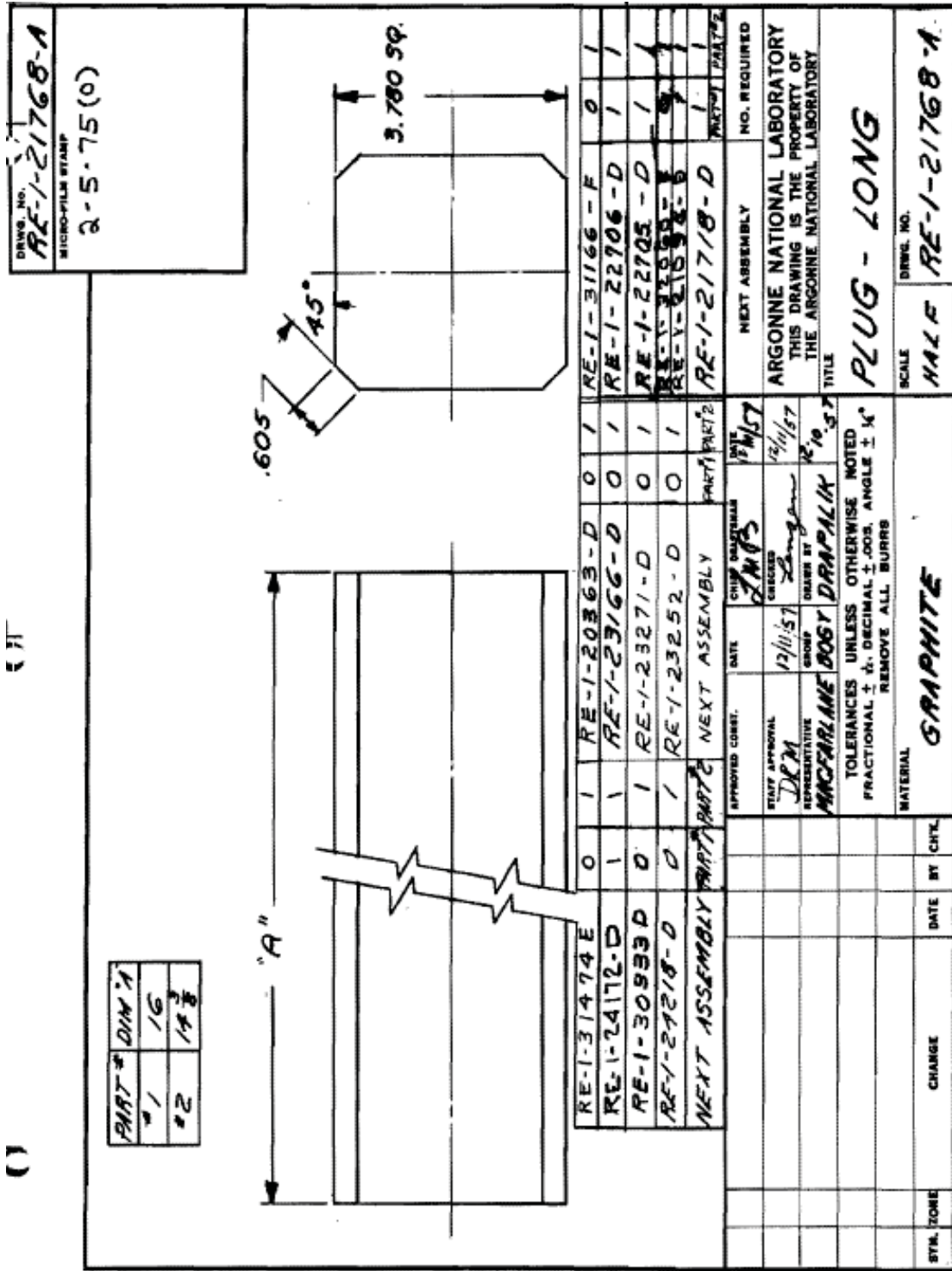


Figure A3: TREAT Fuel Assembly Reflector Block (Long).

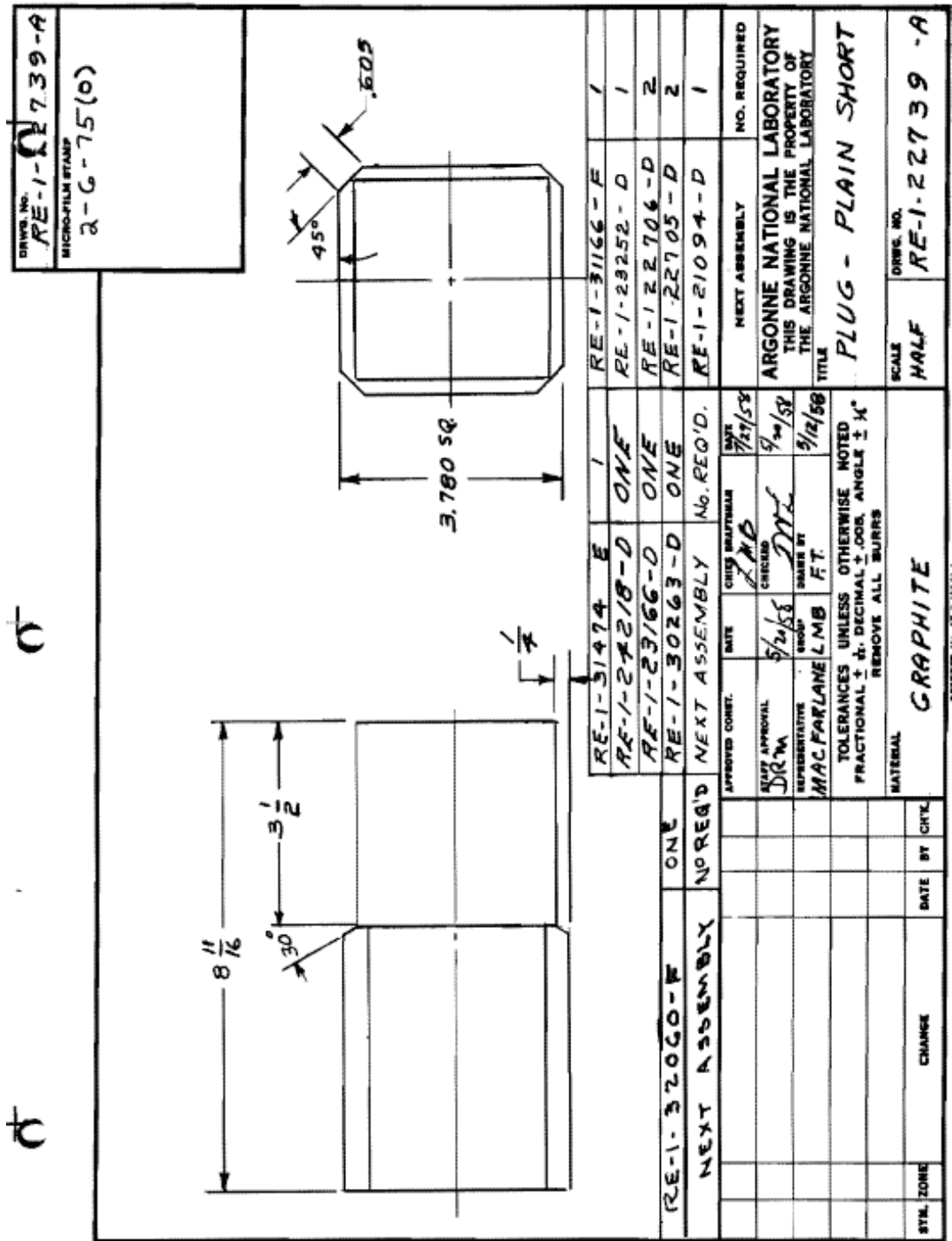
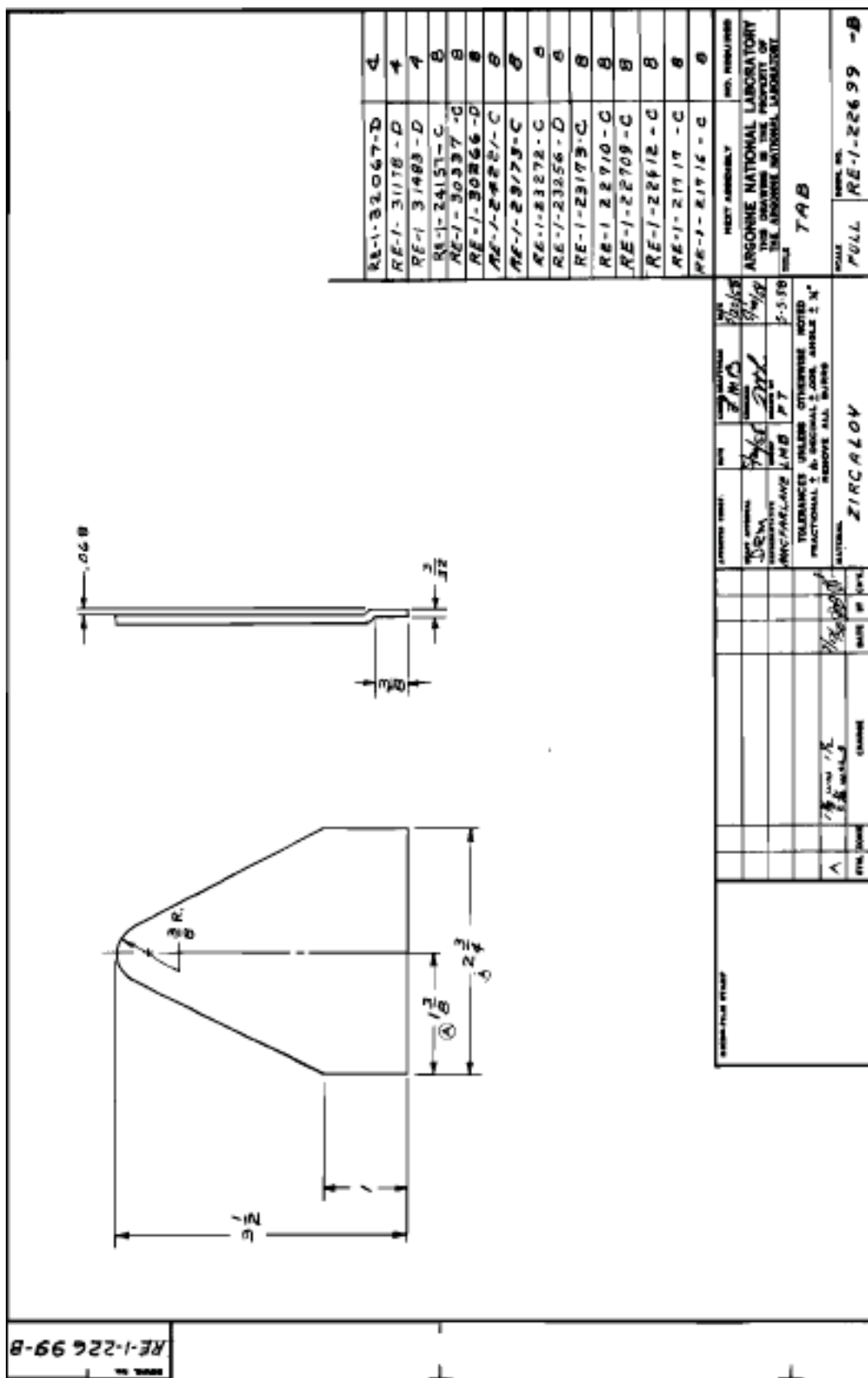
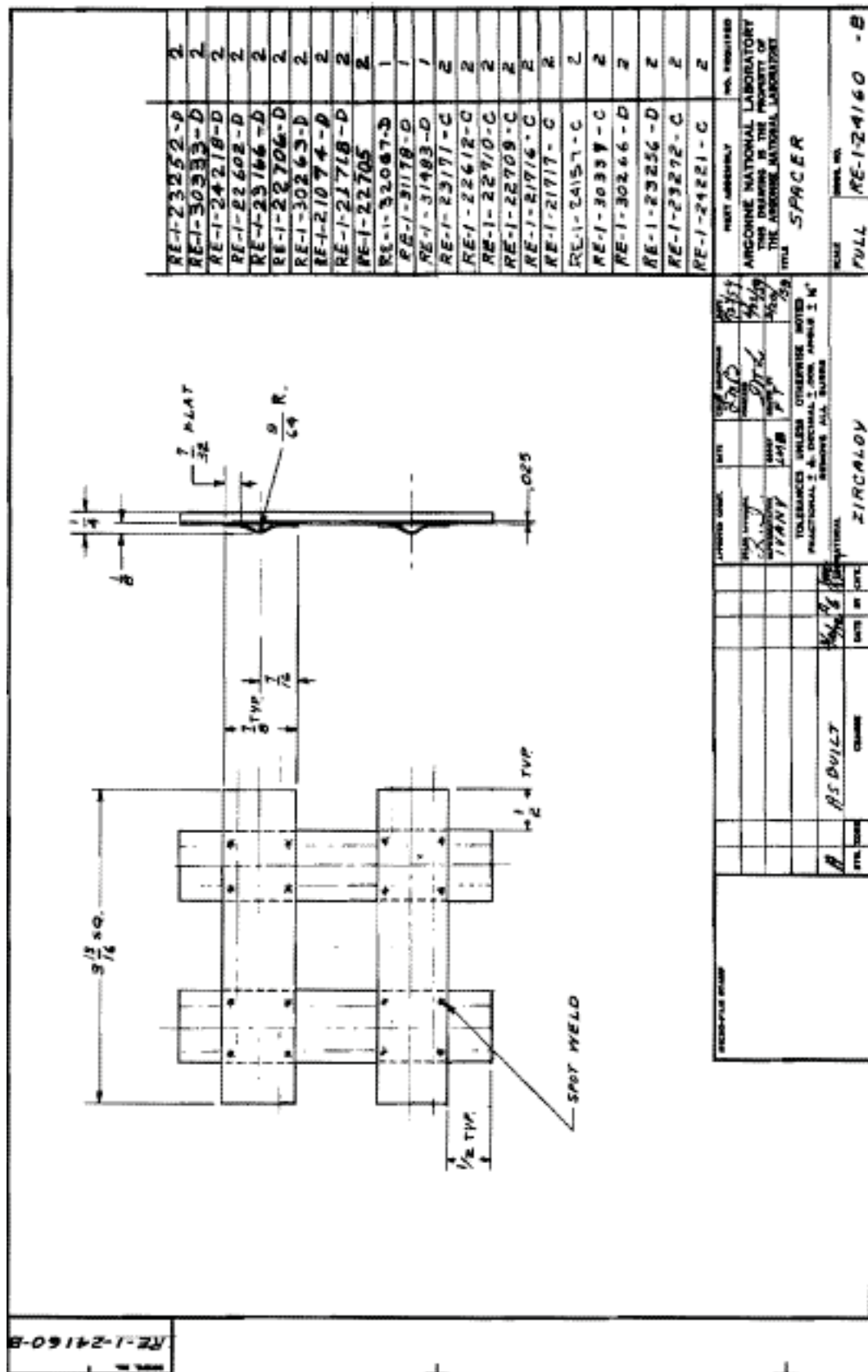


Figure A4: TREAT Fuel Assembly Reflector Block (Short).



Figure A7: TREAT Fuel Assembly Fuel Section.





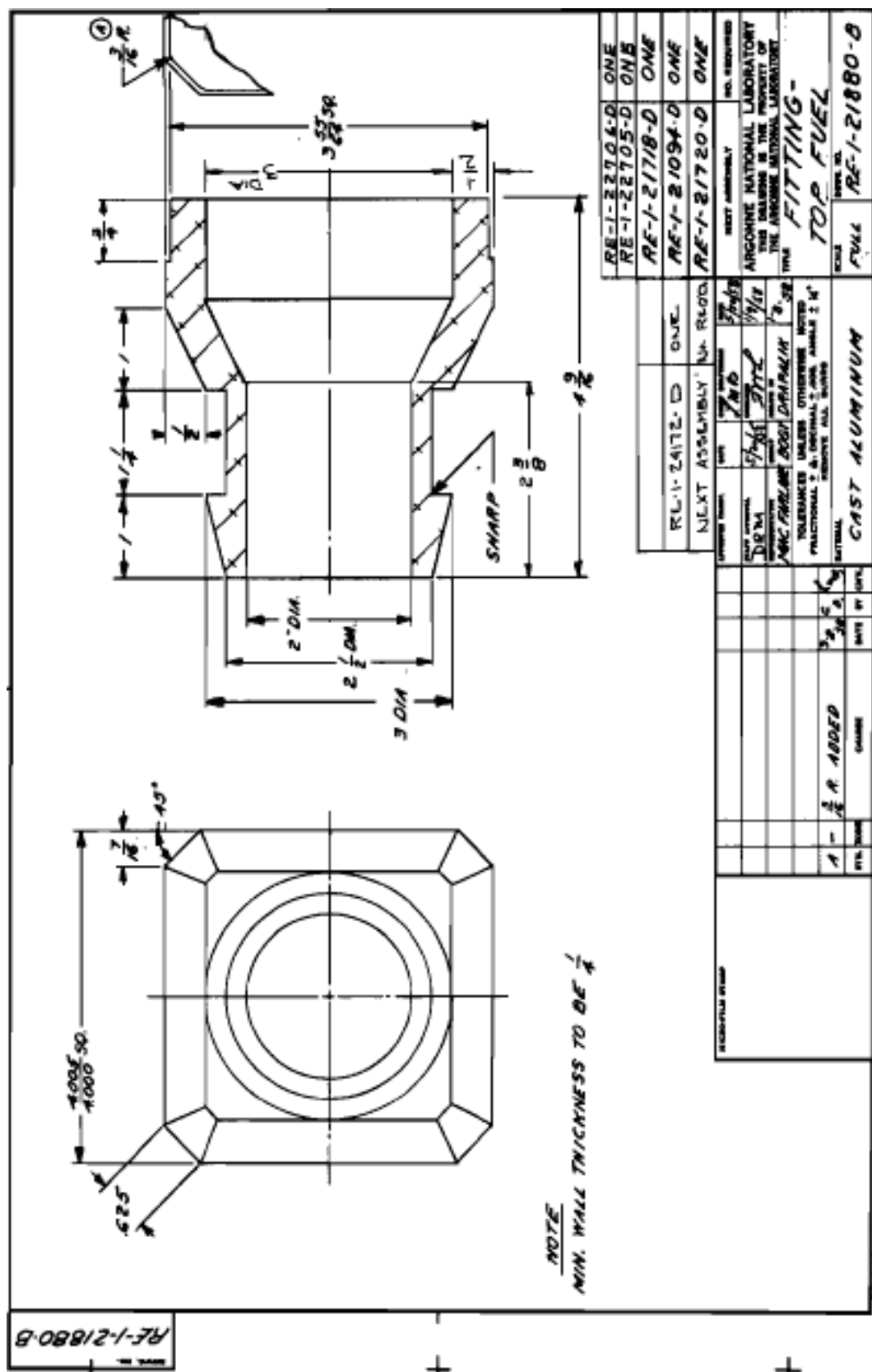


Figure A10: TREAT Fuel Assembly Top handling fixture for TREAT fuel element.

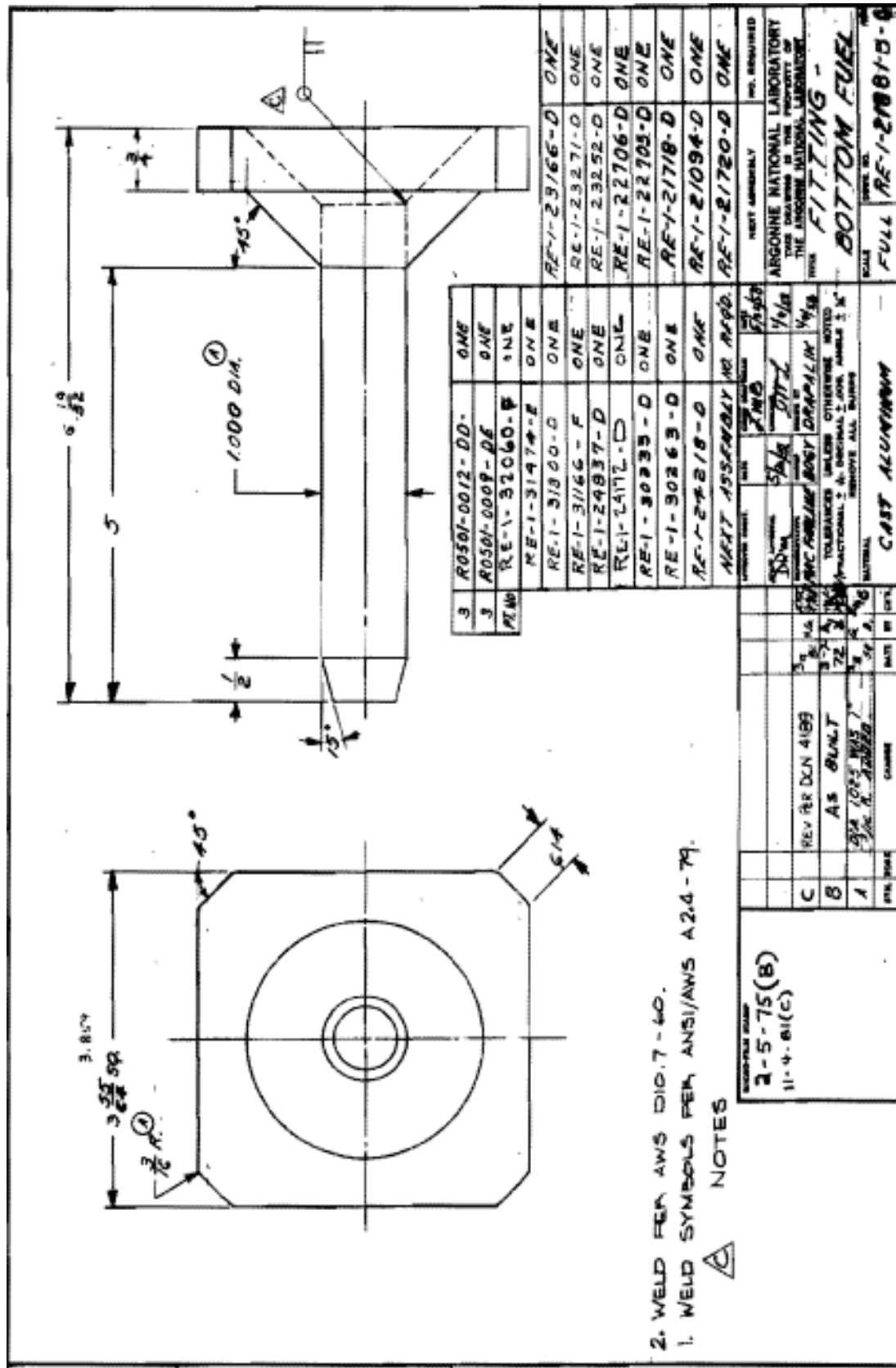


Figure A11: TREAT Fuel Assembly bottom support pin.

APPENDIX B: MESH FILE

```
#####
#####
reset
##Starting from bottom
##Reflector Block Coordinates
create vertex 0.03713989 0.048006 0.01905
create vertex 0.048006 0.03713989 0.01905
create vertex 0.048006 -0.03713989 0.01905
create vertex 0.03713989 -0.048006 0.01905
create vertex -0.03713989 -0.048006 0.01905
create vertex -0.048006 -0.03713989 0.01905
create vertex -0.048006 0.03713989 0.01905
create vertex -0.03713989 0.048006 0.01905
##Fuel Block Coordinates
create vertex 0.037268167 0.04826 0.61355
create vertex 0.04826 0.037268167 0.61355
create vertex 0.04826 -0.037268167 0.61355
create vertex 0.037268167 -0.04826 0.61355
create vertex -0.037268167 -0.04826 0.61355
create vertex -0.04826 -0.037268167 0.61355
create vertex -0.04826 0.037268167 0.61355
create vertex -0.037268167 0.04826 0.61355
##Al cladding Coordinates
##Outside Coordinates
create vertex 0.03906668 0.050292 0
create vertex 0.050292 0.03906668 0
create vertex 0.050292 -0.03906668 0
create vertex 0.03906668 -0.050292 0
create vertex -0.03906668 -0.050292 0
create vertex -0.050292 -0.03906668 0
create vertex -0.050292 0.03906668 0
create vertex -0.03906668 0.050292 0
##Inside Coordinates
create vertex 0.03827793 0.049022 0.01905
create vertex 0.049022 0.03827793 0.01905
create vertex 0.049022 -0.03827793 0.01905
create vertex 0.03827793 -0.049022 0.01905
create vertex -0.03827793 -0.049022 0.01905
create vertex -0.049022 -0.03827793 0.01905
create vertex -0.049022 0.03827793 0.01905
create vertex -0.03827793 0.049022 0.01905
##Zr cladding Coordinates
##Undeformed
##Outside Coordinates
create vertex 0.03906668 0.050292 0.59134
create vertex 0.050292 0.03906668 0.59134
create vertex 0.050292 -0.03906668 0.59134
create vertex 0.03906668 -0.050292 0.59134
create vertex -0.03906668 -0.050292 0.59134
create vertex -0.050292 -0.03906668 0.59134
create vertex -0.050292 0.03906668 0.59134
create vertex -0.03906668 0.050292 0.59134
##Inside Coordinates
create vertex 0.038672305 0.049657 0.59134
create vertex 0.049657 0.038672305 0.59134
create vertex 0.049657 -0.038672305 0.59134
create vertex 0.038672305 -0.049657 0.59134
create vertex -0.038672305 -0.049657 0.59134
create vertex -0.049657 -0.038672305 0.59134
```

```

create vertex -0.049657 0.038672305 0.59134
create vertex -0.038672305 0.049657 0.59134
##Reflector help cut Coordinates
create vertex 0.03827793 0.049022 0.60484
create vertex 0.049022 0.03827793 0.60484
create vertex 0.049022 -0.03827793 0.60484
create vertex 0.03827793 -0.049022 0.60484
create vertex -0.03827793 -0.049022 0.60484
create vertex -0.049022 -0.03827793 0.60484
create vertex -0.049022 0.03827793 0.60484
create vertex -0.03827793 0.049022 0.60484
##Square Reflector Cut Coordinates
creat vertex 0.041656 0.041656 0.60484
creat vertex 0.041656 -0.041656 0.60484
creat vertex -0.041656 -0.041656 0.60484
creat vertex -0.041656 0.041656 0.60484
##Zirc Spacer Cut Coordinates
##Cut 1 Coordinates
create vertex 0.01349375 0.01349375 0.60720
create vertex 0.01349375 -0.01349375 0.60720
create vertex -0.01349375 -0.01349375 0.60720
create vertex -0.01349375 0.01349375 0.60720
##Cut 2 Coordinates
create vertex 0.04841875 0.03571875 0.60720
create vertex 0.04841875 0.01349375 0.60720
create vertex 0.03571875 0.01349375 0.60720
create vertex 0.03571875 -0.01349375 0.60720
create vertex 0.04841875 -0.01349375 0.60720
create vertex 0.04841875 -0.03571875 0.60720
create vertex 0.03571875 -0.03571875 0.60720
create vertex 0.03571875 -0.04841875 0.60720
create vertex 0.01349375 -0.04841875 0.60720
create vertex 0.01349375 -0.03571875 0.60720
create vertex -0.01349375 -0.03571875 0.60720
create vertex -0.01349375 -0.04841875 0.60720
create vertex -0.03571875 -0.04841875 0.60720
create vertex -0.03571875 -0.03571875 0.60720
create vertex -0.04841875 -0.03571875 0.60720
create vertex -0.04841875 -0.01349375 0.60720
create vertex -0.03571875 -0.01349375 0.60720
create vertex -0.03571875 0.01349375 0.60720
create vertex -0.04841875 0.01349375 0.60720
create vertex -0.04841875 0.03571875 0.60720
create vertex -0.03571875 0.03571875 0.60720
create vertex -0.03571875 0.04841875 0.60720
create vertex -0.01349375 0.04841875 0.60720
create vertex -0.01349375 0.03571875 0.60720
create vertex 0.01349375 0.03571875 0.60720
create vertex 0.01349375 0.04841875 0.60720
create vertex 0.03571875 0.04841875 0.60720
create vertex 0.03571875 0.03571875 0.60720
##End of Coordinates
##Create curves
##Reflector Block Curves
create curve vertex 1 2
create curve vertex 2 3
create curve vertex 3 4
create curve vertex 4 5
create curve vertex 5 6
create curve vertex 6 7
create curve vertex 7 8
create curve vertex 8 1
##Fuel Block Curves
create curve vertex 9 10

```

```

create curve vertex 10 11
create curve vertex 11 12
create curve vertex 12 13
create curve vertex 13 14
create curve vertex 14 15
create curve vertex 15 16
create curve vertex 16 9
##Al Cladding Curves
##Outside Curves
create curve vertex 17 18
create curve vertex 18 19
create curve vertex 19 20
create curve vertex 20 21
create curve vertex 21 22
create curve vertex 22 23
create curve vertex 23 24
create curve vertex 24 17
##Inside Curves
create curve vertex 25 26
create curve vertex 26 27
create curve vertex 27 28
create curve vertex 28 29
create curve vertex 29 30
create curve vertex 30 31
create curve vertex 31 32
create curve vertex 32 25
##Zr Cladding Curves
##Undeformed
##Outside Curves
create curve vertex 33 34
create curve vertex 34 35
create curve vertex 35 36
create curve vertex 36 37
create curve vertex 37 38
create curve vertex 38 39
create curve vertex 39 40
create curve vertex 40 33
##Inside Curves
create curve vertex 41 42
create curve vertex 42 43
create curve vertex 43 44
create curve vertex 44 45
create curve vertex 45 46
create curve vertex 46 47
create curve vertex 47 48
create curve vertex 48 41
##Zr End Cap Cut Curves
create curve vertex 49 50
create curve vertex 50 51
create curve vertex 51 52
create curve vertex 52 53
create curve vertex 53 54
create curve vertex 54 55
create curve vertex 55 56
create curve vertex 56 49
##Square Reflector Cut Curves
create curve vertex 57 58
create curve vertex 58 59
create curve vertex 59 60
create curve vertex 60 57
##Zirc spacer cut Curves
create curve vertex 61 62
create curve vertex 62 63
create curve vertex 63 64

```

```

create curve vertex 64 61
create curve vertex 65 66
create curve vertex 66 67
create curve vertex 67 68
create curve vertex 68 69
create curve vertex 69 70
create curve vertex 70 71
create curve vertex 71 72
create curve vertex 72 73
create curve vertex 73 74
create curve vertex 74 75
create curve vertex 75 76
create curve vertex 76 77
create curve vertex 77 78
create curve vertex 78 79
create curve vertex 79 80
create curve vertex 80 81
create curve vertex 81 82
create curve vertex 82 83
create curve vertex 83 84
create curve vertex 84 85
create curve vertex 85 86
create curve vertex 86 87
create curve vertex 87 88
create curve vertex 88 89
create curve vertex 89 90
create curve vertex 90 91
create curve vertex 91 92
create curve vertex 92 65
##End curves
##Create Surfaces
##Reflector Block Surface
create surface curve 1 2 3 4 5 6 7 8
##Fuel Block Surface
create surface curve 9 10 11 12 13 14 15 16
##Al Cladding Surface
##Outside Surface
create surface curve 17 18 19 20 21 22 23 24
##Inside Surface
create surface curve 25 26 27 28 29 30 31 32
##Zr Cladding Surface
##Undeformed
##Outside Surface
create surface curve 33 34 35 36 37 38 39 40
##Inside Surface
create surface curve 41 42 43 44 45 46 47 48
##Square reflector help cut Surface
create surface curve 49 50 51 52 53 54 55 56
##Square Reflector Cut Surface
create surface curve 57 58 59 60
##Zr Spacer Cut Surface
create surface curve 61 62 63 64
create surface curve 65 66 67 68 69 70 71 72 73 74 75 76 77 78 79 80 81 82 83 84 85 86 87
88 89 90 91 92
##End of surface ##These create surface bodies
##Start surface copies ##These create surface bodies
surface 1 copy move z 0.36513 ##to end long RB bottom and start short RB bottom
surface 11 copy move z 0.22066 ##to end short RB bottom
surface 2 copy move z 0.20161 repeat 6 ##fuel blocks ##repeated six times for 6 fuel
blocks
surface 3 copy move z 0.59134375 ##to end al clad outside bottom
surface 4 copy move z 0.5913437 ##to end al clad inside bottom
surface 5 copy move z 1.254125 ##to end zr clad outside
surface 6 copy move z 1.254125 ##to end zr clad inside
surface 12 copy move z 1.2271 ##to start top short RB

```

```

surface 23 copy move z 0.22066 ##to end top short and start long RB
surface 24 copy move z 0.40640 ##to end top long RB
surface 3 copy move z 1.84547 ##to start top al clad outside
surface 4 copy move z 1.82642 ##to start top al clad inside
surface 26 copy move z 0.63261875 ##to end top al clad outside
surface 27 copy move z 0.61357 ##to end top al clad inside
surface 7 copy move z -0.0889 ##to finish bottom cut help
surface 8 copy move z -0.0889 ##to finish bottom cut
surface 7 copy move z 1.2271 ##to start top cut
surface 8 copy move z 1.2271 ##to start top cut
surface 32 copy move z 0.0889 ##to end top cut
surface 33 copy move z 0.0889 ##to end top cut
surface 9 copy move z 0.00635 ##to end spacer bottom cut
surface 10 copy move z 0.00635 ##to end spacer bottom cut
surface 9 copy move z 1.21603 ##to start top spacer cut
surface 10 copy move z 1.21603 ##to start top spacer cut
surface 38 copy move z 0.00635 ##to end top spacer cut
surface 39 copy move z 0.00635 ##to end top spacer cut
##end of surfaces
##start volumes
create volume loft surface 1 11 ##long reflector bottom block vol 42
create volume loft surface 11 12 ##short reflector bottom block vol 43
create volume loft surface 2 13 ##fuel block 1 vol 44
create volume loft surface 13 14 ##fuel block 2 vol 45
create volume loft surface 14 15 ##fuel block 3 vol 46
create volume loft surface 15 16 ##fuel block 4 vol 47
create volume loft surface 16 17 ##fuel block 5 vol 48
create volume loft surface 17 18 ##fuel block 6 vol 49
create volume loft surface 23 24 ##short reflector top block vol 50
create volume loft surface 24 25 ##long reflector top block vol 51
create volume loft surface 3 19 ##aluminum can outside bottom vol 52
create volume loft surface 4 20 ##aluminum can inside bottom vol 53
create volume loft surface 5 21 ##zr can outside vol 54
create volume loft surface 6 22 ##zr can inside vol 55
create volume loft surface 26 28 ##aluminum can outside top vol 56
create volume loft surface 27 29 ##aluminum can inside top vol 57
create volume loft surface 7 30 ##bottom reflector block cut vol 58
create volume loft surface 8 31 ##bottom reflector block cut vol 59
create volume loft surface 32 34 ##top reflector block cut vol 60
create volume loft surface 33 35 ##top reflector block cut vol 61
create volume loft surface 9 36 ##spacer cut bottom vol 62
create volume loft surface 10 37 ##spacer cut bottom vol 63
create volume loft surface 38 40 ##spacer cut top vol 64
create volume loft surface 39 41 ##spacer cut top vol 65
##delete all surface bodies that were used to create volumes
delete volume 1 2 3 4 5 6 7 8 9 10 11 12 13 14 15 16 17 18 19 20 21 22
delete volume 23 24 25 26 27 28 29 30 31 32 33 34 35 36 37 38 39 40 41
##subtract volume 51 from volume 50
subtract volume 53 from volume 52 ##complete aluminum bottom can
subtract volume 55 from volume 54 ##complete zr can
subtract volume 61 from volume 60 ##create reflector cut top
subtract volume 62 from volume 63 ##create cut spacer
subtract volume 60 from volume 50 ##complete top reflector cut
subtract volume 57 from volume 56 ##complete aluminum top can
subtract volume 59 from volume 58 ##create reflector cut bottom
subtract volume 64 from volume 65 ##create cut spacer
subtract volume 58 from volume 43 ##complete spacer cut
##creating the end cap for the zr can
##end cap coordinates
create vertex 0.037268167 0.04826 0.60484
create vertex 0.04826 0.037268167 0.60484
create vertex 0.04826 -0.037268167 0.60484
create vertex 0.037268167 -0.04826 0.60484
create vertex -0.037268167 -0.04826 0.60484

```

```

create vertex -0.04826 -0.037268167 0.60484
create vertex -0.04826 0.037268167 0.60484
create vertex -0.037268167 0.04826 0.60484
##end cap curves
create curve vertex 1013 1014
create curve vertex 1014 1015
create curve vertex 1015 1016
create curve vertex 1016 1017
create curve vertex 1017 1018
create curve vertex 1018 1019
create curve vertex 1019 1020
create curve vertex 1020 1013
##end cap surface
create surface curve 1201 1202 1203 1204 1205 1206 1207 1208
##create surface copies for volumes
surface 388 copy move z 0.00236 ##ends bottom end cap
create volume loft surface 388 389 ##complete bottom end cap
volume 68 copy move z 1.22474 ##complete top end cap
#####
#####
##At this point a complete geometry is created but there was difficultly
##meshing portions of the geometry. Run the problem down to here to
##see the geometry.
##From this point we delete the undeformed zr can (54), the spacers (63 65),
##and the sheet bodies (66 67) that were used to create the end caps.
#####
#####
delete volume 54 66 67 63 65
## Zr cladding coordinates undeformed
create vertex 0.0390667 0.050292 0.59134
create vertex 0.050292 0.0390667 0.59134
create vertex 0.050292 -0.0390667 0.59134
create vertex 0.0390667 -0.050292 0.59134
create vertex -0.0390667 -0.050292 0.59134
create vertex -0.050292 -0.0390667 0.59134
create vertex -0.050292 0.0390667 0.59134
create vertex -0.0390667 0.050292 0.59134
create vertex 0.0388037 0.049657 0.59134
create vertex 0.049657 0.0388037 0.59134
create vertex 0.049657 -0.0388037 0.59134
create vertex 0.0388037 -0.049657 0.59134
create vertex -0.0388037 -0.049657 0.59134
create vertex -0.049657 -0.0388037 0.59134
create vertex -0.049657 0.0388037 0.59134
create vertex -0.0388037 0.049657 0.59134
##zr cladding coordinates deformed
##Starting at top right corner (outside coordinates)
create vertex 0.0390666786 0.0502919984 0.61355
create vertex 0.0502919984 0.0390666786 0.61355
create vertex 0.0488949984 0.023440007 0.61355
create vertex 0.0488949984 -0.023440007 0.61355
create vertex 0.0502919984 -0.0390666786 0.61355
create vertex 0.0390666786 -0.0502919984 0.61355
create vertex 0.023440007 -0.0488949984 0.61355
create vertex -0.023440007 -0.0488949984 0.61355
create vertex -0.0390666786 -0.0502919984 0.61355
create vertex -0.0502919984 -0.0390666786 0.61355
create vertex -0.0488949984 -0.023440007 0.61355
create vertex -0.0488949984 0.023440007 0.61355
create vertex -0.0502919984 0.0390666786 0.61355
create vertex -0.0390666786 0.0502919984 0.61355
create vertex -0.023440007 0.0488949984 0.61355
create vertex 0.023440007 0.0488949984 0.61355
##Starting at top right corner (inside coordinates)

```



```

create vertex 0.0388036530 0.0496569984 0.61355
create vertex 0.0496569984 0.0388036530 0.61355
create vertex 0.04826 0.023282192 0.61355
create vertex 0.04826 -0.023282192 0.61355
create vertex 0.0496569984 -0.0388036530 0.61355
create vertex 0.0388036530 -0.0496569984 0.61355
create vertex 0.023282192 -0.04826 0.61355
create vertex -0.023282192 -0.04826 0.61355
create vertex -0.0388036530 -0.0496569984 0.61355
create vertex -0.0496569984 -0.0388036530 0.61355
create vertex -0.04826 -0.023282192 0.61355
create vertex -0.04826 0.023282192 0.61355
create vertex -0.0496569984 0.0388036530 0.61355
create vertex -0.0388036530 0.0496569984 0.61355
create vertex -0.023282192 0.04826 0.61355
create vertex 0.023282192 0.04826 0.61355
##End of coordinates
##Start curves
##zr can curves
create curve vertex 1069 1070
create curve vertex 1070 1071
create curve vertex 1071 1072
create curve vertex 1072 1073
create curve vertex 1073 1074
create curve vertex 1074 1075
create curve vertex 1075 1076
create curve vertex 1076 1069
create curve vertex 1077 1078
create curve vertex 1078 1079
create curve vertex 1079 1080
create curve vertex 1080 1081
create curve vertex 1081 1082
create curve vertex 1082 1083
create curve vertex 1083 1084
create curve vertex 1084 1077
create curve vertex 1085 1086
create curve vertex 1086 1087
create curve vertex 1087 1088
create curve vertex 1088 1089
create curve vertex 1089 1090
create curve vertex 1090 1091
create curve vertex 1091 1092
create curve vertex 1092 1093
create curve vertex 1093 1094
create curve vertex 1094 1095
create curve vertex 1095 1096
create curve vertex 1096 1097
create curve vertex 1097 1098
create curve vertex 1098 1099
create curve vertex 1099 1100
create curve vertex 1100 1085
create curve vertex 1101 1102
create curve vertex 1102 1103
create curve vertex 1103 1104
create curve vertex 1104 1105
create curve vertex 1105 1106
create curve vertex 1106 1107
create curve vertex 1107 1108
create curve vertex 1108 1109
create curve vertex 1109 1110
create curve vertex 1110 1111
create curve vertex 1111 1112
create curve vertex 1112 1113
create curve vertex 1113 1114

```

```

create curve vertex 1114 1115
create curve vertex 1115 1116
create curve vertex 1116 1101
##end of curves
##zr can surfaces
create surface curve 1265 1266 1267 1268 1269 1270 1271 1272
create surface curve 1273 1274 1275 1276 1277 1278 1279 1280
create surface curve 1281 1282 1283 1284 1285 1286 1287 1288 1289 1290 1291 1292 1293
1294 1295 1296
create surface curve 1297 1298 1299 1300 1301 1302 1303 1304 1305 1306 1307 1308 1309
1310 1311 1312
##end of surfaces
##zr can surface copies for volumes
surface 410 copy move z 1.254095 ##surface 414
surface 411 copy move z 1.254095 ##surface 415
surface 412 copy move z 1.209675 ##surface 416
surface 413 copy move z 1.209675 ##surface 417
##end of copies
##zr can volumes
create volume loft surface 410 412
create volume loft surface 411 413
create volume loft surface 416 414
create volume loft surface 417 415
create volume loft surface 412 416
create volume loft surface 413 417
##end of volumes
subtract volume 79 from volume 78 ##complete undeformed zr can bottom section
subtract volume 81 from volume 80 ##complete undeformed zr can top section
subtract volume 83 from volume 82 ##complete deformed zr can center section
delete volume 70 71 72 73 74 75 76 77 ##delete sheet bodies that created zr can
##create octant of fuel assembly
webcut volume all with plane xplane noimprint nomerge
delete volume 84 85 86 87 88 89 90 91 92 93 94 95 96 97 98 99 100
webcut volume all with plane yplane noimprint nomerge
delete volume 101 102 103 104 105 106 107 108 109 110 111 112 113 114 115 116 117
webcut volume all with plane xplane offset 0 rotate 45 about z noimprint nomerge
delete volume 118 119 120 121 122 123 124 125 126 127 128 129 130 131 132 133 134
#####
#####
##There was difficulty merging fuel to zr can and getting it to mesh. The
##solution was delete the fuel blocks and creating one fuel block.
#####
#####
##delete out multiple fuel blocks and create a single fuel block
delete volume 44 45 46 47 48 49
##create single fuel block coordinates
create vertex 0.037268167 0.04826 0.61355
create vertex 0.04826 0.037268167 0.61355
create vertex 0.04826 -0.037268167 0.61355
create vertex 0.037268167 -0.04826 0.61355
create vertex -0.037268167 -0.04826 0.61355
create vertex -0.04826 -0.037268167 0.61355
create vertex -0.04826 0.037268167 0.61355
create vertex -0.037268167 0.04826 0.61355
##end coordinates
##create single fuel block curves
create curve vertex 1965 1966
create curve vertex 1966 1967
create curve vertex 1967 1968
create curve vertex 1968 1969
create curve vertex 1969 1970
create curve vertex 1970 1971
create curve vertex 1971 1972
create curve vertex 1972 1965
##end curves

```

```

##create single fuel block surface
create surface curve 2705 2706 2707 2708 2709 2710 2711 2712
##create surface copy for volume
surface 1132 copy move z 1.209675 ##surface 1133
##create single fuel block
create volume loft surface 1132 1133
delete volume 135 136 ## delete surface bodies
##cut the new single fuel block into an octant
webcut volume all with plane xplane noimprint nomerge
delete volume 138
webcut volume all with plane yplane noimprint nomerge
delete volume 139
webcut volume all with plane xplane offset 0 rotate 45 about z noimprint nomerge
delete volume 140
##merge volumes
merge volume 42 43 ##long reflector bottom block with short reflector bottom block
merge volume 50 51 ##long reflector top block with short reflector top block
merge volume 52 78 80 82 56 ##aluminum cans with zr can
merge volume 68 43 ##bottom end cap with bottom short reflector block
merge volume 69 50 ##top end cap with top short reflector block
imprint volume 137 82 ##imprint fuel block onto zr can inside surface
merge volume 137 82 ##merge fue block onto zr can inside surface
volume 52 78 80 82 56 size auto factor 8 ##mesh interval
mesh volume 52 78 80 82 56
volume 42 43 137 50 51 68 69 size auto factor 4 ##mesh interval
mesh volume 42 43 137 50 51 68 69
block 1 volume 137 ##Fuel
block 2 volume 68 69 ##end cap
block 3 volume 42 43 50 51 ##reflector
block 5 volume 78 80 82 ##Zr can
block 4 volume 52 56 ##Al can
sideset 1 surface 1167 1173 ##outside fuel surface
sideset 2 surface 574 1124 ##inside Zr 3 can surface
sideset 3 surface 793 981 805 808 990 880 882 1048 891 1057 ##outside reflector surface
sideset 4 surface 902 1064 920 1079 ##inside al can surface
sideset 5 surface 432 950 1106 468 960 1116 504 970 1126 ##outside zr can surface
sideset 6 surface 1076 916 ##outside Al top surface
sideset 7 surface 906 1067 ##outside Al bottom surface
sideset 8 surface 1165 1166 ##outside fuel end surfaces
sideset 9 surface 1088 1095 ##inside end cap end surfaces
sideset 10 surface 1075 ##Al top end surface
block all element type HEX8 ##these are first order elements
##Name the volumes
volume 42 rename 'Long Reflector Block Bottom'
volume 43 rename 'Short Reflector Block Bottom'
volume 50 rename 'Short Reflector Block Top'
volume 51 rename 'Long Reflector Block Top'
volume 52 rename 'Al-6063 Can Bottom'
volume 56 rename 'Al-6063 Can Top'
volume 68 rename 'End Cap Bottom'
volume 69 rename 'End Cap Top'
volume 78 rename 'Zr-3 Can Bottom Section'
volume 80 rename 'Zr-3 Can Top Section'
volume 82 rename 'Zr-3 Can Center Section'
volume 137 rename 'Fuel Block'
##Name the blocks
block 1 name "Fuel"
block 2 name "End Cap"
block 3 name "Reflector"
block 4 name "Al-6063 Can"
block 5 name "Zr-3 Can"
##Name the sidesets
sideset 1 name "Fuel Surface"
sideset 2 name "Zr-3 Can Inside Surface"

```

```
sideset 3 name "Reflector Surface"
sideset 4 name "Al-6063 Can Inside Surface"
sideset 5 name "Zr-3 Can Outside Surface"
sideset 6 name "Al-6063 Top Can Outside Surface"
sideset 7 name "Al-6063 Bottom Can Outside Surface"
sideset 8 name "Fuel End Surfaces"
sideset 9 name "End Can Surfaces"
sideset 10 name "Al-6063 Can End Surfaces"
##End of names
export mesh '/Users/heatbk/Desktop/Parametrics/simple_single_fuel_block.e' overwrite
#####
#####
```

Note: In some cases the command line is split between two lines in order to fit into the document horizontally. Before running this file those commands that have been split into two lines need to be resolved. A command must be all on one line.

Example:

create curve 5 7 8 9 10 11

NOT

create curve 5 7 8

9 10

APPENDIX C: INPUT FILE

```
#####
#####
[Problem]
    coord_type = xyz
[]

[GlobalParams]
    quadrature = true
    family = LAGRANGE
[]

[Mesh] #Call for the Mesh File.
    file = simple_single_fuel_block.e
    patch_size = 1000 # For contact algorithm
[]

[Variables] # Define dependent variables and initial conditions.
    [./temp] # Give the fuel and initial temperature of 300 K.
        initial_condition = 300
    [../]
[]

[Functions]
    [./sh_func] #Specific Heat of fuel as a function of temperature.
        type = PiecewiseLinear
        x = '273 311 366 422 477 533 589 644 700 755 811'
        y = '647 730 847 958 1062 1160 1250 1331 1404 1468 1522'
    [../]
    [./k_func] #Thermal Conductivity of fuel as a function of
        #temperature.
        type = PiecewiseLinear
        x = '338 394 458 475 583 588 733 811'
        y = '22 22 21 21 20 20 18 18'
    [../]
    [./fission_func] #Volumetric fission rate as a function of time.
        type = PiecewiseLinear
        x = '0 1'
        y = '1.57e15 1.57e15'
    [../]
    [./t_infinity1]
        type = PiecewiseLinear
        x = '0 100000'
        y = '300 350'
    [../]
    [./t_infinity2]
        type = PiecewiseLinear
        x = '0 1'
        y = '300 300'
    [../]
    [./t_infinity3]
        type = PiecewiseLinear
        x = '0 100000'
        y = '300 350'
    [../]
```

```

[]

[AuxVariables]
[./fission_rate]
    block = 1
[../]
[./gap_cond]
    order = CONSTANT
    family = MONOMIAL
[../]
[]

[Kernels] # Define kernels for the various terms in the PDE system
[./heat] #Gradient term in heat conduction equation.
    type = HeatConduction
    variable = temp
[../]
[./heat_ie] #Time term in heat conduction equation.
    type = HeatConductionTimeDerivative
    variable = temp
[../]
[./heat_source] #Source term in heat conduction equation
    type = NeutronHeatSource
    variable = temp
    block = 1
    fission_rate = fission_rate
    energy_per_fission = 3.28451e-11
[../]
[]

[AuxKernels]
[./fissionrate]
    type = FissionRateAux
    variable = fission_rate
    block = 1
    value = 1
    function = fission_func
    # 1 watt = 3.121E10 fissions per second
[../]
[]

[BCs] #Boundary Conditions
[./Zr_conv]
    type = ConvectiveFluxFunction
    T_infinity = t_infinity1
    boundary = 5
    coefficient = 70
    variable = temp
[../]
[./Al_conv_top]
    type = ConvectiveFluxFunction
    T_infinity = t_infinity2
    boundary = 6
    coefficient = 103
    variable = temp
[../]
[./Al_conv_bottom]

```

```

        type = ConvectiveFluxFunction
        T_infinity = t_infinity3
        boundary = 7
        heat_transfer_coefficient = 109
        variable = temp
    [.../]
[]

[Materials] # Define material behavior models and input material
property data.
    [./fuel_thermal]
        type = HeatConductionMaterial
        block = 1
        temp = temp
        thermal_conductivity_temperature_function = k_func
        specific_heat_temperature_function = sh_func
    [.../]
    [./fuel_density]
        type = Density
        density = 1720
        block = 1
    [.../]
    [./graphite_thermal]
        type = HeatConductionMaterial
        block = 3
        temp = temp
        thermal_conductivity_temperature_function = k_func
        specific_heat_temperature_function = sh_func
    [.../]
    [./graphite_density]
        type = Density
        density = 1720
        block = 3
    [.../]
    [./al_clad]
        type = HeatConductionMaterial
        block = 4
        temp = temp
        thermal_conductivity = 215
        specific_heat = 900
    [.../]
    [./alclad_density]
        type = Density
        block = 4
        density = 2700
    [.../]
    [./zr_clad]
        type = HeatConductionMaterial
        block = 5
        temp = temp
        thermal_conductivity = 14.4
        specific_heat = 276
    [.../]
    [./zrclad_density]
        type = Density
        block = 5
        density = 6533

```

```

[../]
[/zrcap_thermal]
  type = HeatConductionMaterial
  block = 2
  temp = temp
  thermal_conductivity = 14.4
  specific_heat = 276
[../]
[/zrcap_density]
  type = Density
  block = 2
  density = 6533
[../]
[]

[AuxBCs]
[/conductance]
  type = MaterialRealAux
  property = gap_conductance
  variable = gap_cond
  boundary = '1 3 8'
[../]
[]

[ThermalContact] #This is for gaps between blocks (i.e. fuel and zr-3
                  #can)
[/air_gap1]
  type = GapHeatTransfer
  variable = temp
  master = 2 #put master on coarser surface regardless of which is
clad or fuel.
  slave = 1
  emissivity_1 = 0.98
  emissivity_2 = 0.9
  gap_conductivity = 0.0
[../]
[/air_gap2]
  type = GapHeatTransfer
  variable = temp
  master = 4
  slave = 3
  gap_conductivity = 0.0454
  emissivity_1 = 0.98
  emissivity_2 = 0.05
[../]
[/zr_gap]
  type = GapHeatTransfer
  variable = temp
  master = 9
  slave = 8
  gap_conductivity = 0.15
[../]
[]

[Executioner]

# PETSC options:

```



```

#   Petsc options
#   Petsc options name
#   Petsc options value
#
# controls for linear iterations
#   l_max_its
#   l_tol
#
# controls for nonlinear iterations
#   nl_max_its
#   nl_rel_tol
#   nl_abs_tol
#
# time control
#   start_time
#   dt
#   optimal_iterations
#   iteration_window
#   linear_iteration_ratio

type = Transient

#Preconditioned JFNK (default)
solve_type = 'PJFNK'

petsc_options = '-ksp_gmres_modifiedgramschmidt'
petsc_options_iname = '-ksp_gmres_restart -pc_type -pc_composite_pcs
-sub_0_pc_hypre_type -sub_0_pc_hypre_boomeramg_max_iter -
sub_0_pc_hypre_boomeramg_grid_sweeps_all -sub_1_sub_pc_type -
pc_composite_type -ksp_type -mat_mffd_type'
petsc_options_value = '201 composite hypre,asm
boomeramg 2 composite hypre,asm
lu multiplicative fgmres ds'

line_search = 'none'

l_max_its = 100
l_tol = 8e-3

nl_max_its = 15
nl_rel_tol = 1e-4
nl_abs_tol = 1e-10

start_time = 0
n_startup_steps = 1
end_time = 300000
num_steps = 5000

dtmax = 10000
dtmin = 1

[./TimeStepper]
type = AdaptiveDT
dt = 2e2
optimal_iterations = 6
iteration_window = 2
linear_iteration_ratio = 100

```

```

[../]
[]

[Postprocessors] # Define postprocessors
                  # (some are required as specified above;
                  # others are optional; many others are available)

[./Fuel_Temp_Avg]
  type = ElementAverageValue
  block = 1
  variable = temp
[../]
[./Zr-3_Clad_Temp_Avg]
  type = ElementAverageValue
  block = 4
  variable = temp
[../]
[./Al-Clad_Temp_Avg]
  type = ElementAverageValue
  block = 5
  variable = temp
[../]
[./Reflector_Temp_Avg]
  type = ElementAverageValue
  block = 3
  variable = temp
[../]
[./Rod_Total_Power]
  type = ElementIntegralPower
  variable = temp
  block = 1
  fission_rate = fission_rate
[../]
[./flux_from_clad] # area integrated heat flux from the cladding
  type = SideFluxIntegral
  variable = temp
  boundary = 2
  diffusivity = thermal_conductivity
[../]
[./flux_from_fuel] # area integrated heat flux from the fuel
  type = SideFluxIntegral
  variable = temp
  boundary = 1
  diffusivity = thermal_conductivity
[../]
[./_dt] # time step
  type = TimestepSize
[../]
[./nonlinear_its] # number of nonlinear iterations at each timestep
  type = NumNonlinearIterations
[../]
[]

[Output] # Define output file(s)
  interval = 1
  output_initial = true
  exodus = true

```

```
perf_log = true
max_pps_rows_screen = 25
[]
#End
#####
#####
```
